DIFFUSION STUDY IN THE Fe-Co-Ni-Au SYSTEM USING THE PENETRATION TENDENCY APPROACH

By

FERNANDO COSME RIZZO ASSUNCAO

A DISSERTATION PRESENTED TO THE GRADUATE COUNCIL OF
THE UNIVERSITY OF FLORIDA
IN PARTIAL FULFILLMENT OF THE REQUIREMENTS FOR THE
DEGREE OF DOCTOR OF PHILOSOPHY

UNIVERSITY OF FLORIDA

1978

Dedicated

To My Wife and Son

ACKNOWLEDGEMENTS

During the course of my studies at the University of Florida, the collaboration of several people was significant. It is pleasing, at the end of the journey, to have the chance to reveal my gratitude for those who, by their helpful assistance, were instrumental to the successful completion of this work.

First, I would like to express my appreciation to the chairman of my advisory committee, Dr. Robert T. DeHoff. In fact, I feel very fortunate for the opportunity of working under his supervision. The exposure to his teaching and scientific methods has greatly influenced my personal views over the past few years. His continuous guidance and motivation provided me with the necessary enthusiasm to overcome several instances of discouragement.

To the members of my committee, I am indebted for their helpful advice and collaboration throughout the course of my studies. Dr. Robert E. Reed-Hill, who kindly provided one of the alloys used in this investigation, lent valuable suggestions regarding the mechanical processing of the alloys. Dr. Albert G. Guy's provision of bibliographic material was particularly important during the writing of this dissertation. Dr. Andrawus I. Khuri's technical comments on the statistical manipulation of the data and his unstinting advice on the subject of matrix theory are deserving of special thanks.

In the early stages of this study, I collaborated with Dr. Arun M. Gokhale and Mr. Coimbatore V. Iswaran in both the experimental and theoretical aspects of the project. Their association is gratefully acknowledged.

To Mr. Wayne Acree, I offer my thanks for his unselfish assistance and orientation during the microprobe analysis of the samples. His collaboration was decisive in developing my skills in that analytical technique.

Technical assistance by Mr. Carlos B. Silva and Mr. Ewald Hartung in the preparation of this manuscript is greatly appreciated.

I would like to extend my appreciation to Mrs. Vicki Turner for the assistance she provided in typing the semi-annual reports to my sponsors. Her dependable and accurate typing of this dissertation from my handwritten originals is well deserving of thanks.

The financial support of the Brazilian Research Council, CNPq, and of the Catholic University at Rio de Janeiro, PUC/RJ, during this three and one-half year long program is gratefully acknowledged.

The project in which this investigation was developed is supported by a grant from the National Science Foundation (NSF). My thanks are offered to that agency.

TABLE OF CONTENTS

Page

ACKNOWLEDGEMENTS.. iii

LIST OF FIGURES... vii

ABSTRACT.. xii

CHAPTER

1 INTRODUCTION.. 1

2 REVIEW OF MULTICOMPONENT DIFFUSION........................ 4
  - Introduction... 4
  - Applications of Fick's Law............................. 6
  - Phenomenological Theory................................ 13
  - Ternary Studies on Diffusion........................... 18
  - Examples of Theoretical Studies on Ternary Diffusion... 21
  - Experimental Determination of D's...................... 25
  - Ternary Studies in Nonmetallic Systems................. 29
  - New Approaches to Multicomponent Diffusion............. 33
  - Conclusions.. 43

3 RELATIVE PENETRATION TENDENCY VIEWPOINT................... 44
  - Introduction... 44
  - Linear Approximation Approach.......................... 46
  - Application of the LAA to the Two-Phase Case........... 53
  - Conclusions.. 67

4 EXPERIMENTAL METHODS...................................... 70
  - Introduction... 70
  - The Fe-Ni-Co-Au System................................. 72
  - Preparation of Samples................................. 74
  - Conclusions.. 91

5 EXPERIMENTAL RESULTS AND DISCUSSION....................... 93
  - Introduction... 93
  - Kirkendall Shifts...................................... 93
  - Results and Discussions of Composition Paths........... 108
  - Conclusions.. 152

TABLE OF CONTENTS - continued.

Page

CHAPTER

6 CONCLUSIONS.. 153

APPENDIX

DETERMINATION OF PHASE BOUNDARIES IN TERNARY SYSTEMS USING TWO-PHASE BINARY DIFFUSION COUPLES.................. 156

REFERENCES.. 195

BIOGRAPHICAL SKETCH... 201

LIST OF FIGURES

Figure		Page
2.1	Diffusion with no concentration gradient. Effect of the diffusivity of component 1 on the shape of the composition path. Numbers on the figure indicate the value of D_1	31
2.2	Representation of a composition P in S^2 using the two bases $\{\hat{\gamma}\}$ and $\{\hat{\theta}\}$	36
2.3	Diffusion paths for an infinite couple PQ. The eigenvectors ν_1 and ν_2 are indicated. Path 1: $\lambda_1 = \lambda_2$; Path 2: $\lambda_1 = 6\lambda_2$; Path 3: $\lambda_1 \to \infty\lambda_2$	39
2.4a	Illustration of a forbidden path on S^2	41
2.4b	Restrictions on eigenvectors and [D] at the boundary	42
3.1	Penetration tendency model for a ternary couple in a system where the penetration tendencies are independent of composition	47
3.2	Penetration tendency model for a ternary couple in a system where the penetration tendencies are composition dependent	51
3.3	Penetration tendency for a quaternary couple	54
3.4	Penetration tendency for a binary two-phase couple displaying a planar interface	56
3.5	Effect of the width and location of the two-phase field on the motion of the interface	59
3.6	Penetration tendency for a ternary two-phase couple displaying a planar interface	61
3.7	Ternary two-phase system assuming an ideal solution model for both phases	63
4.1	Binary diagrams in the system Fe-Ni-Co-Au	73

LIST OF FIGURES - continued.

Figure Page

4.2 Ternary isotherms of the Fe-Ni-Co-Au system at 900°C....... 75

4.3 Quaternary system Fe-Ni-Co-Au at 900°C.................... 76

4.4 Typical arrangement of the samples for the diffusion study.. 78

4.5 Sequence of operations for specimen preparation........... 83

5.1 Pattern of Kirkendall shifts in couples of type A/B........ 98

5.2 Pattern of Kirkendall shifts in couples of type A/AB....... 100

5.3 Pattern of Kirkendall shifts in couples for the ternary couples. a) Fe-Co-Au; b) Fe-Ni-Au; c) Fe-Co-Ni; d) Co-Ni-Au... 103

5.4 Pattern of Kirkendall shifts in couples of type AB/CD...... 107

5.5a Concentration profile for couple Fe/NiCo.................. 110

5.5b Concentration profile for couple Ni/FeCo.................. 111

5.5c Concentration profile for couple FeNi/Co.................. 112

5.5d Concentration profile for couple FeCo/FeNi................ 113

5.5e Concentration profile for couple FeNi/NiCo................ 114

5.5f Concentration profile for couple FeCo/NiCo................ 115

5.6 Composition paths in the system Fe-Ni-Co.................. 117

5.7a Concentration profile for couple AuNi/Fe.................. 119

5.7b Concentration profile for couple FeNi/Au.................. 120

5.7c Concentration profile for couple Ni/AuFe.................. 121

5.7d Concentration profile for couple AuFe/FeNi................ 122

LIST OF FIGURES - continued.

Figure Page

5.7e Concentration profile for couple AuFe/AuNi................. 123

5.7f Concentration profile for couple FeNi/AuNi................. 124

5.7g Penetration tendency model for couple FeNi/AuNi............ 125

5.8 Composition paths in the system Fe-Ni-Au.................. 126

5.9 Comparison of paths in the systems Fe-Ni-Co and Fe-Ni-Au... 127

5.10a Concentration profile for couple AuCo/AuNi................. 129

5.10b Concentration profile for couple Ni/AuCo.................. 130

5.10c Concentration profile for couple Au/NiCo.................. 131

5.10d Concentration profile for couple Co/AuNi.................. 132

5.10e Concentration profile for couple NiCo/AuNi................. 133

5.11 Composition paths in the system Au-Ni-Co.................. 135

5.12a Concentration profile for couple AuCo/Fe.................. 138

5.12b Concentration profile for couple AuCo/AuFe................. 139

5.12c Concentration profile for couple AuCo/FeCo................. 140

5.12d Concentration profile for couple FeCo/Au.................. 141

5.12e Concentration profile for couple Co/AuFe.................. 142

5.12f Concentration profile for couple AuFe/FeCo................. 143

5.13 Composition paths in the system Au-Fe-Co.................. 145

5.14a Concentration profile for couple AuCo/FeNi................. 147

5.14b Concentration profile for couple AuFe/NiCo................. 148

5.14c Concentration profile for couple AuNi/FeCo................. 149

LIST OF FIGURES - continued.

Figure Page

5.15a Composition path for couple AuFe/NiCo...................... 150

5.15b Composition path for couple CoFe/AuNi...................... 151

A1 Ternary system displaying a miscibility gap................ 158

A2 Lattice parameter variation with composition............... 159

A3 Concentration profile in a diffusion couple................ 161

A4 Diffusion couple using a binary two-phase alloy............ 163

A5 Composition profiles in a two-phase structure.............. 164

A6 Initial and later stages of a local diffusion couple....... 166

A7 Composition profile across a particle in a two-phase structure.. 168

A8 Effect of a phase boundary on a two-phase diffusion couple.. 170

A9 Different concentration profiles resulting from phase boundary diffusion... 173

A10 Selection of couple to illuminate two-phase field.......... 175

A11 Different two-phase cases in which the technique can be used... 177

A12 Composition path in a quaternary system displaying a miscibility gap.. 180

A13 Application of the technique to the determination of a quaternary two-phase field.............................. 183

A14a Microprobe results for the NiCo/AuCo couple................ 184

A14b Microprobe results for the AuNi/AuCo couple................ 185

A14c Microprobe results for the Ni/AuCo couple.................. 186

LIST OF FIGURES - continued.

Figure		Page
A15	Collection of results for the Au-Ni-Co system	188
A16a	Microprobe results for the couple FeCo/AuCo	190
A16b	Microprobe results for the couple AuFe/AuCo	191
A16c	Microprobe results for the couple Fe/AuCo	192
A17	Collection of results for the Au-Fe-Co system	193

Abstract of Dissertation Presented to the Graduate Council
of the University of Florida in Partial Fulfillment of the Requirements
for the Degree of Doctor of Philosophy

DIFFUSION STUDY IN THE Fe-Co-Ni-Au SYSTEM USING THE PENETRATION TENDENCY APPROACH

By

Fernando Cosme Rizzo Assunção

December 1978

Chairman: Robert T. DeHoff
Major Department: Materials Science and Engineering

Diffusion in the system Fe-Ni-Co-Au at 900°C was investigated in the present study. Aspects of the diffusion behavior of the four components were interpreted using the penetration tendency viewpoint. An algorithm for treating diffusion in semi-infinite two-phase couples displaying a planar interface has been presented, yielding some qualitative insights into the role of the location and width of the two-phase field in determining the motion of the interface.

Analysis of the pattern of Kirkendall shifts in binary, ternary, and quaternary couples of the system Fe-Ni-Co-Au produced a ranking of penetration tendencies for the elements in the decreasing order Fe, Au, Co, Ni.

Analysis of the composition paths for the same couples confirmed the validity of the proposed ranking. The penetration tendencies of all

components are larger in the region of compositions close to the AuNi 50-50 atomic percent alloy. The low melting point of this alloy is probably responsible for the observed effect. The results for couples containing the AuNi alloy indicate that Au out penetrates Fe in that particular region of compositions.

A new technique for the determination of multiphase ternary isotherms using binary two-phase couples was used to obtain the phase boundaries of the AuCo two-phase field in the ternary systems Au-Ni-Co and Au-Fe-Co. The description of the technique has been incorporated in the present study.

CHAPTER 1
INTRODUCTION

The continuous and increasing utilization of multicomponent alloys in all sectors of today's industry clearly indicates an irreversible trend in the area of selection and development of materials. As the availability of these alloys expands, new applications are found and new compositions are investigated. No matter what elements are present, it is almost certain that diffusion will be involved in the preparation, processing or application of these new alloys.

Studies of diffusion in metals have been concentrated mostly in pure metals or binary alloys. In such studies, the use of the Fickian approach has provided a good framework for describing the diffusion process. The atomistic and continuum aspects of the phenomenon can be interrelated through the descriptor used in the approach, the diffusion coefficient. Due to its similarity with the problem of heat flow, the subject of atomic diffusion has been treated in many texts in conjunction with heat conduction, under the broad designation of transport phenomena. The possibility of using the same mathematical description for both problems has justified the employment of a unified treatment.

For systems with more than two components, application of Fick's laws is no longer a convenient way for describing diffusion. Besides requiring a huge experimental effort to permit evaluation of the diffusion coefficients, the understanding of the processes actually taking place is gradually lost for each new component considered. As a result, the diffusion coefficients become a collection of numbers to which one cannot in general assign a physical meaning.

A review of the studies on binary and ternary diffusion is provided in Chapter 2, with emphasis being given to the limitations of the phenomenological (Fickian) approach as a basis for studying the multicomponent problem.

The recognition that a theory successful in describing the binary problem could not be extended satisfactorily to higher order systems prompted the proposition of a new approach to multicomponent diffusion, the penetration tendency viewpoint. In Chapter 3, this approach is reviewed and expanded to include the case of an infinite two-phase diffusion couple displaying a planar interface.

In the present investigation the penetration tendency approach was used to investigate diffusion in the quaternary system Fe-Ni-Co-Au. Kirkendall shifts and composition paths were measured to generate a qualitative model for the penetration tendencies of the four components involved. The experimental results are presented and discussed in Chapter 5, and the conclusions are described in Chapter 6.

To permit the theoretical description of the two-phase problem in ternary systems, the boundaries and tie lines of the two-phase field must be known at the temperature of the treatment. A new technique for obtaining the ternary isotherms in multiphase systems was developed in this study and yielded satisfactory results. The description of the technique is given in the Appendix.

CHAPTER 2
REVIEW OF MULTICOMPONENT DIFFUSION

Introduction

In the opening remarks of his work on the theory of heat, Fourier (1) indicated a basic and interesting dilemma: "Primary causes are unknown to us; but are subject to simple and constant laws, which may be discovered by observation, the study of them being the object of natural philosophy." As he proceeds in his discussion, the importance of experimental observation in helping to distinguish and define the elementary properties which determine the action of heat is emphasized. After these basic properties are established, then the body of mathematical analysis can be used to reveal the laws which this element obeys.

One of the intrinsic properties he used in founding his theory was the difference in which different bodies conduct heat through the interior of their masses. After this was done, the whole theory of heat conduction was developed, based fundamentally on three entities: (1) heat flux, (2) thermal conductivity, (3) temperature gradient. Once the relation among them was established (flux proportional to force), an energy balance produced the equation to be used in problems of heat conduction. Following that, the mathematics took over, and the development of the theory was dependent on the progress of the calculus. As a matter of fact, it could be said that both fields registered parallel growth, and Fourier's contribution to the field of mathematics was outstanding. In any event, the theory was firmly established.

During the development of a theory, there are times when the complexity of the problem under study is significant. In some cases, the establishment of boundary conditions and existence of solutions become crucial, and it may be necessary to look back at the physical problem to discard inconsistent conditions or physically meaningless solutions. It is thus desirable that the descriptors of the problem are suited to such analysis. This was the case with the theory for heat conduction. The basic elements involved in the theory were of such a simple nature that they could be easily monitored with respect to anomalous behavior and in order to determine the range of values the variables could assume one would not have to go beyond very simple physical arguments (for example, (1) the temperature in any point of an isolated system cannot get lower than the minimum temperature initially present, or (2) the thermal conductivity must always be positive).

Taking into consideration the success of Fourier's theory for heat transfer, it seemed very natural to extend its results to the problem of mass transfer. After all, the similarity of problems was striking and the solutions were already available. With this idea, Adolf Fick (2) suggested that during diffusion the ratio between the flux of atoms across a given plane and the concentration gradient was a constant characteristic of the material, to be called diffusivity.

$$D = \frac{-J}{\partial C/\partial x} \tag{2.1}$$

In this relation, known as Fick's first law, D has units of $[\text{length}]^2/[\text{time}]$, usually cm^2/sec, J has units of atoms (or grams)/cm^2 sec and C is given in atoms (or grams)/cm^3.

If we consider the accumulation of atoms in a given region of the system, conservation of mass required, for one dimensional flow,

$$\frac{\partial C}{\partial t} = -\frac{\partial J}{\partial x} \tag{2.2}$$

so that

$$\frac{\partial C}{\partial t} = -\frac{\partial}{\partial x}\left(-D\frac{\partial C}{\partial x}\right) = \frac{\partial}{\partial x}\left(D\frac{\partial C}{\partial x}\right) \tag{2.3}$$

This relation is known as Fick's second law. If it is assumed that D is independent of x, then

$$\frac{\partial C}{\partial t} = D\frac{\partial^2 C}{\partial x^2} \tag{2.4}$$

Solutions for this equation are readily available for numerous boundary and initial conditions (2-5), most of them borrowed from the heat conduction literature.

Applications of Fick's Law

It is interesting to study the conditions under which Fick's laws are applicable. The first law, being a definitional relation, can always be used; however, as one will see later, there are cases in which the application is useless. Consider now the second law. To be used in the form of eqn. (2.4), the diffusivity has to be constant, a situation very special and usually encountered only for couples presenting small difference in composition. In most of the cases one has to deal with eqn. (2.3), whose solution is not as straightforward, although it has long been established (6,7).

Using the Boltzmann-Matano analysis (7), one makes a change of variable,

$$\lambda = x/\sqrt{t} \tag{2.5}$$

so that

$$\begin{cases} \partial\lambda/\partial x = 1/\sqrt{t} \\ \partial\lambda/\partial t = -\lambda/2t \end{cases} \tag{2.6}$$

Substituting in eqn. (2.3) one gets

$$-\frac{\lambda}{2}\frac{dc}{d\lambda} = \frac{d}{d\lambda}\left(D\frac{dc}{d\lambda}\right) \tag{2.7}$$

Integrating from one end of the couple (C^-) to the composition of interest (C):

$$-\frac{1}{2}\int_{C^-}^{C} \lambda dC = D\frac{dc}{d\lambda}\Big]_{C^-}^{C} = D\frac{dc}{d\lambda}\Big]^{C} \tag{2.8}$$

After a diffusion experiment, t is fixed so that one can change back to x and t in eqn. (2.8) and obtain

$$-\frac{1}{2t}\int_{C^-}^{C} x dc = D\frac{dc}{dx}\Big]^{C} \tag{2.9}$$

from which the diffusion coefficient D can be obtained for every composition C by means of the above equation and the experimentally determined penetration curve. Once the curve is determined for a given couple, all information necessary for studying diffusion at that temperature has been obtained since in λ space the penetration curve is time invariant. A more detailed treatment of the method can be found elsewhere (5,8).

Now that one has seen some applications of Fick's laws it is appropriate to observe the looseness of language with which the equations were applied. It was not mentioned during all discussion above if there was only one diffusing species, as was the case in heat conduction. In fact, there are many situations in which this condition is observed, for example diffusion of an interstitial element in a rigid lattice, such as carbon in austenite, or diffusion of a radioactive tracer in a stable isotope of the same element, where only one species can be monitored. However, in a binary substitutional alloy, there is no reason to believe that only one species is diffusing or, if both diffuse, that their diffusivities should be the same.

Now, if one considers the penetration curve for a binary couple and applies Fick's law for one of the components, one obtains a diffusion coefficient that characterizes the process. Since the concentration profiles for the two species are symmetric, the same diffusion coefficient would result if one had selected the other component for the analysis. In other words, the diffusivity obtained from such experiment is related to the ability of the two components to interdiffuse and eliminate compositional gradients, not a measure of the ability of individual species to diffuse in the crystal.

As far as being able to calculate penetration depths and diffusion coefficients for binary alloys, the use of Fick's laws proved to be advantageous. However, for those interested in describing the mechanism of diffusion, the diffusivity produced by the analysis was of little application. It would be desirable that the diffusion coefficients could be related to more fundamental parameters, such as mobilities or atomic jump frequencies of each species.

By the late 1940's, several mechanisms had been proposed; among them was the vacancy mechanism. When Kirkendall, in the last of his papers on diffusion in the CuZn system (9-11), reported the movement of inert markers and suggested that one explanation could be based on the difference in diffusivity between Cu and Zn, the validity of the vacancy mechanism seemed established. Although the experimental confirmation of the effect was finally made only some years later (12), its observation enabled Darken (13) to explain Kirkendall's results and to relate the interdiffusion coefficient to other "intrinsic" coefficients, which would measure the ability of each component to diffuse in the crystal. First, as suggested by Seitz (14), Darken recognized the fact that the two components diffused at different rates; there is a net flow of mass across the original interface between the two metals with the result that there is a gain in mass on the side of the slowest moving species. If one assumes constancy of density and accepts the vacancy mechanism, there will be creation of vacancies on the side of the slowest component and annihilation of vacancies on the other side.

As a consequence, the sample "grows" on one side and "shrinks" on the other. If the ends of the couple are fixed in space, markers initially located at the original interface will indicate the movement of lattice planes caused by this effect.

A central point in Darken's analysis is the choice of reference frame. If one selects a frame fixed with respect to the lattice planes (and markers) one can define the flux of each component across a lattice plane by

$$J_A = -D_A\frac{\partial C_A}{\partial x} \quad \text{and} \quad J_B = -D_B\frac{\partial C_B}{\partial x} \tag{2.10}$$

where D_A and D_B are called intrinsic diffusion coefficients. Every plane in the diffusion zone will be moving with a velocity v with respect to the ends of the couple; this velocity varies along the diffusion direction, being zero outside the diffusion zone. It would be very complicated to treat several different reference frames, each one travelling at a different velocity. It is simpler to select the reference frame fixed with respect to the end of the couple and write the expression for the new flux using the fact that there is a relation among the fluxes defined in different reference frames. With respect to the end of the couple, the flux of, say, A across a plane fixed in space will consist of the flux J_A given above due to diffusion, plus a contribution C_Av due to the movement of the lattice. Thus,

$$\left\{\begin{array}{l} J'_A = J_A + C_A v = -D_A \frac{\partial C_A}{\partial x} + C_A v \\ J'_B = J_B + C_B v = -D_B \frac{\partial C_B}{\partial x} + C_B v \end{array}\right. \qquad (2.11)$$

With respect to the end of the couple the fluxes of A and B are equal (interdiffusion) so that

$$J'_A + J'_B = 0 \qquad (2.12)$$

Also,

$$C_A + C_B = C = \text{constant} \therefore \frac{\partial C_A}{\partial x} = -\frac{\partial C_B}{\partial x} \qquad (2.13)$$

And one gets

$$(D_A - D_B)\frac{\partial C_A}{\partial x} = Cv \therefore v = (D_A - D_B)\frac{\partial N_A}{\partial x} \qquad (2.14)$$

where $N_A = C_A/C$.

Substituting the expression for v in one of the equations [(2.11)]:

$$J'_A = -D_A \frac{\partial C_A}{\partial x} + C_A(D_A - D_B)\frac{\partial N_A}{\partial x} = [-D_A + N_A D_A - N_A D_B]\frac{\partial N_A}{\partial x}$$

$$\therefore J'_A = (N_B D_A + N_A D_B)\frac{\partial C_A}{\partial x} \qquad (2.15)$$

Comparing this expression with that for interdiffusion [eqn. (2.1)] one can write

$$\tilde{D} = N_B D_A + N_A D_B \qquad (2.16)$$

This expression made it possible to relate the experimentally determined $\tilde{D}$ with the intrinsic diffusion coefficients D_A and D_B. Darken also showed that the intrinsic D's could be related to the tracer diffusivities:

$$D_A = D_A^*[1 + \frac{\partial \ell n \gamma_A}{\partial \ell n N_A}] \qquad (2.17)$$

The problem of diffusion in a binary system was thus reasonably under control; the contribution of Fick's law had been significant.

For those working on the atomistic approach to diffusion, the task was still incomplete. Expressions for D in terms of fundamental parameters just kept growing in size, as many corrections had to be used to take into account different effects (correlation, vacancy wind effect, etc.). Although the two approaches, continuum and atomistic, do not necessarily focus on the same goals, it is desirable that both interact in a supportive way, since much understanding can be gained from the process when such a unified picture is available. However, as the theory was extended to multicomponent systems many difficulties were uncovered and both approaches had to fight for their survival. As a result, each one followed a different route with few attempts (15-18) being made to bring them together. If one compares Fick's law problems with the success of Fourier's equation, it becomes clear that one difference among treatments concerns the possibility of more than one flux in problems of mass transfer as opposed to the single heat flux in the area of heat conduction. It is common in physics to go from one component to multicomponent space without great difficulty, so that it does not seem advisable to drop the theory without some struggle.

Phenomenological Theory

The basis for a theory on multicomponent diffusion was laid down by Onsager (19) in his treatise on irreversible processes. In 1945, he (20) addressed the problem of multicomponent diffusion directly. For an n-component system, the flux of each species is assumed to be a linear function of all forces acting in the system. For an isobaric, isothermal and otherwise simple system, it is common to express the fluxes as

$$\begin{aligned} J_1 &= -L_{11}\,\nabla\mu_1 - L_{12}\,\nabla\mu_2 \ldots -L_{1n}\,\nabla\mu_n \\ J_2 &= -L_{21}\,\nabla\mu_1 - L_{22}\,\nabla\mu_2 \ldots -L_{2n}\,\nabla\mu_n \\ &\vdots \\ J_n &= -L_{n1}\,\nabla\mu_1 - L_{n2}\,\nabla\mu_2 \ldots -L_{nn}\,\nabla\mu_n \end{aligned} \qquad (2.18)$$

where the L_{ij}'s are the phenomenological coefficients and the μ_i's represent the chemical potential of component i. The phenomenological coefficients may depend on temperature and composition but are independent of the forces. If the fluxes and forces are properly defined, the coefficients L_{ij} are related by Onsager's relations (19).

$$L_{ij} = L_{ji} (i \neq j;\ i,j = 1,2,\ldots n) \qquad (2.19)$$

The experimental verification of Onsager's relation in multicomponent diffusion has been reported several times in liquid systems (21-24), and in solid ternary systems (25-27). The use of eqns. (2.18) is not convenient, however, from a practical standpoint since the phenomenological coefficients and chemical potential gradients are not parameters amenable to experimental observation.

Instead, the fluxes in eqn. (2.18) are defined using concentration gradients as driving forces and the resulting expressions are

$$\begin{aligned} J_1 &= -D_{11}\,\nabla C_1 - D_{12}\,\nabla C_2 \ldots -D_{1n}\,\nabla C_n \\ J_2 &= -D_{21}\,\nabla C_1 - D_{22}\,\nabla C_2 \ldots -D_{2n}\,\nabla C_n \\ &\vdots \\ J_n &= -D_{n1}\,\nabla C_1 - D_{n2}\,\nabla C_2 \ldots -D_{nn}\,\nabla C_n \end{aligned} \tag{2.20}$$

where now the diffusion coefficients D_{ij} have been defined to relate that part of the flux J_i of species i due to the concentration gradient ∇C_j of component j. Equations relating the D_{ij}'s with the phenomenological coefficients L_{ij}'s can then be derived from eqns. (2.19) and (2.20) if both sets of fluxes are identically defined. In this manner, experimentally determined D's can be used to test Onsager's reciprocal relations. While such tests may contribute to confirm the generality of Onsager's treatment, their importance to the field of multicomponent diffusion is confined to reducing the number of off-diagonal coefficients necessary to describe the different fluxes. The reason for this limited contribution results from the lack of physical significance for the diffusion coefficients when eqns. (2.20) are redefined to take into account additional relations among the fluxes and among the driving forces.

For interdiffusion fluxes (volume-fixed reference frame) one can use relations of the kind

$$\sum_{i=1}^{n} p_i\,J_i = 0 \qquad \text{and} \qquad \sum_{k=1}^{n} q_k\,\nabla C_k = 0 \tag{2.21}$$

to reduce the set of eqns. (2.20) to n-1 fluxes and n-1 concentration gradients. By regrouping and redefining the diffusion coefficients, a new set of equations is obtained containing $(n-1)^2$ coefficients. It should be recognized, however, that the choice of which component will be considered the dependent one is arbitrary and any of n different square matrix of coefficients may be defined. It is common (28) to use a superscript to indicate the dependent component. A tilde will be used to characterize interdiffusion (chemical) coefficients. The new set of equations, in condensed form, becomes

$$J_i = -\sum_{k=1}^{n-1} \tilde{D}^n_{ik} \nabla C_k \qquad (i = 1,2,\ldots n-1) \tag{2.22}$$

$$J_n = -\sum_{i=1}^{n-1} J_i \tag{2.23}$$

as opposed to the old set

$$J_i = -\sum_{k-1}^{n} \tilde{D}_{ik} \nabla C_k \qquad (i = 1,2,\ldots n) \tag{2.24}$$

The two sets of coefficients are related by

$$\tilde{D}^n_{ik} = \tilde{D}_{ik} - \tilde{D}_{in} \tag{2.25}$$

As is apparent from inspection of eqn. (2.25) the physical meaning of $\tilde{D}^n_{ik}$ is by no means obvious, showing a composite effect between the originally meaningful coefficients $\tilde{D}_{ik}$ and $\tilde{D}_{in}$ to describe the contribution exerted by the concentration gradient ∇C_k to the flux J_i. It is appropriate to reflect about the implications of such a result. If one considers the n-diagonal coefficient $\tilde{D}^n_{ii}$, which is related to the flux of i under its own concentration gradient, it is found that its value is affected by which element is chosen as dependent component. Further, the sign of $\tilde{D}^n_{ii}$ may be positive or negative, without necessarily implying the direction of flow of component i.

If one attempts to define the fluxes relative to the lattice planes (intrinsic fluxes), the expression for each flux is given by

$$J_i = - \sum_{k=1}^{n-1} D_{ik} \nabla C_k \qquad (i = 1,2,\ldots n) \tag{2.26}$$

and the D_{ik}'s are called intrinsic diffusion coefficients. Again one can use a relation among the concentration gradients to reduce the number of terms describing each flux if one assumes

$$C_T = \sum_{i=1}^{n} C_i = \text{constant} \tag{2.27}$$

The fluxes are then expressed by

$$J_i = - \sum_{k=1}^{n} D^n_{ik} \nabla C_k \qquad (i = 1,2,\ldots n) \tag{2.28}$$

$$J_v = - \sum_{i=1}^{n} J_i \tag{2.29}$$

where J_v represents the flux of vacancies across a given lattice plane. The fact that the fluxes J_i of the n components are not linearly dependent makes the matrix of coefficients asymmetric, since there are n fluxes J_i and n-1 concentration gradients ∇C_k. As in the case of interdiffusion it is not clear what physical meaning can be attributed to the resulting intrinsic coefficients.

The basic purpose of this discussion is simply to provide a picture of the kind of descriptors the diffusion coefficients are, and for that reason no attempt will be made to cover the phenomenological theory of diffusion. It should be pointed out however that the theory is fully consistent and is successfully applied in many problems where the availability of thermodynamic and kinetic data is large. On the other hand, in the case of multicomponent diffusion, the situation is markedly disadvantageous. The methods for obtaining diffusion coefficients in ternary systems are slow and tedious besides not being precise, due to extensive processing of the raw data. When one considers systems of higher order the situation may be defined as chaotic. As of this writing, no new method had been suggested to obtain diffusion coefficients in quaternary systems, and yet, none of the methods in use for the ternary case can be extended to those systems.

Two intersecting paths are necessary in order to calculate D's in ternary systems. For quaternary systems, intersection of three paths would be required. Chances that the composition paths of three independent couples will cross in a common point in compositional space are negligible.

One of the goals of this investigation is to point out the severe limitations of the Fickian approach to treat diffusion in higher order systems. The need for a new approach cannot be overemphasized. In fact, the common trend has been one of patiently hoping that the classical approach will ultimately yield solutions to these complex problems. Many years ago, on recognizing the limitations of the binary treatment to address the problem of diffusion in higher order systems one investigator warned: "... it is clear that diffusion in a multicomponent system cannot be adequately described by a simple extension of the method currently used for binary systems." It is therefore puzzling that since that time, most of the work reported in multicomponent diffusion is basically devoted to supporting such extensions, while only a few attempts have been made to develop new viewpoints. When one considers that those prophetic words were spoken in a seminar on diffusion, in 1950, by Darken (29), one cannot avoid wondering why people have not dedicated more time in search of a new approach.

Ternary Studies on Diffusion

Studies on ternary systems have been plentiful. While they are performed by different investigators using different techniques, it can be said that one common goal of most studies is the determination of diffusion coefficients. As explained in the previous section, the experimental determination of diffusion coefficients is likely to be confined to ternary systems in view of the need for intersecting paths at the composition of interest. As a result, experimental studies in quaternary systems are not centered on obtaining diffusion coefficients. Most of the work reported in the literature refers to specific alloys, without any attempt to generate a systematic survey over a region of compositions in the quaternary system. The only alloys investigated are those presenting peculiar properties or those of commercial importance. Although such empirical approaches have been an important factor in the progress of materials science, it is rather natural to expect (30) that a theoretical methodology would provide a better framework to investigators working on those systems. The relative penetration tendency viewpoint, which was used in this investigation to explore the quaternary system Fe-Ni-Co-Au, holds promise toward the development of such a framework. It is believed that the results reported in this study represent the first attempt to systematically describe diffusion over an entire quaternary system.

In order to provide a background to the discussion of the results, a brief review of ternary studies will be made. This review is not intended to be comprehensive; those interested in the subject are referred elsewhere (26,27,31).

Darken's experiment (32) in 1949 provided a stirring effect on the theory of ternary solid state diffusion. By welding an Fe-C alloy to an Fe-C-Si alloy of the same carbon content, he showed that after a long diffusion anneal at 1050°C the carbon atoms had been redistributed over a significant distance on both sides of the interface. The explanation for this uphill diffusion necessarily revealed the limitations of Fick's law as a basis for describing diffusion in systems with more than two components. Darken proposed that carbon had diffused down its chemical potential gradient, due to its higher thermodynamic activity, on the side containing silicon. A plot of the composition path, that is, the sequence of compositions in the couple along the diffusion zone, resulted in an S-shaped curve.

The explanation for this curved path was based on the difference in diffusion velocity of carbon and silicon. At that time no importance was given to the information contained in the composition path.

Some years later, Rhines et al. (33) reported diffusion experiments in brass-bronze couples, indicating the formation of S-shaped composition paths. In this case, the explanation for the curved path was based on the variation of the relative diffusion velocities of tin and zinc, since it was known that zinc diffused faster than tin in copper (34). Analysis of the composition paths showed the paths bending away from the fast moving species.

The first study focussing on the behavior of composition paths was published by Rhines and Clark (35), based on metallography and x-ray diffraction of diffusion layers formed in the system Al-Mg-Zn at 335°C. Despite the complexity of the system under study, those authors were able to generate a set of rules governing the formation of diffusion paths in single-phase and multiphase ternary systems. Their work was later criticized by Kirkaldy and Fedak (36) for being essentially metallographic. It was found, during diffusion studies in two-phase ternary couples in the systems Fe-Ni-Cr and Cu-Zn-Sn, that the possibility of nonplanar interfaces or isolated precipitates in ternary systems may lead to erroneous metallographic interpretation. This requires a much more complete analysis of the structure, including microanalysis of the diffusion zone, to avoid the risk of misleading results.

In the following year, Kirkaldy and Brown (37) published a series of theorems and rules pertaining to the construction of diffusion paths in ternary isotherms. These rules encompassed Rhines' previous rules and included the concept of the virtual diffusion path, developed in the previous paper (36).

When Clark (38) reported some conventions for plotting the diffusion paths in multiphase ternary couples in the isothermal section of a ternary phase diagram, the apparatus for representing diffusion paths was complete. Nonetheless, few studies have been made focussing on the relation between composition path and microstructure. In an extensive investigation of the system Cu-Ni-Zn (39,40), this kind of analysis was included.

Examples of Theoretical Studies on Ternary Diffusion

Kirkaldy's studies of multicomponent diffusion marked the first systematic attempt to describe the complexities of the problem. In a series of papers (41-45) he discussed a number of general theoretical problems pertaining to multicomponent diffusion in metals. Such studies included the solution for the semi-infinite case (41,42) using a procedure similar to the Boltzmann-Matano analysis. He satisfactorily described (41) Darken's results (32) and reported diffusion coefficients for carbon and silicon from the analysis. Using Onsager's principle of microscopic reversibility (20) and the second law of thermodynamics, he derived (42) some conditions that should prevail among the diffusion coefficients in order to assure consistency between those two principles. He also found that for many physically acceptable choices of D's and boundary conditions, the equations would give negative concentrations in the distribution. He suggested that new principles should be developed to handle such cases. Following Zener's solution (46) for the growth of precipitates in a binary system, he solved the ternary problem (43) for two-phase systems and applied the result to transformations in steel. Due to the lack of data in the two systems under investigation (Fe-C-Si and Fe-C-Mn), the conclusions derived in that paper were more of a qualitative nature with regard to the effect of manganese and silicon on the hardenability of steels. Next he treated the motion of planar phase interfaces (44), obtaining a solution for the general case of N phases of an n-component system. Recognizing the possibility of marker movement in systems where vacancy mechanism operates, he showed that such motion would not invalidate his results (since he used interdiffusion fluxes) but new diffusion coefficients would be needed to evaluate the velocity of the markers. He finally published a general theorem for construction of multicomponent solutions from solutions of the binary diffusion equation (45). Derivations for steady state and transient equilibrium were indicated. In the last paper of the series (17), he treated interstitial diffusion in dilute ternary austenites. By using the statistical theory of diffusion suggested by Seitz (15), he tried to bridge the gap between the atomistic approach and the phenomenological theory. Due to large experimental and analytical errors he did not claim that the attempt had been successful.

To complement such extensive studies, Coates, another investigator from Kirkaldy's group, attacked other areas of theoretical interest previously unexplored. He first discussed the stability of planar interfaces (47) using perturbation theory. Although very successful in hydrodynamic studies (48), the method proved too complicated to be of practical interest. The criteria for stability derived from the theory involved too many parameters, all of them collected in very long equations. On the other hand, the theory successfully confirmed earlier claims that the onset of instability could be indicated by the diffusion path becoming tangent to the boundary of the two-phase field. In other words, if the two-phase field was known and the diffusion path could be predicted, it would be possible to identify which couples in a system were potentially bound to develop nonplanar interfaces. Experimental observation of some α-β couples in the system Cu-Ni-Zn comprised the qualitative test for the theory. The author described the possibility of deriving the composition paths. Using the phase diagram information and the diffusion data available, application of Kirkaldy's solutions (44) would produce the composition path for planar interfaces. At this point, it is appropriate to consider the imprecision that could be present in such calculations. In all of Kirkaldy's solutions, it is assumed that the diffusion coefficients are constant. In multiphase systems, an average D should be used to describe the diffusion in each phase. If one just considers the α region of the Cu-Ni-Zn system, variations in the tracer diffusivity of the three components as large as one hundred times have been reported (31) between alloys of roughly the same content of copper but different contents of Ni and Zn. It therefore seems unlikely that the use of an average D for each component in the α phase will produce a reliable composition path upon which one can draw conclusions about the stability of the α-β interface. Coates did not report any calculated path in his study. The relative penetration tendency approach, with its ability to predict composition paths could be well suited to such analysis.

Following his work on interface stability, Coates (49) reported an elegant treatment for precipitate growth in ternary systems. An interesting feature of the treatment was the recognition that in order to maintain a velocity compatible with the different diffusivities of the solutes, the system could initially pick a tie line not passing through the gross composition of the original alloy. Again, in order to make the problem tractable, the assumption of constant diffusion coefficients was made. The cross coefficients D_{ij} were also neglected.

Because of these simplifying assumptions, extension of his treatment to quaternary systems is straightforward (50).

A careful evaluation of the theoretical developments reported by Kirkaldy's group makes it clear that if extension of binary methods is an adequate procedure for treating multicomponent diffusion, then much of the work has already been done. It is doubtful that new analytical solutions can be derived for the problems discussed above without introducing assumptions to make them tractable. On the other hand, it is also true that those solutions do not satisfy the standards of a theory approaching completion. Furthermore, excessive experimental work is necessary to produce the input data required in each case. The question here is: "Should one insist upon the Fickian approach despite all the above mentioned limitations?" Enough evidence seems to have accumulated to suggest that instead of continuing to change the craftsman one should start thinking about changing the tools.

Experimental Determination of D's

Much of the work reported on ternary systems in the last fifteen years has been directed, at least in part, toward the determination of diffusivities and/or thermodynamic activities. Several methods have been suggested for the experimental evaluation of chemical (41, 51-54) and intrinsic (55,56) diffusivities. A brief review of the most accepted methods in each case will be presented.

1) Interdiffusion Coefficients

Following the Boltzmann-Matano analysis for binary diffusion, Kirkaldy (41) extended the procedure to obtaining interdiffusion coefficients in ternary systems by seeking solutions of the form $C_i = C_i(\lambda)$, $\lambda = x/\sqrt{t}$ to the two simultaneous nonlinear equations

$$-\frac{\lambda}{2}\frac{dC_i}{dx} = \sum_{k=1}^{2} \frac{d}{d\lambda}[\tilde{D}^3_{ik}\frac{dC_k}{d\lambda}] \qquad (i = 1,2) \qquad (2.30)$$

Equation (2.30) can be integrated once to obtain

$$\int_{C_{i\circ}}^{C_i} \lambda dC_1 = -2[\tilde{D}^3_{i1}\frac{dC_1}{d\lambda} + \tilde{D}^3_{i2}\frac{dC_2}{d\lambda}]_{C_i} \qquad (2.31)$$

In order to solve eqn. (2.31), two independent diffusion couples having a common composition C_i are required. Evaluation of the integral and derivation of eqn. (2.31) from experimentally obtained concentration profiles yields a pair of equations relating each $\tilde{D}^3_{i1}$ and $\tilde{D}^3_{i2}$. Ziebold and Ogilvie (51) suggested two modifications to improve the precision of the method without changing the basic principles of the technique. Ziebold's analysis is recognized as the most convenient method for determining interdiffusion coefficients of semi-infinite diffusion couples. Studies have been reported of evaluation of the chemical $\tilde{D}$'s using one of the above analyses in the systems Fe-C-Si (41), Cu-Ag-Au (27,51), Cu-Ni-Zn (26,57), Fe-Ni-Co (25), Cu-Zn-Mg (58) and Fe-Ni-Al (59).

2) Intrinsic Diffusion Coefficients

A method for experimentally determining intrinsic coefficients was presented by Philibert and Guy (56). In an extension of a method originally developed for binary alloys (60,61), they integrated eqn. (2.2) to obtain an expression for the total cumulative flux past a marker plane. The resulting equation is

$$A_i = \int_o^t J_i \, dt = -\int_o^t (D_{i1}^3 \frac{\partial C_1}{\partial x} + D_{i2}^3 \frac{\partial C_2}{\partial x}) dt \qquad (i = 1,2,3) \qquad (2.32)$$

Integrating eqn. (2.32) for a marker plane of constant composition one gets

$$A_i = -2t(D_{i1}^3 \frac{\partial C_1}{\partial x} + D_{i2}^3 \frac{\partial C_2}{\partial x})_{marker} \qquad (i = 1,2,3) \qquad (2.33)$$

Using two independent couples with identical marker compositions, one can experimentally obtain the A_i's and the $\partial C_j/\partial x$'s and then calculate the six D_{ij}^3's. The need for different couples presenting the same compositions at the marker planes strongly limits the applicability of the method for sandwich-like samples. An interesting alternative to overcome this difficulty was the use of vapor-solid diffusion couples by Dayananda and Grace (58) in the system Cu-Zn-Mn. By placing the inert markers at the vapor-solid interface and using different alloys under the same vapor source, they were able to maintain a constant concentration at the interface. Depending on the depth of burial of the markers, the composition at that plane would be slightly different from the interface composition but for practical purposes almost identical. Experimental determination of intrinsic D's has also been reported in other ternary systems (62-64).

A method for obtaining intrinsic diffusivities from interrelation among the tracer, chemical and intrinsic diffusion coefficients was reported by Wan (26), who investigated the Cu-Ni-Zn system at 900°C. In his work he compared three different ways for obtaining the intrinsic coefficients. The first one was based on four relations among the chemical and intrinsic diffusion coefficients (65), together with an expression relating the velocity of the markers with the intrinsic diffusivities (66). In order to obtain the six intrinsic D's another equation is necessary. As in the case of Philibert and Guy (56), he suggested the use of two independent couples with intersecting paths. The possibility of the common composition being located away from the markers was circumvented by estimating the "lattice velocity" at the intersecting composition. The other method of evaluation used interrelations among the chemical potentials and the tracer and intrinsic diffusivities (65). He then compared the intrinsic D's obtained from these two methods with those obtained by the relations among tracer, chemical and intrinsic diffusivities. The values obtained using the estimated lattice velocity did not agree very well with the values obtained with the other two methods, whose agreement was excellent.

As one can see from the description of these methods, evaluation of diffusion coefficients is a tedious and laborious process. Further, in most cases the composition at which the coefficients will be calculated is unknown before the experiment, since the point where the paths intersect is not evident from the choice of couples.

Ternary Studies in Nonmetallic Systems

It would seem natural that diffusion studies in related fields could be directly incorporated to our analysis of multicomponent diffusion. Unfortunately, that is not the case. Diffusion in liquids and glasses does not present some of the problems usually encountered in the description of diffusion in crystals. On the other hand, the study of diffusion in metals has the advantage that effects of ionic charges during motion of the species need not be considered. It is also true that, even when such peculiarities are recognized, difference in notation or terminology may confuse an investigator unaware of such problems. This point will be illustrated in one of the two papers to be discussed.

The first describes a model for multicomponent diffusion by Cooper (67). The purpose of the paper is to give a physical basis for the phenomenological equations for multicomponent diffusion. The author seeks to express the coefficients of the phenomenological equation in terms of independently measurable tracer diffusion coefficients and partial volume of the various species. Unfortunately, the resulting expressions are cumbersome and do not appear to be likely to have analytical solutions in the general case, as pointed out by the author in the paper. In following the derivations on that study, it was observed that what the author called "self diffusivity" is normally referred to as "intrinsic diffusivity" in the literature. Hopefully, such differences in nomenclature between the fields of glasses and metals will be erased in due time.

The other study describes an analysis of ternary diffusion by Oishi (68). Solutions of diffusion equations and calculated concentration distribution were presented. He expressed the interdiffusion fluxes in terms of intrinsic diffusion coefficients and applied the conservation condition for two independent components. Oishi obtained solutions in closed form for the simultaneous differential equation by considering the diffusion equations as linear differential equations. For those cases in which the diffusion equations cannot be approximated as linear, a procedure of finite difference was carried out. By using the solutions, characteristics of ternary diffusion such as the curved diffusion path on the composition diagram, diffusion with no initial gradient, and uphill diffusion were demonstrated quantitatively.

If one considers one of the examples described in the paper, another limitation of the Fickian approach may be illustrated. For the case of diffusion with no initial gradient the theory predicts that if D_2 and D_3 are not equal (see Fig. 2.1), species 1 must diffuse, even with no initial gradient and as a result of its diffusion the composition path will be curved. In order to substantiate the argument, Oishi calculated some paths using several sets of values for the diffusion coefficients D_1, D_2, and D_3. It was found that the smaller is D_1, the more the path deviates from a straight line. Based on his proposed explanation that component 1 diffuses because D_2 and D_3 are different, it is concluded that the lower is the value of the

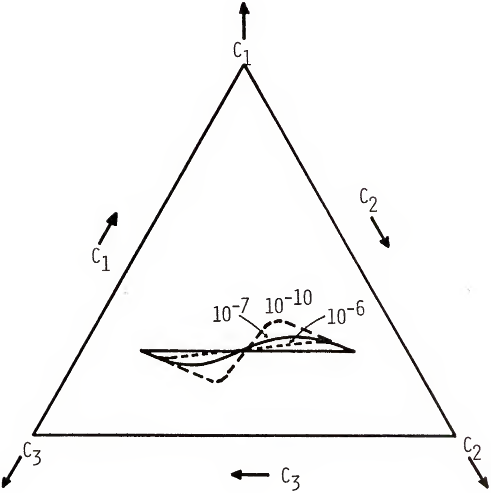

Fig. 2.1. Diffusion with no concentration gradient. Effect of the diffusivity of component 1 on the shape of the composition path. Numbers on the figure indicate the value of D_1.

diffusivity D_1 the more component 1 diffuses. This is exactly opposite from what one would expect for a component with low diffusivity. Such a conclusion clearly results from the lack of physical significance to be assigned to the diffusion coefficients. As a matter of fact, the paper (68) did not describe how the "intrinsic coefficients" were defined, reference being made to another study by the same author (69). It is possible, then, that what Oishi termed intrinsic diffusivity is in fact a different set of coefficients. Oishi's reference was incomplete and the referred paper could not be located. If this is so, it serves to prove the point that the phenomenological theory, when applied to multicomponent diffusion, can produce misleading interpretations by allowing different sets of coefficients to be defined. Since the criteria to pick the most convenient set will vary depending on the area of interest (liquids, metals, ceramics), the chances of obtaining a unified picture with consistent terminology are slim. In any event, whatever set of coefficients is defined to describe the above problem, the result would be the same. The reason for that comes from the inability of the Fickian approach to relate to the processes that are taking place in the system. As a consequence, every change in the concentration of a given species is attributed to a flux of that species, even when physical analysis of the process suggests that such a flux is improbable. It is not surprising therefore that in the example given above, if one considers the case when $D_1 = 0$, one would conclude that redistribution of component 1 would be maximum. As will be shown later, the relative penetration tendency viewpoint explains the same situation without requiring diffusion of species 1. Besides providing a physically meaningful insight into the problem, the concepts involved in the description of the method are extremely simple.

New Approaches to Multicomponent Diffusion

During the last decade, two new approaches have been suggested for treating the problem of multicomponent diffusion. One of them presented a vector space treatment (70) using the [D] matrix of coefficients as a natural extension of the coefficient D for binary diffusion. The other approach (71) introduced a completely different viewpoint in which the total flows of atoms are studied in terms of new descriptors, called penetration tendencies. In the next chapter, this latter approach will be reviewed and expanded to include the description of two-phase systems. The remainder of this section will be devoted to describing the vector space treatment.

The basic strategy of the suggested approach (70) is the use of the eigenvalues and eigenvectors of the diffusion matrix to permit an easier comprehension of the phenomena. Although the use of eigenvalues to calculate diffusion behavior had already been reported in other studies (72,73), the advantages resulting from the uncoupling of the diffusion equations had not been fully explored. Furthermore, the suggested approach has the merit of including the composition paths in the description of the diffusion problem.

Consider the generalized Fick's law of diffusion for an n component system,

$$J_i = -\sum_k D_{ik}\, \rho\, \nabla C_k \qquad (i = 1,2,\ldots n-1) \tag{2.34}$$

where ρ is a density, C_k is some fractional concentration and J_i is the flux defined in some reference frame which leaves only (n-1) independent fluxes. A set of units for ρ, C_k and J_i could be respectively mol/cm^3, mol fraction, and mol/cm^{2}s.

The fractional concentrations are related by

$$\sum_i^n C_i = 1 \tag{2.35}$$

so that only (n-1) fractions are independent. Restricting the analysis to one-dimensional space, eqn. (2.34) can be written

$$J_i = -\sum_k D_{ik}\, \rho\, \frac{\partial C_k}{\partial x} \tag{2.36}$$

Consider now a real space of (n-1) dimensions, S^{n-1}, described by a set of orthonormal basis vectors $\{\hat{\gamma}\}$. If one associates one basis vector to each one of the independent species, one can represent the flux, the concentration gradient and the composition as vectors in S^{n-1}.

$$J = J_1\hat{\gamma}_1 + J_2\hat{\gamma}_2 + \ldots + J_{n-1}\hat{\gamma}_{n-1} \tag{2.37}$$

$$\frac{\partial C}{\partial x} = \left(\frac{\partial C_1}{\partial x}\right)\hat{\gamma}_1 + \left(\frac{\partial C_2}{\partial x}\right)\hat{\gamma}_2 + \ldots + \left(\frac{\partial C_{n-1}}{\partial x}\right)\hat{\gamma}_{n-1} \tag{2.38}$$

$$C = C_1\hat{\gamma}_1 + C_2\hat{\gamma}_2 + \ldots + C_{n-1}\hat{\gamma}_{n-1} \tag{2.39}$$

While J and $\frac{\partial C}{\partial x}$ have all S^{n-1} as their range, the composition vector C is limited to the region defined by

$$C_i \geq 0 \qquad \sum_{i=1}^{n-1} C_i \geq 1 \tag{2.40}$$

The representation of the $\{\hat{\gamma}\}$ basis for a ternary system is shown in Fig. 2.2. One composition P is represented by its description using the $\{\hat{\gamma}\}$ basis as well as an alternative basis $\{\hat{\nu}\}$.

Rewriting eqn. (2.36) in matrix form,

$$J = -[D]\rho \frac{\partial C}{\partial x} \tag{2.41}$$

where [D] is a square matrix of order (n-1). One can make use of the available theory of linear algebra (74) to simplify the equation. If the matrix [D] has real positive eigenvalues, one can find another set of basis vectors $\{\nu\}$, in which the representation of J, $\frac{\partial C}{\partial x}$, and C is more convenient. When one uses this alternative basis $\{\nu\}$, the equation corresponding to (2.41) involves a diagonal matrix $[\lambda]$ having as its elements the eigenvalues of [D]. The resulting flux equations are then uncoupled and can be solved analytically without difficulty.

It can be shown (75) that [D] is the product of a mobility matrix [L], and a thermodymamic matrix [G], both of which are symmetric and positive definite. This ensures that [D] has positive real eigenvalues and can always be diagonalized. To diagonalize [D] one finds its eigenvalues $(\lambda_1, \lambda_2, \ldots \lambda_{n-1})$ and its normalized eigenvectors $(\nu_1, \nu_2, \ldots \nu_{n-1})$ by solving the characteristic equation

$$[D - \lambda I]\gamma = 0 \tag{2.42}$$

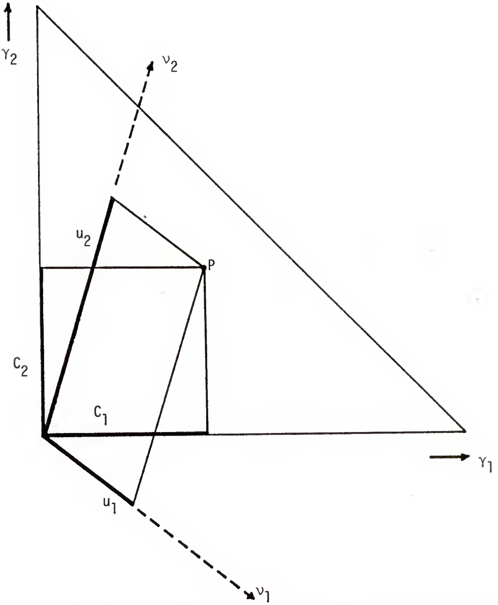

Fig. 2.2. Representation of a composition P in S^2 using the two bases {$\hat{\gamma}$} and {$\hat{\nu}$}.

Using the eigenvectors $\gamma_1, \gamma_2, \dots \gamma_{n-1}$ one can define the matrix [B] which transforms the representation of a vector in S^{n-1} from the original {γ} basis to the new {ν} basis formed by the eigenvectors ν_1, ν_2, etc. Using H and U to represent the flux J and composition C, respectively, in the new basis {ν}, it is clear that

$$H = [B]J \qquad \text{and} \qquad U = [B]C \tag{2.43}$$

The relation between U and C in S^2 is illustrated in Fig. 2.2.

Operating on both sides of eqn. (2.41) from the left and introducing the identity matrix $[I] = [B]^{-1}[B]$ into the first term on the right-hand side, one gets

$$-\frac{1}{\rho}[B]J = [B][D][B]^{-1}[B]\frac{\partial C}{\partial x} \tag{2.44}$$

But $[\lambda] = [B][D][B^{-1}]$ so that

$$-\frac{1}{\rho}H = [\lambda]\frac{\partial U}{\partial x} \tag{2.45}$$

And instead of coupled equations one gets (n-1) independent equations. If ρ and [D] are assumed to be independent of composition, Fick's second law becomes

$$\frac{\partial C}{\partial t} = [D]\frac{\partial^2 C}{\partial x} \tag{2.46}$$

which can be converted, in a like manner, to

$$\frac{\partial U}{\partial t} = [\lambda]\frac{\partial^2 U}{\partial x^2} \tag{2.47}$$

a set of (n-1) uncoupled binary diffusion equations, for which solutions are readily available (3,4).

By analyzing the solutions of eqn. (2.47) for several cases, the authors developed simple rules pertaining to the shape of the composition paths. For diffusion in an infinite couple they observed that: 1) near its extremities the diffusion path always parallels the direction of the fastest eigenvector (the one associated with the larger eigenvalue; 2) for a straight line path the path must parallel an eigenvector (when all λ's are equal, any vector is an eigenvector); 3) the path always lies within an alternate pair of parallelograms (or higher dimensional analogs) obtained by joining the midpoint m with the endpoints p and q by lines parallel to eigenvectors (Fig. 2.3).

The emphasis of the analysis, however, was directed to the fact that the diffusion path alone gives the information necessary to determine the ratios of all the elements of [D].

Experimental observation in the system $CaO-K_2O-SiO_2$ (76) suggested that the eigenvectors for this system do not change direction as a function of temperature, but the ratio of the eigenvectors decreases as the temperature increases. In a study of interdiffusion in the system $K_2O-SrO-SiO_2$ (77), it was found that the eigenvalues and eigenvectors and hence [D] are independent of the direction in compositional space between the end member compositions. It should be pointed out, however, that in both studies the couples investigated covered a small region of composition.

Consider now the possibility that [D] is constant over a region of the compositional space. If one considers a couple near the boundary

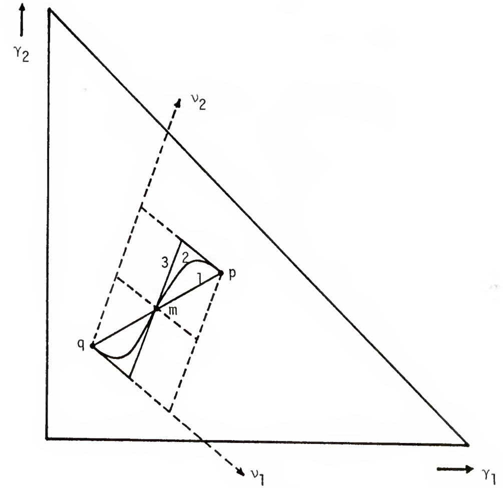

Fig. 2.3. Diffusion paths for an infinite couple PQ. The eigenvectors ν_1 and ν_2 are indicated. Path 1: $\lambda_1 = \lambda_2$; Path 2: $\lambda_1 = 6\lambda_2$; Path 3: $\lambda_1 \rightarrow \infty\lambda_2$.

as indicated in Fig. 2.4a, one concludes that the path may extend beyond the limits of composition in the case of constant [D]. Since this is forbidden from the definition of composition, one sees that the eigenvectors cannot have arbitrary directions. Near the boundaries the major eigenvectors have to parallel the boundary, as indicated in Fig. 2.4b. A consequence of this restriction is to limit the case of constant [D] to small regions of the compositional triangle.

Consider now what happens when [D] is not constant. In this case the operator $\frac{\partial C}{\partial x}$ and [D] do not commute in eqn. (2.3) and the equivalent to eqn. (2.46) is

$$\frac{\partial C}{\partial t} = \frac{\partial}{\partial x}[[D]\rho \frac{\partial C}{\partial x}] \tag{2.48}$$

This equation cannot be uncoupled by a linear transformation of the basis vectors as was done before. In summary, as a result of the composition dependence of [D] the partial differential equations become nonlinear and the equations cannot be uncoupled by a linear transformation of [D]. Since it was shown that [D] will in general vary, the limitations of the treatment are obvious and once again numerical methods have to be called for.

An interesting conclusion of the approach just described has to do with the requirement that [D] must vary in a multicomponent system. The fact that most of the analytical solutions available in the literature assume a constant D endorses several claims made in this investigation about the limitations of the Fickian approach.

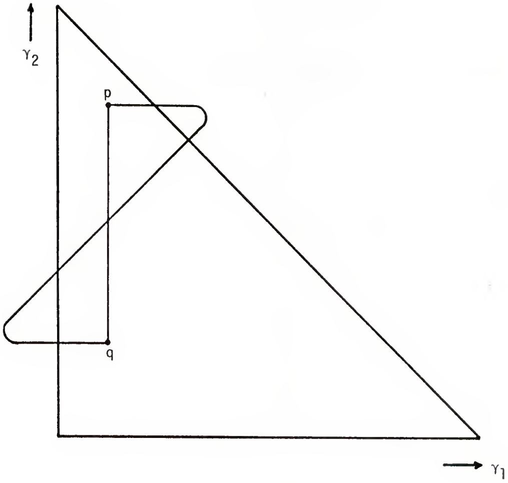

Fig. 2.4a. Illustration of a forbidden diffusion path on S^2.

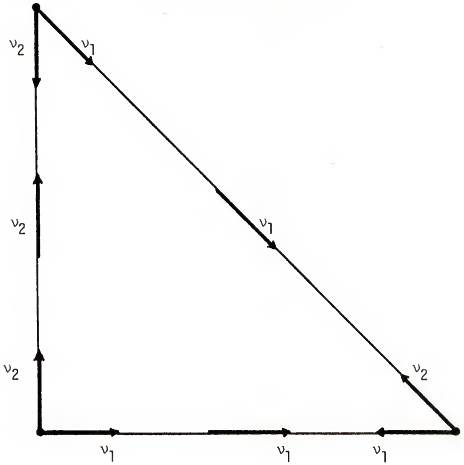

Fig. 2.4b. Restrictions on eigenvectors and [D] at the boundary.

A final comment is appropriate regarding the use of eigenvectors and their influence on the shape of the composition path. If one could relate the eigenvectors to some physical variation taking place in the system, one could probably understand why an eigenvector located on the boundary should parallel that boundary. Further, one could be able to have some feeling about the directions of the eigenvectors from the knowledge of the D's. This is definitely not the case. The eigenvectors are produced by a matrix transformation and no specific directions are expected *a priori*. As will be seen in the next chapter, the features of the composition path are described by the penetration tendency viewpoint and can be easily predicted and understood with a minimum input information about the system.

Conclusions

A critical evaluation of the subject of multicomponent diffusion has been attempted. In this review the limitations and complexities of the Fickian approach have been exposed with the hope that more investigators will recognize the urgent need for a formalism more suited to the intricacies of multicomponent diffusion. To permit extensive coverage of some points considered basic to the discussion, part of the literature review had to be sacrificed. It is therefore possible that many investigations worthy of mention will not be found in this work.

CHAPTER 3
RELATIVE PENETRATION TENDENCY VIEWPOINT

Introduction

The limitations of the phenomenological theory in describing diffusion in multicomponent systems prompted Anusavice (31) and DeHoff to suggest a new approach to the problem which they termed the relative penetration tendency viewpoint. Although approximate, the proposed approach is physically meaningful and can be extended without difficulty to multicomponent systems, having as its principal virtue the fact that it is simple. Using as input the ratio of tracer diffusivities of the species in the system Cu-Ni-Zn at 900°C, they were able to predict Kirkendall shifts and composition paths for several couples located in the Cu-rich α phase.

In their analysis of the diffusion problem, Anusavice and DeHoff used the linear approximation approach (LAA), which assumed linear concentration profiles of the diffusing species. That was not intended, by any means, to suggest that the real concentration profiles were actually straight lines. The purpose of such an assumption was strictly to simplify the analysis. As pointed out in that investigation, the use of a more realistic curve would not affect the outcome of the analysis, although it would substantially decrease its simplicity.

Following that work, the approach was applied by Wan (26) to additional couples of the system Cu-Ni-Zn, and nine other isomorphous systems. Predictions for the systems Fe-Ni-Co and Cu-Ni-Zn were in excellent agreement with the experimental observations. The Kirkendall shift pattern in all nine isomorphous systems could be qualitatively explained if the three elements of each system were assigned penetration tendencies in a given order. The composition paths in the systems Fe-Ni-Pd and Fe-Ni-Co were in agreement with the general principles of the LAA. Composition paths for the systems Ag-Au-Pd, Au-Cu-Ni and Au-Cu-Pd were not obtained; experimental difficulties on those systems made the microprobe results unreliable. Four other ternary systems, namely Fe-Co-Pd, Co-Ni-Pd, Cu-Ni-Pd and Au-Ni-Pd, displayed composition paths which were inconsistent with the predicted paths, as derived from observation of the Kirkendall shifts. Out of six samples investigated in each of the nine isomorphous systems, only two were analyzed for composition path determination. This limited sampling precluded any theoretical study from being made based on the paths. It was concluded therefore that the general rules of the LAA could not explain the observed inconsistencies. A more developed approach of the penetration tendency viewpoint should be used to treat those systems.

Wan also analyzed the data of other investigators using a modified LAA. He found excellent agreement between the predicted and measured paths for the system Fe-Ni-Co (25) by choosing a penetration tendency model 5:3:3 for the LAA. For the system Au-Ag-Cu (27), a model of penetration depths with a constant ratio 12:1:1 brought fairly good agreement between the predicted and measured paths.

In analyzing the Cu-Ni-Zn system, Wan and DeHoff (78) showed that the original agreement (79) between predicted and measured paths could be much improved if the compositional dependence of the penetration tendencies are assumed to lie on a helical surface, and the ratio of penetration depths is also concentration dependent. The predicted Kirkendall shift in this case matches excellently with the measured values.

The ability of the penetration tendency approach to adjust to the complexities of each system without losing its conceptual simplicity makes it an ideal tool for the description of multicomponent diffusion. After successful applications in an isomorphous system, it was necessary to extend the theory to cover the two-phase case. An algorithm to treat the problem has been developed and will be described in this chapter. To permit a gradual buildup of the theory, the fundamentals of the LAA will be briefly reviewed.

Linear Approximation Approach

Consider a semi-infinite ternary couple formed by joining a 50-50 AB alloy to a 50-50 BC alloy of an isomorphous system as indicated in Fig. 3.1a. It is assumed that component A is the fastest moving species and component C is the slowest. Also, normal diffusion behavior is assumed. After a diffusion anneal, each component will have penetrated the side where its concentration was lower. To simplify the argument, the resulting concentration profiles are approximated by

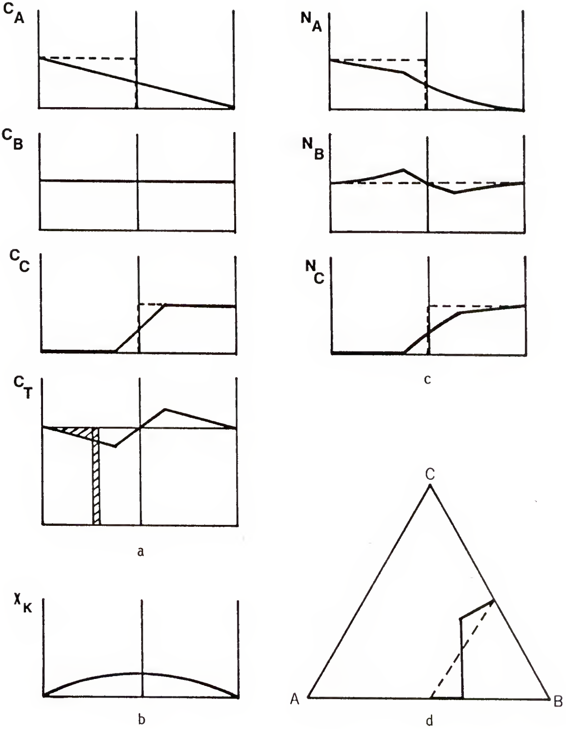

Fig. 3.1. Penetration tendency model for a ternary couple in a system where the penetration tendencies are independent of composition.

straight lines in Fig. 3.1a. As mentioned earlier, this simplification does not affect the general characteristics of the outcome of the analysis. Having drawn the assumed concentration profiles, one can identify for each component a distance of penetration (X_A^+) and a distance of draw (X_A^-). Those penetration depths are the descriptors for the penetration tendency viewpoint.

During an actual diffusion experiment, the imbalance in the flux of atoms generates a flux of vacancies along the diffusion zone. To maintain the equilibrium concentration, vacancies are created in one side and destroyed in the other, giving rise to the Kirkendall effect.

Consider now a conceptually rigid lattice where the species are allowed to redistribute without maintaining a constant concentration of atoms per unit volume. This is the situation depicted in Fig. 3.1a, where the bottom curve, which is the sum of the other three, represents the total concentration of atoms as a function of distance in the couple after the redistribution has occurred. As evident in that figure, there is a deficiency of atoms in the left side and an excess of atoms in the right side. After all species have been redistributed, the lattice is allowed to relax, bringing the total concentration of atoms to its equilibrium value at each position, and producing a Kirkendall shift. The shift experienced by the lattice plane located at x_1 is proportional to the hatched area indicated in Fig. 3.1b, and can be calculated as a function of position, as shown in that figure.

To obtain the composition path, one has simply to divide the concentration of each species by the total concentration of atoms at each point along the diffusion zone. This will produce the atomic fractions, which are used to plot the paths in the ternary diagram. Looking at the atomic fraction curves for the three components, Fig. 3.1c, one may be surprised to observe that component B presents an undulation in its profile, although it was assumed that component B did not redistribute at all. As the reader may have guessed, this is the explanation for Oishi's puzzling result (68) about diffusion in systems with no initial concentration gradient.

When one analyzes chemically a diffusion sample to obtain the concentration profiles, the results are usually reported in units of atomic fraction as opposed to atoms/cm^3. There is no way therefore to distinguish if the concentration of a given species increased due to actual increase in the number of atoms of that species or due to a decrease in the number of atoms of another species. In other words, trying to relate the experimentally determined concentration profiles with fluxes of a given species is not a recommendable practice since fluctuations in the fractional concentration may occur without necessarily implying motion of that species.

Looking at the resulting composition paths in Fig. 3.1d, one can identify the characteristic S-shape curve. Some guidelines may be obtained from the analysis of the path. The two basic principles governing the shape of the path are: 1) The terminal regions of the path are controlled by the fast moving species A. Consequently the end points of the path will always be pointing toward or away from component A. In the specimen this implies that only component A has its concentration altered on those regions although the fractional concentrations of B and C may be affected. 2) The center portion of the path is controlled by the slow moving species C and points more or less toward the C corner. This region usually contains the intersection of the path with the gross composition line. Referring to Fig. 3.1a, one sees that in the central region of the specimen, component C is the one presenting the steepest concentration gradient. This is revealed in the composition paths by a line tending to point toward the C corner.

These principles may be fully explored to generate a pattern of composition paths based on the location of the end couple compositions. It is possible therefore to anticipate the shape of the diffusion path for a given couple when a model for the penetration tendencies of the system is available.

In the example illustrated above, the penetration tendency of each species was assumed to be the same in both sides of the couple. A model can be derived where the penetration tendencies are assumed to be dependent on composition, resulting in different penetration depths in each side of the couple, as illustrated in Fig. 3.2a for the same couple. If one follows the simple analysis of the LAA, the composition path and Kirkendall shifts may be predicted for this case where the penetration depths for all species are assumed to be larger on the AB side of the couple. As expected, both the Kirkendall shift and the

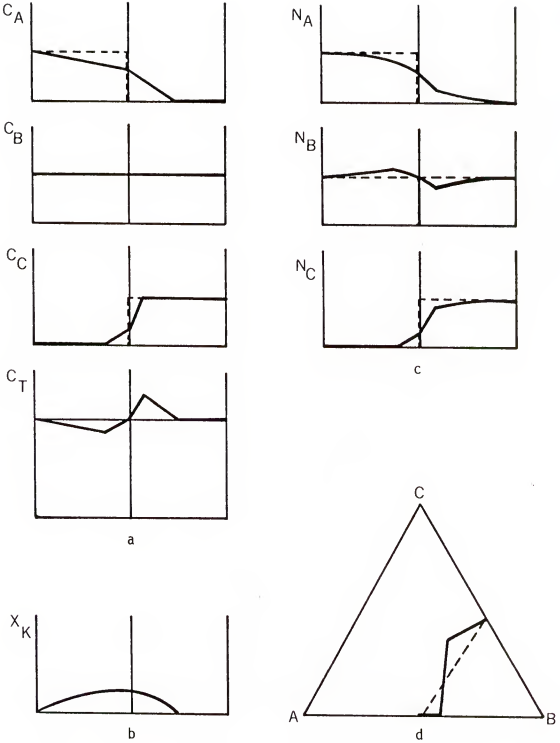

Fig. 3.2. Penetration tendency model for a ternary couple in a system where the penetration tendencies are composition dependent.

composition path are affected. The curve representing the Kirkendall shift along the diffusion zone (Fig. 3.2b) loses its original symmetry, indicating that the size of the diffusion zone is not symmetrical with respect to the original interface. On the composition path, similarly, the crossover point is shifted toward the end point where the penetrations are higher, in this case the AB side (see Fig. 3.2c). The explanation for this distortion of the composition path can be easily obtained from mass balance considerations in Fig. 3.2a. Due to the difference in penetration depths, the concentration of each species at the interface will not bisect the two original concentrations. The need for balancing the two triangular areas to ensure conservation of each species brings the concentration at the interface closer to that corresponding to the side where the penetrations are larger. The displacement of the crossover point, accordingly, gives information with regard to the compositional dependence of the penetration tendencies.

The ability of the LAA to predict composition paths and Kirkendall shifts in a systematic way over the whole ternary diagram is especially interesting. The fact that this is done using such simple arguments is extremely convenient.

The extension of the approach to quaternary and higher order systems is straightforward, since each component is treated independently. One can expect therefore that the same principles derived for the ternary case will apply in other multicomponent systems. Also, it is possible that additional principles will be generated upon each increase in the number of components.

To illustrate how the LAA could be applied to quaternary systems, one model assuming the penetration tendencies to be in the order A>B>C>D will be treated. For the quaternary system indicated in Fig. 3.3a, consider the couple formed by joining the 50-50 binary alloys AB and CD. After a diffusion anneal the assumed concentration profiles would be as indicated in Fig. 3.3b and the atomic fractions as in Fig. 3.3c. The existence of an "A controlled region" at the extremities of the diffusion zone and a "D controlled region" at the center of the couple is evident. In the spatial representation this translates into a path that points toward the A corner at its ends and is somewhat directed toward the D corner at the center in accordance with the principles dicussed before. The segments of line joining the ends of the path with the center represent the effect of the intermediate species on the path. The prediction of Kirkendall shifts is similarly done using the C_T curve.

A detailed analysis for the quaternary system could be done exploring the effect of the ratio of penetration tendencies on the Kirkendall shifts and on the shape of the path. This analysis would serve no purpose since no new concept would evolve from such a study.

Application of the LAA to the Two-Phase Case

In this section an algorithm for treating the possibility of a diffusion path crossing a two-phase field will be presented. Clearly,

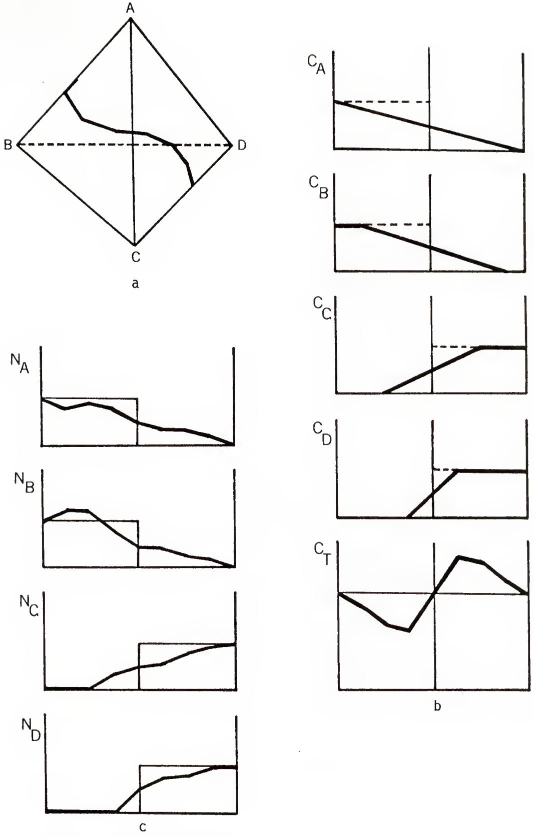

Fig. 3.3. Penetration tendency model for a quaternary couple.

the nature of the problem requires a more complex description. Although the more involved treatment will be reflected in the discussion, the simplicity of the approach is not lost. The following discussion will be restricted to the case of a planar interface.

1) Binary Two-Phase Couple

For the binary system illustrated in Fig. 3.4a, consider a diffusion couple formed by joining pure metals A and B. After a diffusion anneal, the couple will display an interface where the phases α and β are in equilibrium, with the concentrations being given by the phase diagram. In Fig. 3.4b a hypothetical situation is illustrated. The purpose of this figure is to introduce the elements involved in the analysis. For each component, say A, one can define a depth of penetration (X_A^+) and a depth of draw (X_A^-). At the interface, the concentration of each species will satisfy the equilibrium condition according to its coefficient of distribution (e.g. $N_A^\beta = k_A\, N_A^\alpha$, where $N_A^\alpha = C_A^\alpha/C_A^\alpha{+}C_B^\alpha$ and $N_A^\beta = C_A^\beta/C_A^\beta{+}C_B^\beta$ are atomic fractions). Finally the position of the interface, ξ, has to be the same for both components.

One can now write a mass balance equation for each component, as indicated in Fig. 3.4c. Using the relation

$$I + J = J + K + L \qquad (3.1)$$

one can write

$$\tfrac{1}{2}(X_i^- + \xi)(C_i^- - C_i^\alpha) = \xi(C_i^- - C_i^+) + \tfrac{1}{2}(C_i^\beta - C_i^+)(X_i^+ - \xi) \qquad (i = 1,2) \qquad (3.2)$$

from which an expression for ξ can be derived,

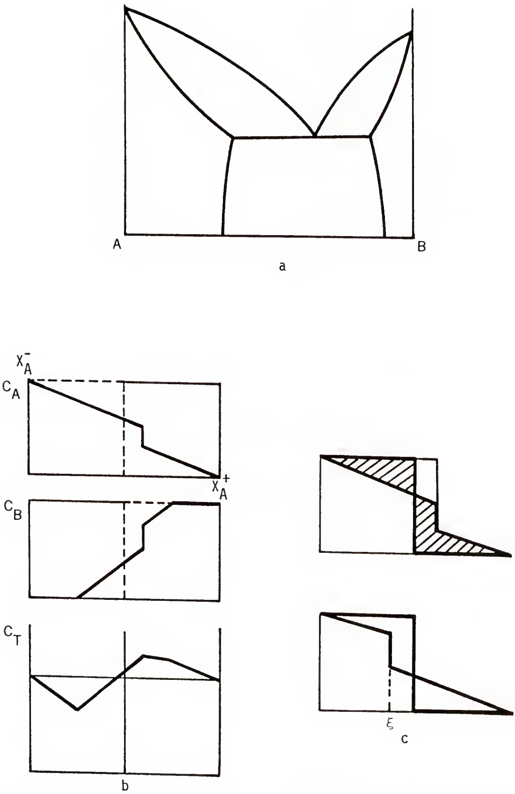

Fig. 3.4. Penetration tendency model for a binary two-phase couple displaying a planar interface.

$$\xi = \frac{X_i^+(C_i^\beta - C_i^+) + X_i^-(C_i^\alpha - C_i^-)}{(C_i^\alpha - C_i^\beta) + (C_i^- - C_i^+)} \tag{3.3}$$

yielding two equations for ξ.

Using the phase diagram information (k_A, k_B) and defining $C_T^\alpha = C_A^\alpha + C_B^\alpha$ and $C_T^\beta = C_A^\beta + C_B^\beta$ one can write

$$N_A^\beta = k_A\, N_A^\alpha \quad \therefore \quad \frac{C_A^\beta}{C_T^\beta} = k_A \frac{C_A^\alpha}{C_T^\alpha} \tag{3.4}$$

$$N_B^\beta = k_B\, N_B^\alpha \quad \therefore \quad \frac{C_B^\beta}{C_T^\beta} = k_B \frac{C_B^\alpha}{C_T^\alpha} \tag{3.5}$$

At this point, one has obtained four equations (two mass balances and two phase diagram conditions) to relate the five unknowns (C_A^α, C_A^β, C_B^α, C_B^β, and ξ). Another equation is necessary to permit solution of the problem. Because all five unknowns are related to the interface, it is convenient to look for some condition at the interface. The lack of any physical argument to suggest a better equation to the problem resulted in the arbitrary assumption that the total concentration of atoms in the α and β phases is the same at the interface. In other words,

$$C_A^\alpha + C_B^\alpha = C_A^\beta + C_B^\beta \tag{3.6}$$

as illustrated in Fig. 3.4b with a continuous curve for C_T. Although such an assumption is plausible, it is not backed by any theoretical or practical argument. Nevertheless, once the fifth equation is incorporated in the study, solutions for the problem may be obtained.

It is instructive to follow the effect of the width and location of the two-phase field on the displacement of the interface. Consider Fig. 3.5 where several situations are represented. As one can see on that figure, the position of the two-phase field with respect to the end couple compositions is one of the factors determining the direction of motion of the interface. Comparing Figs. 3.5a and 3.5b, it is concluded that the interface will move toward the side whose composition is closer to the two-phase field. The effect of the width of the two-phase field is illustrated in Figs. 3.5c and 3.5d. The wider is the two-phase field, the smaller is the interface displacement. This effect has to be observed in combination with the previous one, dealing with the position of the two-phase field. As shown in Figs. 3.5e and 3.5f, the interface does not move if the interface concentrations straddle the end compositions of the couple. Finally, in Figs. 3.5g and 3.5h, the effect of the two-phase field in reducing the total flow of the components is indicated. The Kirkendall shift, being produced by the imbalance of these flows, is expected to be reduced.

Before describing the two-phase ternary case, it is appropriate to assess the performance of the penetration tendency model. Despite the increased complexity brought about by the presence of an interface, the description of the diffusion problem using the LAA remains simple and the predictions of the theory can be understood in view of the meaningful descriptors used in the approach.

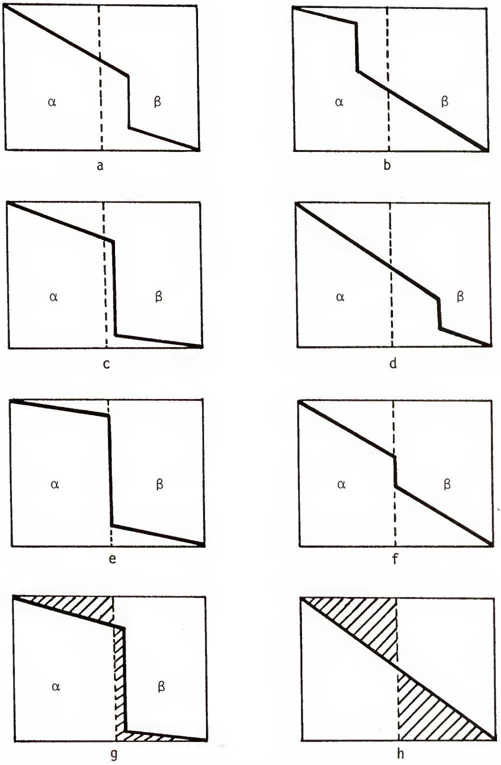

Fig. 3.5. Effect of the width and location of the two-phase field on the motion of the interface.

2) Ternary Two-Phase Couple

Consider now a ternary system presenting a two-phase field as indicated in Fig. 3.6a. If a couple is formed by joining pure A to a 50-50 BC alloy, a possible set of concentration profiles could look like that in Fig. 3.6b. As in the case of the binary system, the problem can be solved with the help of the mass balance equations and the distribution coefficients k_i (obtained from the phase diagram). The equations available for solution are three mass balance (one for each species) and three equilibrium conditions at the interface. These equations should relate seven unknowns (C_A^α, C_A^β, C_B^α, C_B^β, C_C^α, C_C^β, and ξ), so that again one has to rely on the arbitrary condition $C_T^\alpha = C_T^\beta$.

In order to exploit the pattern of Kirkendall shifts, composition paths, and interface displacements of a given system, one must first assume a model for the two-phase field. This is a very difficult task if one attempts to model an actual two-phase field. It is found in most of the cases, that the distribution coefficients k_i vary in a somewhat arbitrary manner across the two-phase field, making the modelling of the tie lines impractical. Even when the tie lines can be modeled, the solution of the problem requires that the system picks the tie line which will suit it best. This usually involves some numerical method to sort out the winner.

To gain some insight on how the different factors (penetration tendencies, location and width of two-phase field, end couple compositions) affect the pattern of Kirkendall shifts, composition paths and

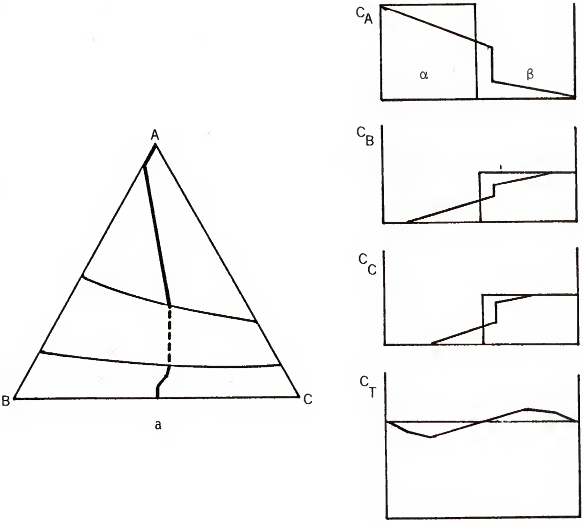

a

b

Fig. 3.6. Penetration tendency model for a ternary two-phase couple displaying a planar interface.

interface displacement, a computational model was developed (80) to explore the simplest possible case. An ideal solution model was assumed for both phases (Fig. 3.7), in which the distribution coefficients are constant across the two-phase field. By altering the location and width of the two-phase field, interchanging the order of the penetration tendencies and considering different couples in each system, a preliminary survey was completed. The results of that survey have been partially presented (81) and will be more fully reported later (80).

When exploring the effects of all of these factors on the binary and ternary two-phase systems, it was observed that, if some sets of penetration tendencies were applied to some specific two-phase fields, an anomalous result would obtain. The anomaly consisted in the displacement of the interface being larger than the penetration tendency of the slowest component. No explanation has yet been found for this phenomenon. It may be derived from the improper use of one equation (obviously $C_T^{\alpha} = C_T^{\beta}$) or from some inconsistency related to the arbitrary assignment of penetration tendencies to the components.

The anomaly observed in the preceding survey indicates that some modification is necessary in the treatment to permit fully consistency of results. It should be noticed, however, that the recognition of the problem, namely, the interface moving beyond the penetration of one species, was immediate, because of the simplicity of concepts involved. As discussed before with regard to the description of heat conduction,

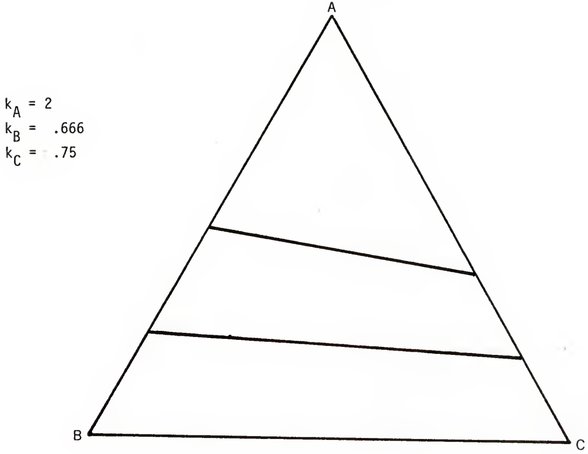

Fig. 3.7. Ternary two-phase system assuming an ideal solution model for both phases.

this possibility derives from the utilization of physically meaningful descriptors. Under these circumstances, the investigator is able to discard inconsistent results by simple inspection.

The pattern of Kirkendall shifts for the two-phase case is also affected by the anomaly, so that definite conclusions will not be advanced at this stage. On the other hand, from the very nature of the phenomenon, some qualitative principles may be established. In particular, if a series of ternary couples is investigated, analysis of the direction of the shifts reveals the relative ratio of penetration, that is, the components can be assigned a ranking of penetration tendencies (higher, medium, lower). The Kirkendall shifts will be usually directed toward the side of the couple richer in the fastest moving species (see Fig. 3.6b).

During the analysis of the penetration tendency approach for isomorphous systems (71), it was found that, except for some particular dispositions of the end couple compositions, the shifts would always follow the above principle. The exceptions would occur when the concentration of the fastest moving species A was almost the same in both ends of the couple while the intermediate species B had quite distinct contents on each side of the couple. It was understandable therefore, that the bulk flow of component B should be larger than that of component A. In those cases the shift would point toward the B-rich side of the couple. Simple intuition would lead one to the same conclusion; in a couple where the concentration of A is almost constant the Kirkendall shift will measure the difference between the fluxes of B and C. The quantitative agreement between the predicted and measured Kirkendall shifts for the system Cu-Ni-Zn (78) attested to the validity of the model.

For the two-phase case, the pattern of Kirkendall shifts derived from the LAA cannot be relied upon before the observed anomaly is completely understood. It suffices to say that the pattern derived from the LAA (80) also displayed the same principles observed in the isomorphous case. It seems reasonable then, to expect that at least qualitatively, those principles should apply in the two-phase case. In the course of this investigation these qualitative principles were used to indicate the relative penetration tendencies of the four species studied.

The prediction of composition paths for ternary systems exhibiting intervening two-phase fields requires careful consideration. As indicated earlier, a model describing the available tie lines is needed as input information. This is not a diffusion problem, but rather belongs to the field of thermodynamics. Once the two-phase configuration is satisfactorily described, it is possible, using numerical methods (47), to predict the tie line that will be chosen by the system during a semi-infinite diffusion study. The selection is, in summary, made by a trial and error technique. If one can explore the pattern of behavior of the composition path as a function of several factors pertinent to the description of the diffusion problem (end couple compositions, two-phase field width and location, etc.), there is hope that some general guidelines may result from the analysis pertaining to the shape of the path. Despite the current limitation of the penetration tendency viewpoint to address the two-phase case, it seems clear that the approach has all the capabilities to provide this global perspective, as evidenced by the results for isomorphous systems.

Under the assumption that some other condition is missing in the formulation of the problem [to substitute the condition of Eq. (3.6)], an experimental survey is under progress; it is expected that the study of experimental cases will provide a clue to some physical principle overlooked in the original treatment.

3) Quaternary Two-Phase Couple

The strategy for treating the quaternary two-phase system with the LAA is the same used in the previous cases. Four relations are provided by the mass balance condition for each species. The assumption of equilibrium at the interface yields four other equations. Again, an additional equation is needed to make possible the determination of the nine unknowns (four C_i^{α}, four C_i^{β}, and ξ).

The principles controlling the pattern of Kirkendall shifts, composition paths, and interface displacement are essentially unchanged by the inclusion of a new component. The only difference concerns the representation of the composition path, since now a tetrahedron must be used.

The visualization of the path in compositional space is a very convenient way of representing the results of a diffusion experiment.

Unfortunately, one runs out of space when systems with more than four components must be represented. The utilization of a vector space treatment could overcome this limitation. Even if the representation of the path is not extended beyond quaternary systems, all the information revealed by the path is available in the atomic fraction profiles predicted by the LAA.

Conclusions

The linear approximation approach of the penetration tendency viewpoint has been reviewed and expanded in this chapter. Extension of the approach to quaternary systems has been shown to be straightforward and indicated that the same basic principles common to binary and ternary systems apply. An algorithm was presented to treat the case of a two-phase semi-infinite diffusion couple. Although incomplete, the suggested algorithm has yielded definite insights into the effect of the location and width of the two-phase field on the motion of the interface and on the magnitude of the Kirkendall shift.

The limitation of the treatment, in its present stage, seems related to the incomplete formulation of the problem, which gives rise to anomalous results for some boundary conditions. It is hoped that experimental observation will provide the elements necessary to the theoretical breakthrough.

The anomaly does not result from the extension of the treatment to multicomponent systems, being also present in the binary case.

Accordingly, once the ideal formulation for the binary problem is found, the description of a generic n-component system will be possible. This is a consequence of the ability of the LAA to treat multicomponent systems with the same descriptors that are used in the binary case. Because of this, extension of the basic principles to higher order systems is straightforward.

The description of systems with more than four components is well within the grasp of the penetration tendency viewpoint. Although the composition paths cannot be represented in three-dimensional space, the theory may be used to predict the atomic fraction profiles in any system for which the penetration tendencies have been determined or assumed. The sequence of compositions along the diffusion zone may be obtained from the atomic fraction profiles.

In the Fickian approach, for each increase in the number of components, there is a corresponding increase in the complexity of the diffusion problem. At the same time the descriptors of the model become less meaningful and the understanding of the physical processes taking place is lost. As illustrated by Oishi's example, diffusion coefficients may be required to explain fluxes that are artifacts of the treatment of the problem.

When a model is developed, its main objective is to explain a given phenomenon. However, the validity of the model is not judged solely upon the explanation of that phenomenon, but rather on its ability to predict and explain additional phenomena, brought to test its performance.

The time has come to pass judgment on the Fickian approach as a basis for describing multicomponent diffusion.

CHAPTER 4
EXPERIMENTAL METHODS

Introduction

In the present work diffusion in the quaternary system Fe-Ni-Co-Au has been investigated. This is the first step of a project designed to experimentally test the relative penetration tendency viewpoint in systems with more than three components. The whole project includes the study of diffusion in the systems Fe-Ni-Co-Pd, Fe-Ni-Co-Cr and Fe-Ni-Co-V. With such studies it is expected that the basic types of systems will be surveyed, ranging from the simplest isomorphous case (Fe-Ni-Co-Pd at 1200°C) to some multiphase systems with metallic compounds (Fe-Ni-Co-Cr and Fe-Ni-Co-V). Due to experimental problems during the preparation of alloys of the Fe-Ni-Co-Pd system it was decided to begin the program with the system Fe-Ni-Co-Au.

Previous work in ternary systems using the relative penetration tendency concept (26,31) has been confined to isomorphous systems or isomorphous regions of multiphase systems. In those experiments the Kirkendall shifts and composition paths of selected couples were used to check the predictions of the model, which was developed in each case on the basis of the tracer diffusivities of the three elements over the corresponding region of the ternary system. This kind of investigation requires an inordinate amount of specimen preparation if tracer diffusivities are to be measured experimentally (31) over the entire ternary diagram. Evidently, the study of a quaternary system using the same strategy is not practical. The fact that in those studies of ternary systems (26,31) the pattern of Kirkendall shifts and composition paths were always consistent with the predictions of the theory, suggested the possibility of working backward. Instead of using the composition paths to check the model, they were successfully used (26) to generate models of penetration tendencies to describe the diffusion behavior in the systems Fe-Ni-Co (25), Cu-Ni-Zn (26), and Ag-Au-Cu (27).

In the present study, the lack of tracer diffusivity data suggested the utilization of Kirkendall shifts and composition paths to generate a model for the system Fe-Ni-Co-Au. However, the existence of a huge two-phase field not yet determined, together with the current limitation of the LAA for treating two-phase systems, precluded the quantitative completion of the model.

Using the experimentally measured Kirkendall shifts a qualitative model for the penetration tendencies of the four species was derived in the form of a ranking. Independent analysis of the measured composition paths yielded the same ranking of penetration tendencies. The experimental results will be presented in the next chapter.

Any attempt to describe diffusion in a two-phase system requires the knowledge of the two-phase field as a necessary input. A survey of phase diagram availability shows that most of the reported literature is concentrated in binary diagrams (82-85). Publications dealing with multiphase ternary diagrams are usually restricted to regions of the triangular isotherms. For quaternary systems the situation is even worse; most of the reported diagrams are only schematic, as is the one illustrated in Fig. 4.3.

A new technique for determining ternary multiphase diagrams using binary two-phase alloys was employed with success in this investigation. The Au-Co two-phase fields of the system Au-Ni-Co and Au-Fe-Co were determined using the above technique. The potential applicability of the method to determining quaternary two-phase fields is worth mentioning. The method and its applications are described in the Appendix.

The Fe-Ni-Co-Au System

The basic features of the Fe-Ni-Co-Au system may be inferred from the binary phase diagrams involving the constituent elements. The six corresponding diagrams (82) are shown in Fig. 4.1. Based on the available literature (86-88), an educated guess was made to predict the shape of the ternaries and quaternary diagrams at different temperatures, so that the temperature for the diffusion anneal could be selected. During the diffusion experiment it was desirable to use the highest possible temperature in order to minimize the time of anneal. On the other hand, the possibility of forming low melting point regions in the diffusion zone had to be considered.

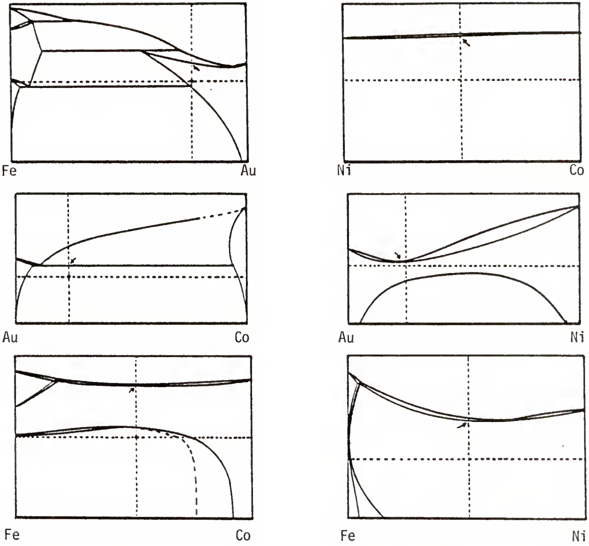

Fig. 4.1. Binary diagrams in the system Fe-Ni-Co-Au.

The presence of a minimum in the solidus curve of the Au-Ni system at 950°C suggests the possibility of a minimum inside the quaternary system at an even lower temperature. If one speculates about the range of temperatures for which all compositions are fcc, it is found that the $\alpha \to \gamma$ transformation in pure iron at 910°C places a lower limit on the temperature range of interest. It was decided then to work at a temperature of 900°C, where bcc iron is stable, and make use of the imposed restriction to obtain some information about the penetration tendencies in the bcc region of the system. In all other studies of the project, the temperature will be in a range where fcc iron is the stable phase. In the present case, out of a total of 45 couples, 14 involve the bcc phase.

A schematic view of the four ternaries and the quaternary systems at 900°C is shown in Figs. 4.2 and 4.3. Indicated in these figures by black dots are the end couple compositions of the specimens used in the investigation.

Preparation of Samples

As indicated in Figs. 4.2 and 4.3, the system Fe-Ni-Co-Au was investigated with diffusion couples formed by unary and binary alloys, selected to uniformly cover the isothermal tetrahedron with a minimum number of couples. In order to characterize more completely the pattern of Kirkendall shifts across the system, binary couples (couples situated along the binary edge of the tetrahedron) were also investigated.

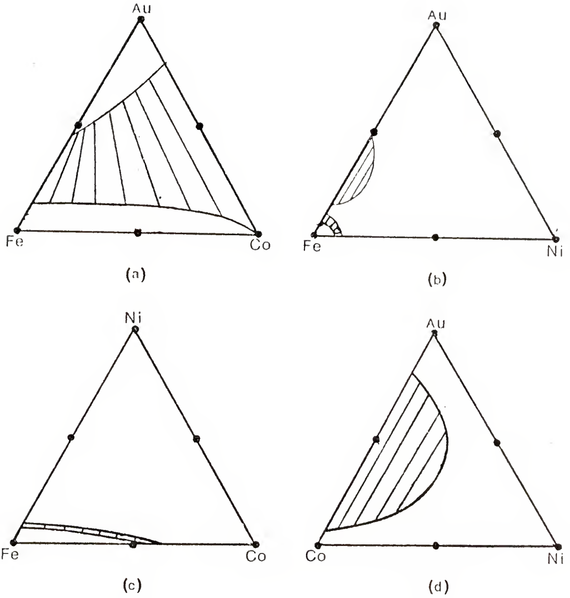

Fig. 4.2. Ternary isotherms of the Fe-Ni-Co-Au system at 900°C.

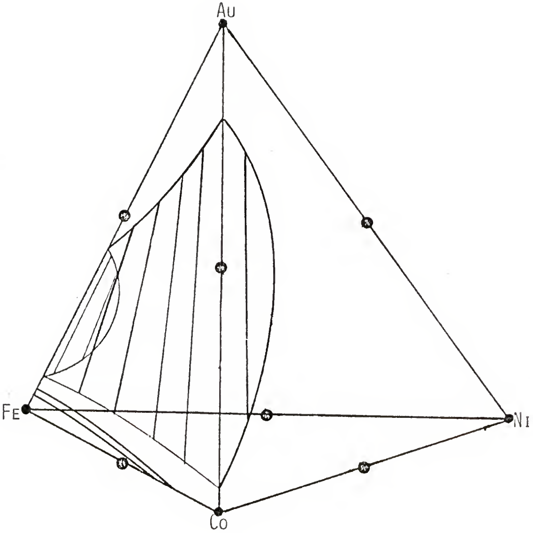

Fig. 4.3. Quaternary system Fe-Ni-Co-Au at 900°C.

Following a suggestion by Wan (26) the alloys were stacked in a sandwich-like arrangement in such a way as to produce identical adjacent interfaces. This configuration facilitates the measurement of Kirkendall shifts, making them more reliable. Some typical arrangements are illustrated in Fig. 4.4. Disks were cut and polished to produce two flat sides parallel to each other. Sandwiches were formed in one of the arrangements described previously, with some fine, inert powder dispersed between adjacent disks to act as markers. After stacking, each sandwich was pressure bonded to produce a continuous, one-piece specimen. Following the bonding operation, two flats were polished diametrally opposed to each other and the position of the markers determined on both sides. The samples were then wrapped in tantalum foils and encapsulated in quartz tubes under a helium atmosphere to minimize oxidation. The encapsulated specimens were then annealed for one week at 900°C, cooled in air to about 400°C and then quenched in cold water. The specimens were removed from the quartz tubes and cut longitudinally in a plane perpendicular to the two flats. After polishing, one half of the sample was used for interface motion measurements and metallographic studies while the other had the Kirkendall shifts measured and was analyzed with the microprobe for determination of composition paths. The above sequence of operations is illustrated in Fig. 4.5. In the following sections, each step in this experimental procedure is described in greater detail.

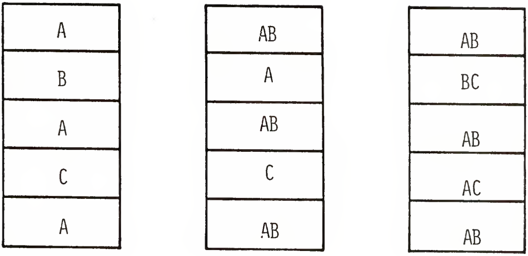

Fig. 4.4. Typical arrangement of the samples for the diffusion study.

Preparation of Alloys

The pure metals used in this investigation were purchased from Materials Research Corporation; the purity of each element is indicated in Table 4.1.

The binary alloys were prepared from these pure metals in an induction furnace, under vacuum, and to a composition approaching 50-50 atomic percent. The convection action promoted by the induction current in the molten alloy reduced the occurrence of segregation effects. After cooling, the solidified ingots (ϕ = 1/2" = 1.27 cm) were swaged to a diameter approaching 1/4" (.635 cm) and annealed under a helium atmosphere to ensure homogenization and produce large grained structures. With the exception of the Au alloys, hot swaging was necessary to prevent internal cracking of the rods. Cobalt, originally in the form of 1/2" (1.27 cm) diameter rods, was also hot swaged. After the annealing operation the rods were machined to 1/4" (.635 cm) diameter in order to remove any oxidized layer eventually formed.

The Ni-Co alloy was kindly provided by Dr. R. E. Reed-Hill from a surplus of Cribb's (89) work. The composition of the alloy was 60 at% Co.

Cutting, Polishing and Stacking

The homogenized alloy or pure metal rod of 1/4" (.635 cm) diameter was cut into disks about 1/8" (.3175 cm) in thickness on a diamond cut-off machine. Each disk was then polished through 600 grit, soft SiC grinding paper so that the two surfaces of the disk were nearly

Table 4.1
Purity of Metals Used in the Study

Metal	Grade	Purity
Fe	MARZ*	99.99
Ni	VP	99.99
Co	MARZ	99.99
Au	VP	99.99

*MARZ is a registered trademark of Materials Research Corporation.

parallel. Due to the small size of the disks, an aluminum jig was made to hold the specimen and facilitate its alignment. The dimensions of the cylindrical opening in the jig were such as to perfectly match the lateral surface of a 1/4" (.635 cm) disk. This provided a convenient way for obtaining two parallel surfaces during the polishing. The parallelism between the two faces after the final 600 polishing was checked with a micrometer to within .05°. Following the selection of alloys to form a given sandwich, polished disks of these alloys were stacked in the proper order with some fine Al_2O_3 (<50 μ) or ThO_2 (<20 μ) powder evenly dispersed between them. The whole stack was then rechecked with the micrometer to ensure that the top and the bottom surfaces were parallel. With the stack held together by the pressure of the micrometer heads, transparent tape was wrapped around the specimen to permit its handling.

Pressure Bonding

The wrapped specimen was placed between the loading rod and the head bar of a pressure bonding apparatus. To isolate the specimen a disk of tantalum foil was placed between the top surface of the specimen and the loading rod. A second disk was placed between the bottom surface and the head bar. In this way, the possibility of the specimen sticking to the apparatus after the bonding was minimized.

The bonding apparatus utilized was the same used by Wan (27,90,91), allowing control of temperature, pressure and atmosphere. After positioning the specimen, pressure was applied to the loading rod and the tape removed. A Vycor tube was then inserted, isolating the system and permitting atmosphere control. The Vycor tube was evacuated after flushing with argon and a vertical furnace raised to surround the apparatus.

The temperatures of bonding varied from 750°C to 850°C depending on the alloy involved. Specimens containing Au or Au alloy were bonded at the lower temperatures. Several specimens had to be bonded more than one time because the temperature and pressure required to bond, say, the Au/AuFe interface would be too low for the bonding of the adjacent Au/Fe interface. The pressure of two-phase interfaces increased the difficulty of the bonding operation. On the other hand, the excessive plasticity of Au prevented the use of higher pressure on those specimens containing disks of this metal. For all the other couples the temperature of bonding was around 850°C.

The bonding operation was carried out in one thermal cycle. The temperature of the furnace was steadily increased up to the bonding temperature, T_B. At this point the furnace would be turned off and allowed to cool. When the temperature was about 100°C below T_B the furnace was pulled down and the specimen left to cool down inside the evacuated Vycor tube.

Polishing and Measurement

The bonded specimens were removed from the pressure bonding apparatus and mounted in Lucite to facilitate polishing to two diametrally opposed flats as illustrated in Fig. 4.5. After polishing

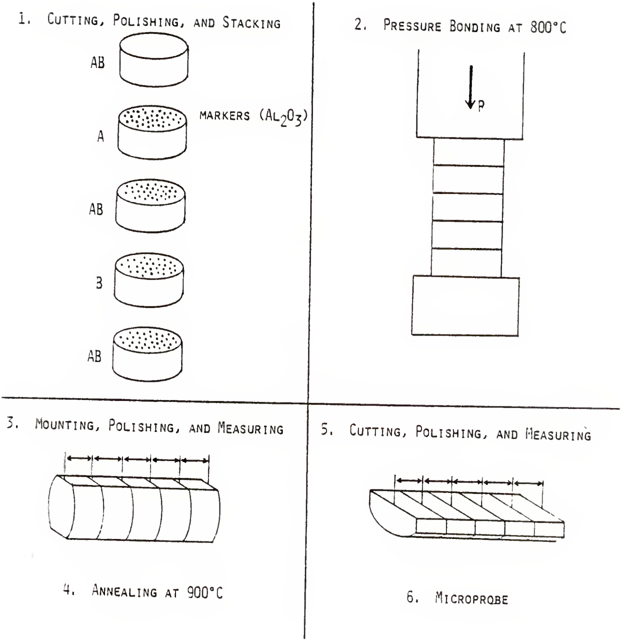
1. Cutting, Polishing, and Stacking
AB
markers (Al$_2$O$_3$)
A
AB
B
AB
2. Pressure Bonding at 800°C
P
3. Mounting, Polishing, and Measuring
4. Annealing at 900°C
5. Cutting, Polishing, and Measuring
6. Microprobe

Fig. 4.5. Sequence of operations for specimen preparation.

through 600 grit, soft SiC paper, the specimens were taken to a Unitron microscope with measuring stage. The position of the markers was measured at five different locations on each flattened side. The average of these five values was used to represent the original position of the interfaces (or markers) on each side. This precaution was necessary to check for the occurrence of buckling or creep of the specimen during the pressure bonding operation. Buckling produces non-parallel interfaces which may affect the precision of the Kirkendall shift measurement. By measuring the original markers' position at two diametrally opposed sides, the bending of the specimen could be detected and corrected for. For some Au-containing specimens, variations in the distance of markers up to 30 μ were found between the two sides. The buckling problem was later solved with the manufacture of another apparatus where the loading rod was more perfectly aligned. After the measurements were completed, the specimens were removed from the Lucite mounting and prepared for the annealing operation.

Encapsulation and Annealing

The measured specimens were wrapped in tantalum foils and encapsulated in Vycor tubes. Helium was used as inert gas and the pressure inside the tubes was set below atmospheric pressure. In this way, the pressure developed at the annealing temperature would not be enough to affect the performance of the encapsulating tube during the long anneal.

The encapsulated specimens were then annealed for one week in a Lyndberg Heavy-Duty glow-bar furnace, at a temperature of 900±1°C.

After one week the encapsulated specimens were removed from the furnace, cooled in air to about 400°C and then quenched in cold water. Although such a cooling cycle does not preserve the phases existent at 900°C, it is rapid enough to prevent diffusion processes from affecting the concentration profiles established at 900°C. On the other hand, it was feared that a very drastic quenching rate could produce some discontinuity at two-phase interfaces.

Specimens containing disks of pure Fe exhibited a considerable loss of this metal by evaporation. However, the bond at the interfaces was sound and the central part of each disk (where the measurements were concentrated) was unaffected.

Cutting and Polishing

The annealed specimens were removed from the Vycor tubes and positioned in a diamond cut-off machine in such a way as to produce a longitudinal cut whose plane was perpendicular to the two flats, as indicated in Fig. 4.5. This would permit a precise measurement of the Kirkendall shifts in any position across the section since the original position of the markers on each extremity (flat sides) had been recorded.

One half of the specimen was used to study the displacement of the interface and the resulting microstructure (80).

The other half was mounted in Lucite and polished through 600 grit, soft SiC grinding paper. Kirkendall shift measurements were then recorded for each specimen. In some cases a slight etching was necessary to reveal the position of the markers.

After the Kirkendall shifts had been measured all the specimens were repolished. This polishing was necessary to remove the etched layer of some specimens and to take them to the 5 μ diamond finish required for microprobe analysis.

Kirkendall Shift Measurements

The position of the markers was again measured in the Unitron microscope with measuring stage. For these measurements, five observations were made at each markers plane, covering 100 μ of a central region of the section. The five observations were evenly spaced 25 μ from each other along the markers plane. An average of these five values yielded the position of the interface, from which the distance between adjacent marker planes was calculated. Since these distances were measured in a central region of the specimen, to obtain the corresponding distances before the diffusion anneal, it was only necessary to average the values obtained in each flat. Thus, even for those specimens where some buckling had occurred, the original distance in the center of the specimen could be estimated.

Subtracting the original distance from the one obtained after the diffusion anneal, and dividing the result by 2, yields the Kirkendall shift.

The precision of the measurement of the Kirkendall shift varied with the kind of interface being analyzed. The standard deviation on the position of markers varied from 1 μ up to 5 μ. It can therefore be concluded that the values for the Kirkendall shift can be assigned a 95% confidence interval of roughly ±10 μ.

Microprobe Analysis

The concentration profiles were determined with an Acton Electron-Probe X-ray Microanalyzer, model MS 64. This equipment was originally a two-channel, four-detector microanalyzer with the ability to measure the intensity of two different x-ray radiations at the same time. The acquisition of a pulse height analyzer, a ratemeter, and a $[10\bar{1}\bar{1}]$ quartz crystal increased the capability of the system for simultaneous analysis of three different elements.

The x-ray intensities obtained for each component were then converted to weight and atomic percent using a version of MAGIC (Microprobe Analysis, General Intensity Corrections) developed by Colby (92). MAGIC is a batch-type computer program capable of providing a statistical evaluation of the input data as well as the calculated concentrations.

The operating conditions of the micorprobe were as follows: 20 KV accelerating voltage, 100 nA specimen current and take-off angle of 18°. The diameter of the electron beam was about 1 micron.

The characteristic lines $FeK\alpha$, $NiK\alpha$, $CoK\alpha$, and $AuL\alpha$ were used for the analysis. Elemental standards for these metals were prepared from the same rods used for production of the samples. Intensities for standards and background were determined before and after each run.

Scans along the diffusion direction were made to determine the size of the diffusion zone. Scans parallel to the marker planes were made at different distances to reveal the position of grain boundaries and to check for homogeneity of the specimens. The region for the point count measurements was selected on the basis of these preliminary scans.

A total of twenty-seven couples (twenty-four ternaries and three quaternaries) were analyzed. At least two independent concentration profiles were determined for each couple. In most of the cases small variations were observed among the profiles, although the characteristics of the composition path were essentially unchanged.

To obtain the profiles, point counts were made at 50 to 100 micron intervals at the extremities of the diffusion zone and at 5, 10, and 20 micron intervals in the center of the diffsion zone. The counts were taken at fixed time (10 seconds). At all points the counting measurements were repeated three or four times, depending on the scatter of values. At least once for each point, the focus would be readjusted and the analyzing crystals realigned to check for maximum intensity.

During the processing of data to convert the raw intensities into concentrations, several corrections have to be made (93). These include absorption, atomic number, and fluorescence effects. Each correction is affected by the composition of the region under analysis. In a diffusion couple the concentration varies along the diffusion zone, with the result that if the sample is improperly positioned, the emitted x-rays will travel through regions of different composition before reaching the detector. The corrections employed in the data reduction scheme do not recognize such a possibility and incorrect results may be obtained. It is important therefore that the specimen of a diffusion experiment be positioned in a way that allows the emitted radiation to traverse a region of roughly the same composition before reaching the detectors.

Analyses at interfaces are also subjected to three major effects (94). Two of them, absorption and fluorescence, have already been commented upon, and methods to avoid them described. The third one, spatial resolution, has to do with the fact that the volume in which primary x-rays are produced is much larger than the size of the focussed electron beam. This precludes any attempt at direct measurement of the phase boundary composition. If one considers a steep concentration profile, such as that at a phase boundary, the finite volume from which x-rays are excited would produce a "smearing" in the measured concentration profile. The measured concentration profile is then the mathematical convolution of the probe function (x-ray excitation volume) and the true concentration profile (95). If the probe function can be experimentally determined (96,97), a deconvolution technique can be used to yield the actual concentration profile (98). However, this technique is very difficult to carry out in practice. The best method for estimating interface compositions (99) is to use the known probe function and a predicted true concentration profile to calculate an expected concentration profile. By comparing this calculated profile with experimental data, the true concentration profile at the interface can be evaluated.

The determination of compositions at interfaces using the above method, although viable, requires the use of rather sophisticated computational schemes and numerical methods. This renders the method unsuited for most practical applications. Techniques for obtaining the interface composition without involving this kind of analysis should therefore be welcome. The technique described in the Appendix to determine two-phase fields in ternary isotherms accomplished this goal for the specific case of diffusion couples using two-phase alloys. By choosing an adequate number of regions of the specimen to be analyzed, the interface compositions may be obtained from the analysis of neighboring regions, where the mentioned effects can be avoided.

During a microprobe analysis, the region immediately below the surface of the specimen is essentially being analyzed; for that reason the metallographic section should be truly representative of the specimen. The use of unetched specimens, as flat and scratch-free as possible, is needed to preserve the precision of the analysis. For a wavelength dispersive spectrometer, such as the one used in this investigation, the requirement of flat specimens is still more stringent. Due to the restrictive aspect of Bragg's law, the diffracted intensities are critically affected by undulations in the sample surface.

Imprecision caused by several surface effects have been reported (100-103). It is found that the lower the take-off angle the more pronounced is the effect of surface roughness (101,102). The 18° take-off angle of the instrument used in the present study falls in that low angle category. In addition, difference in hardness between Au and Co produced surface relief in the specimens containing the AuCo two-phase alloy, even though low nap cloths and high wheel speeds were used in polishing the samples. The combination of these two effects makes the possibility of errors due to topography unavoidable. This is another limitation of methods dealing with measurements very close to interfaces, since those regions are usually the most affected by the surface relief. Nonetheless, the results obtained with the proposed technique were reproducible for different couples despite the collection of adverse factors. The redetermination of the phase boundaries of a known system should provide the definitive test about the validity of the technique.

Presence of porosity and, in some cases, cracks in the diffusion zone obviously affect the analytical precision. In each case, the region under analysis was well removed from those locations. It is not believed that the analysis of the diffusion behavior has been significantly affected by either factor.

Conclusions

The experimental methods employed in this investigation have been described. The role of this study as a partial accomplishment of a much broader project dealing with multicomponent diffusion was indicated.

The qualitative nature of the conclusions to be derived from the Kirkendall shift measurements mitigated the need for a more detailed analysis on the effect of porosity on the measured shift. Study of this porosity (104,105) can be helpful in cases where the predictions of the theory are to be compared with experimental results.

The description of the microprobe analysis was more complete in order to provide a background to the introduction of the new technique for determination of multiphase equilibrium diagrams in ternary systems, which is considered a definite contribution from this investigation.

The experimental results and their discussion will be presented in the next chapter.

CHAPTER 5
EXPERIMENTAL RESULTS AND DISCUSSION

Introduction

The penetration tendency viewpoint was used in this investigation to derive some qualitative conclusions with regard to the penetration tendencies of the species forming the quaternary system Fe-Ni-Co-Au. The Kirkendall shifts and composition paths will be presented in this chapter. Analysis of the pattern of shifts will be used to generate a ranking of penetration tendencies. An independent analysis of the composition paths will confirm the validity of the derived ranking. The results and discussion for each case will be presented separately.

Kirkendall Shifts

The Kirkendall shifts for all the couples investigated are presented in Table 5.1, along with some comments describing the nature of the couple involved. The annealing time for each couple is also indicated. In order to provide a uniform basis for comparison, the shifts were corrected to a reference annealing time of one week (168 hrs.). However, no attempt was made in this investigation to explain these values quantitatively: attention was focussed on the direction of the shift. The disposition of the end couple compositions in

Table 5.1
Kirkendall Shifts in the System Fe-Ni-Co-Au

#	COUPLE LEFT	 SHIFT*	 RIGHT	Annealing time at 900°C (hrs)	COMMENTS
	BINARY (TYPE A/B):				
1	Fe	80	Co	168	BCC-FCC couple
2	Fe	52	Ni	168	BCC-FCC couple
3	Co	11	Ni	170	Single phase (FCC)
4	Au	214	Ni	168	Lowest solidus curve
5	Au	19	Co	187	Composition crosses two-phase field (FCC-FCC)
6	Fe	74	Au	-	Crosses two two-phase fields (BCC-FCC-FCC)
	BINARY (TYPE/A AB):				
7	Fe	26	FeNi	192	BCC-FCC couple
8	FeNi	13	Ni	192	Single phase (FCC)
9	Co	45	NiCo	235	Single phase (FCC)
10	NiCo	81	Ni	235	Single phase (FCC)
11	FeCo	54	Co	185	BCC-FCC couple
12	Fe	27	FeCo	185	Single phase (BCC)
13	Fe	96	FeAu	169	Crosses two two-phase fields (BCC-FCC-FCC)
14	FeAu	188	Au	169	Single phase (FCC)
15	NiAu	44	Ni	262	Single phase (FCC)
16	Au	72	NiAu	262	Single phase (FCC)
17	CoAu	21	Co	187	End point is in two-phase field (FCC-FCC)
18	Au	-	CoAu	-	Couple not measured
	QUATERNARY (TYPE AB/CD):				
19	FeNi	76	CoAu	171	Endpoint is in two-phase field (FCC-FCC)
20	NiAu	19	FeCo	187	May cross two two-phase fields (BCC-FCC-FCC+FCC)
21	FeAu	38	NiCo	169	May cross two-phase field (FCC-FCC+FCC)

continued

Table 5.1 - continued.

#	COUPLE LEFT	 SHIFT*	 RIGHT	Annealing time at 900°C (hrs)	COMMENTS
	TERNARY (Fe-Ni-Co):				
22	FeNi	8	Co	188	Single phase (FCC)
23	FeCo	7	Ni	311	Crosses two-phase field (BCC-FCC)
24	Fe	9	NiCo	168	Crosses two-phase field (BCC-FCC)
25	FeCo	13	NiCo	311	Crosses two-phase field (BCC-FCC)
26	FeNi	2	NiCo	168	Single phase (FCC)
27	FeCo	2	FeNi	188	Crosses two-phase field (BCC-FCC)
	TERNARY (Fe-Ni-Au):				
28	FeAu	54	NiAu	167	Single phase (FCC)
29	FeAu	22	FeNi	168	Crosses two-phase field (FCC-FCC)
30	NiAu	19	FeNi	167	NiAu is the high mobility end; single phase (FCC)
31	Au	99	FeNi	168	Single phase
32	FeAu	54	Ni	167	Single phase (FCC)
33	Fe	168	NiAu	167	Crosses two-phase field (BCC-FCC)
	TERNARY (Ni-Co-Au):				
34	CoAu	51	NiAu	216	End point is in two-phase field
35	CoAu	69	NiCo	168	End point is in two-phase field
36	NiAu	4	NiCo	169	Crosses two-phase field (FCC-FCC)
37	Au	79	NiCo	169	Crosses two-phase field (FCC-FCC)
38	CoAu	102	Ni	168	End point is in two-phase field
39	NiAu	64	Co	216	Crosses two-phase field

continued

Table 5.1 - continued.

#	LEFT	SHIFT*	RIGHT	Annealing time at 900°C (hrs)	COMMENTS
		TERNARY (Fe-Co-Au):			
40	FeAu	38	FeCo	168	Crosses two-phase field (FCC+BCC)
41	FeAu	54	CoAu	168	End point is in two-phase field (FCC+FCC)
42	FeCo	88	CoAu	276	End point is in two-phase field (FCC+FCC)
43	FeAu	75	Co	168	Crosses two two-phase fields (FCC-BCC-FCC)
44	Au	43	FeCo	276	Crosses three-phase field (BCC-FCC-FCC)
45	Fe	174	CoAu	168	End point in two-phase field (FCC+FCC), crosses two-phase field (BCC+FCC) and three-phase field (FCC+BCC+FCC)

---

*Shifts presented are in μm, corrected to a reference annealing time of 1 week (168 hrs). All shifts are to the left.

Table 5.1 follows the convention that the measured shift is always directed to the left. Four types of couples may be recognized, and each type will be discussed separately.

1. Binary Couples (Type A/B)

The results for these couples are shown in lines 1 to 6 of Table 5.1 and illustrated in Fig. 5.1. The arrows in that figure are located midway between the end compositions of each couple and indicate the direction of the Kirkendall shifts. The length of each arrow is proportional to the magnitude of the shift.

Consider the couples involving Fe. All shifts for these couples point toward Fe. In terms of the penetration tendency viewpoint, this suggests that Fe is the fastest moving component.

Next consider the couples having Ni as one end point. It is found that all shifts move away from the Ni corner. Accordingly, Ni is assigned the lowest ranking of penetration tendency among these metals.

To decide between Au and Co one observes that in all couples containing Au, except those with Fe, the shift points toward Au. Also, the only couple in which Co is the winning end is that against Ni.

With this piece of information one can suggest a preliminary ranking of the tetrahedron, namely, Fe>Au>Co>Ni.

Previous works (25,26) on the systems Fe-Ni-Co had already indicated the sequence Fe>Co≥Ni for diffusivities (25) and penetration tendencies (26) in a temperature range where Fe was fcc. The

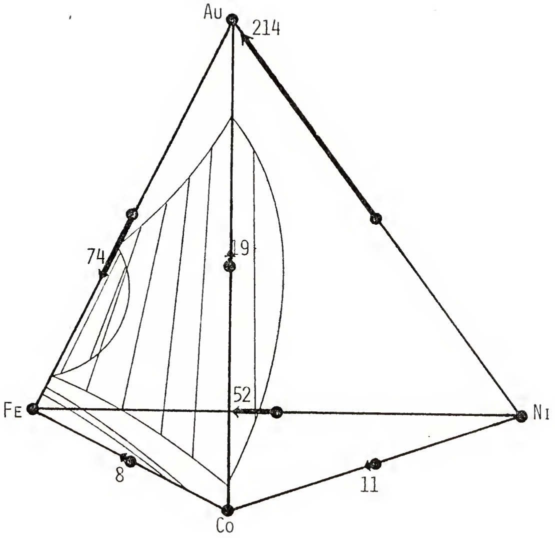

Fig. 5.1. Pattern of Kirkendall shifts in couples of type A/B.

temperature used in this investigation (900°C) produced bcc Fe. It is generally accepted that the more open bcc structure should permit larger diffusivities, so that the observation that Fe out penetrates Ni and Co at 900°C is not surprising. On the other hand, it is not obvious why Fe penetrates further than Au. If one considers the melting points of the two metals it would be logical to select Au as the larger penetrator. However, this result does not constitute an exception. The above mentioned work in the Fe-Ni-Co (26) system had produced similar results, showing that the relative penetration tendencies do not necessarily line up according to the respective melting points.

2. Binary Couples (Type A/AB)

Lines 7 to 18 in Table 5.1 and Fig. 5.2 illustrate the results for these couples. Observe that again Fe is the fastest moving species, as indicated by the direction of arrows in Fig. 5.2. One important result is revealed by couple Au/AuFe. One can see that the direction of the shift is toward the AuFe alloy, even though the fcc structure is the prevalent structure in both sides of the couple. This is an indication that Fe out penetrates Au in the face centered structure, as well as in bcc lattices.

The order of penetration tendencies is not altered with respect to the other components. Analysis of the AuCo/Co couple shows that Au is faster. The couple AuCo/Au was not measured because the sample broke apart after the annealing, due to the fragility of the bond at the welded interface.

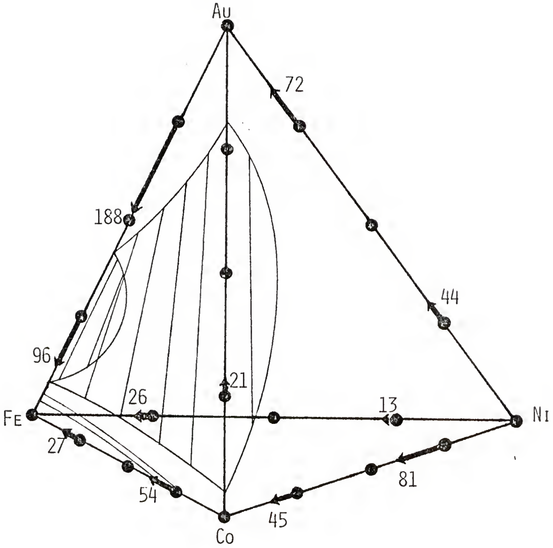

Fig. 5.2. Pattern of Kirkendall shifts in couples of type A/AB.

From the couples Co/NiCo and NiCo/Ni, one concludes that Ni is the slowest moving species. The pattern of shifts along the other edges, namely Fe→Co, Fe→Ni, and Au→Ni, is consistent with the qualitative ranking suggested before. The fact that the magnitude of the shifts along the Fe→Ni edge are the smallest among all the others may appear contradictory since those couples involve the elements with highest and lowest ranking, respectively. This is not the case. The magnitude of the Kirkendall shift is proportional to the imbalance in the total flow of atoms. It depends, therefore, on the total flow of each species, as well as on the difference between those flows. If the depth of penetration of both metals is small, the total flow for each species is also small and the resulting shift, being the difference between two small quantities,will be small. On the other hand, if the depth of penetration for both species is large, the shift will be proportional to the difference between two large quantities. One can, therefore, expect a large shift even if the relative penetration tendencies of the elements are not very different. As will be shown in the next section, the depth of penetration for the couples involving Fe, Ni, and Co are much smaller than for those couples involving pure Au or Au alloys. This explains the seemingly strange observation that the shifts for couples containing Au are usually larger. It should also be pointed out that when the penetration tendencies are concentration dependent, the total flow for both components may be reduced. Couples in which Au is present in only one side display this effect.

3. Ternary Couples (Types A/BC or AB/AC)

Figure 5.3 and lines 22 to 45 in Table 5.1 show the pattern of measured shifts for these types of couples. As indicated there, it is convenient to describe each ternary separately.

The Fe-Ni-Co system (lines 22 to 27, Fig. 5.3c) has all shifts pointing in directions compatible with the ranking Fe>Co>Ni. It is evident from the values on that table that the direction of some shifts could be reversed if one considers the imprecision on the measurements (95% confidence interval of ±10 μ). However, there are strong reasons to believe that the directions of the Kirkendall shifts for those couples are as indicated. First, work on the Fe-Ni-Co system (26) at a higher temperature (1200°C) definitively established Fe as the fastest moving component, while suggesting that Ni and Co have about the same penetration tendency. Second and more importantly, the analysis of the pattern of shifts, together with the results from binary couples, shows consistency between the measured shifts and the predictions of the model. In any event, it is clear that a longer diffusion anneal at this temperature (900°C) is necessary if quantitative conclusions are to be derived from measured shifts in ternary couples of the system Fe-Ni-Co.

The results for the Fe-Ni-Au system (lines 28 to 33, Fig. 5.3b) indicate that the penetration tendencies are in the order Au>Fe>Ni. This conclusion is derived from the couple AuNi/FeNi, in which Fe and Au are in competition and the shift is toward the Au/Ni side. Although

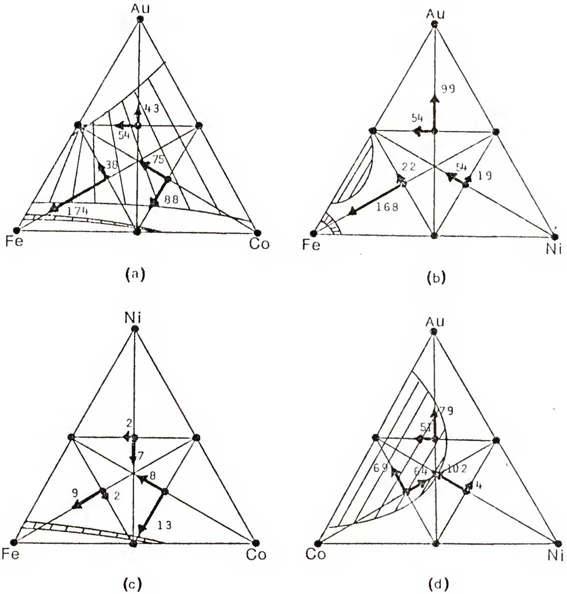

(a)

(b)

(c)

(d)

Fig. 5.3. Pattern of Kirkendall shifts for the ternary couples. (a) Fe-Co-Au; (b) Fe-Ni-Au; (c) Fe-Co-Ni; (d) Co-Ni-Au.

this result contradicts the suggested preliminary ranking, it is possible to recognize its origin. Looking back at the binary phase diagrams, Fig. 4.1, one can see that for an annealing temperature of 900°C, the 50-50 AuNi alloy is very close to its melting point while the FeNi alloy is more than 400°C below its solidus curve. This could result in an increase in the penetration tendencies of all components on the AuNi side of the couple and somehow favor a larger flow of Au from AuNi to FeNi than the opposite flow of Fe. It seems doubtful, however, that one can explain the above result using the simplified picture provided by the LAA. A more sophisticated model of the relative penetration tendency may be necessary to provide the desired explanation.

Analysis of the couple Fe/AuNi offers additional evidence for the contention that Fe is the fastest penetrator. In that couple, the shift points toward the Fe side, despite the high diffusivity condition in the AuNi alloy. Unfortunately, in this particular couple Fe is present in the bcc form, raising the possibility that the body centered structure is the cause of the larger penetration of Fe. From the couple AuFe/AuNi, in which Fe is in the fcc form, the fact that the shift points toward Fe is of no help in resolving the dilemma; although the AuNi alloy has been identified with high penetration tendencies, the Fe is competing with Ni, not with Au, in that particular couple.

The results for the ternary couples of the system Ni-Co-Au (lines 34 to 39, Fig. 5.3d) support the ranking of penetrations Au>Co>Ni, as evidenced by the arrows in Fig. 5.3d. In all cases the shifts point toward the Au-rich side and away from the Ni-rich side of the couple. The very small value for the shift of the couple AuNi-NiCo is also within the statistical range where the direction of the shift could be reversed. It does not seem viable that such a reversal could in fact occur, mainly because in this case Au is competing with Co, one of its habitual losses. It is also possible that the intervening two-phase field could be responsible for the reduced Kirkendall shift.

Analysis of the system Fe-Co-Au (lines 40 to 45, Fig. 5.3a) will provide the elements for the decisive conclusion about the validity of the preliminary ranking. The natural choice for starting the discussion is couple FeCo/CoAu where Fe and Au are brought into competition. Once more, Fe emerges as the highest penetrator. Once more, however, the couple used to sort out the pattern has Fe in the bcc form. In those couples in which each of these metals compete against Co, this last metal comes out a loser (FeAu/FeCo and FeAu/CoAu). This clearly establishes Co as the slowest penetrator in this system. Couples Au/FeCo and Fe/AuCo have shifts directed toward Au and Fe respectively. This suggests that the combined flows of Fe and Co in the first couple do not match the total flow of Au in the opposite direction. The same is true with respect to the couple Fe/AuCo. Fe alone can handle the combined fluxes of Au and Co. When Au and Fe together go against Co in the couple AuFe/Co, the resulting shift is directed to their side of the couple, in agreement with the predictions of the model.

4. Quaternary Couples (Type AB/CD)

It is encouraging that one can extend the same relative penetration tendency ranking to quaternary systems. The results for these couples are illustrated in lines 19 to 21 of Table 5.1 and Fig. 5.4. The binary nature of the end couple compositions prevents any direct comparison among the penetration tendencies of the metals. However, if a ranking for these four elements is assumed, one can qualitatively infer the direction of the shift and explore whether some observed shift contradicts the prediction of the theory.

Starting with the couple FeAu/NiCo, one can see that the shift pointing toward the FeAu side supports the assumption that Fe and Au penetrate more than Ni and Co do.

The result for couple NiAu/FeCo, with the shift pointing toward the NiAu side, is consistent with earlier discussions. The higher penetration of all components in the AuNi region is to be expected due to the proximity of the annealing temperature to the solidus curve for the 50-50 NiAu alloy. Observe that in this particular couple the shift is away from the Fe-rich side despite the bcc structure displayed by the FeCo alloy.

Consider now couple FeNi/CoAu. The shift is directed to the FeNi side supporting the assumption that Fe is the fastest moving species. In this couple Fe is in the same form (fcc) in which it lost to the AuNi alloy. In other words, if one takes into account the peculiarity of the AuNi alloy, it is verified that the only two couples in which

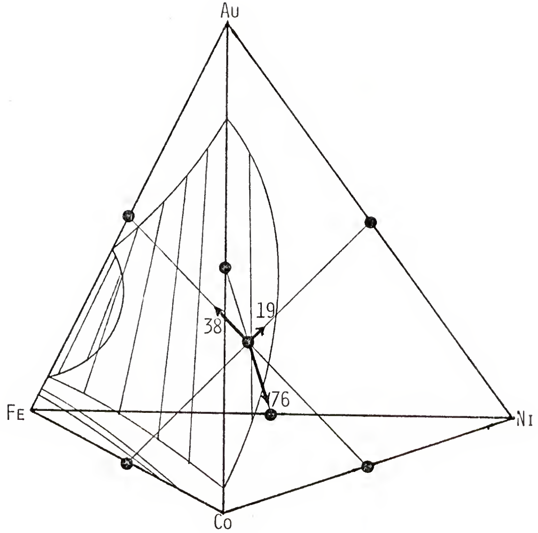

Fig. 5.4. Pattern of Kirkendall shifts in couples of type AB/CD.

the shift was directed away from Fe, that particular alloy was involved. In all other cases, the shift pointed toward the Fe-rich side of the couple, regardless of which metal or alloy was on the other side.

Results and Discussions of Composition Paths

In order to obtain the composition paths, atomic percent concentration profiles were obtained with the microprobe. From these profiles the composition paths were derived and will be presented in this section. The pertinent phase diagrams for the ternaries and quaternary isotherms were not available other than in schematic form. While this does not affect the study of the Fe-Ni-Co and Fe-Ni-Au systems, it strongly limits the analysis of the systems Au-Ni-Co and Au-Fe-Co, even in a qualitative way. For this reason, part of this study was devoted to the determination of the ternary sections of the systems Au-Ni-Co and Au-Fe-Co using the technique described in the Appendix.

For the Au-Fe-Co system, only that part of the diagram comprising the AuCo two-phase field was determined. In the phase diagrams for this system, presented below, the other two-phase fields and three-phase reactions were speculatively estimated.

The discussion in this section will also be aimed at deriving an independent ranking of penetration tendencies for the elements of the system Fe-Ni-Co-Au. As was done before, the discussion will be divided into parts, exploring each subsystem individually.

1. Ternary System Fe-Ni-Co

The concentration profiles for the couples in the system Fe-Ni-Co are shown in Figs. 5.5a to f. In those figures the origin of the distance axis is the location of the two-phase interface. For isomorphous couples the origin represents the Kirkendall markers plane. If the profiles were to be used in a Matano analysis of diffusion coefficient determination, the choice of a single consistent criterion for determining the origin would be required. However, in the present case, the shape of the composition path was the only information sought. Therefore, the microprobe analysis was done on the polished specimens without fiducial marks to locate any particular plane. The initial scan along the diffusion direction yielded the location of the two-phase interface. For isomorphous couples the markers could usually be located in the unetched condition. Thus, the samples did not have to be etched for marker identification and repolished for the microprobe analysis, speeding up considerably the handling of the samples.

For each couple the concentration profile was determined twice in different positions along the bonded interface. Only one set of values is illustrated in Fig. 5.5.

Consider first the couples of the type A/BC, Figs. 5.5a to c. The profiles have the familiar shape, with the exception of couple FeNi/Co, which presents a plateau in composition from about zero to five microns. This suggests that during the cooling process of the couple, some intermediate phase nucleated and grew, producing the above mentioned

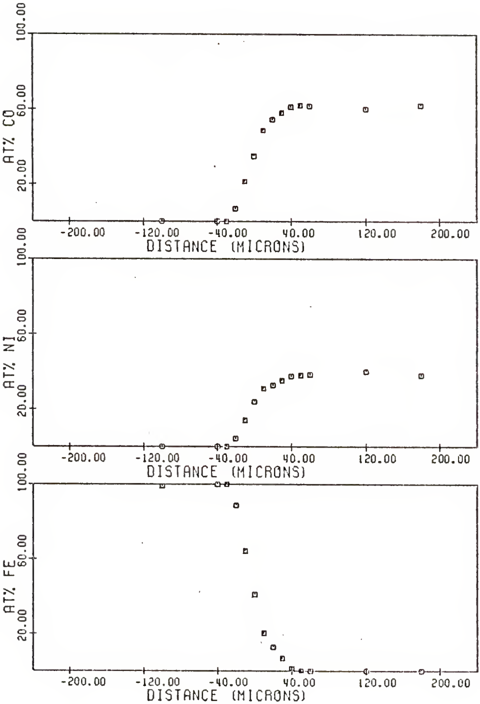

Fig. 5.5a. Concentration profile for couple Fe/NiCo.

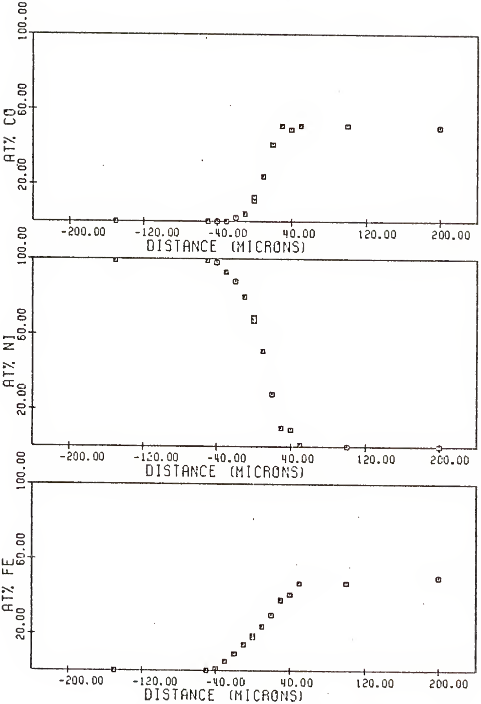

Fig. 5.5b. Concentration profile for couple Ni/FeCo.

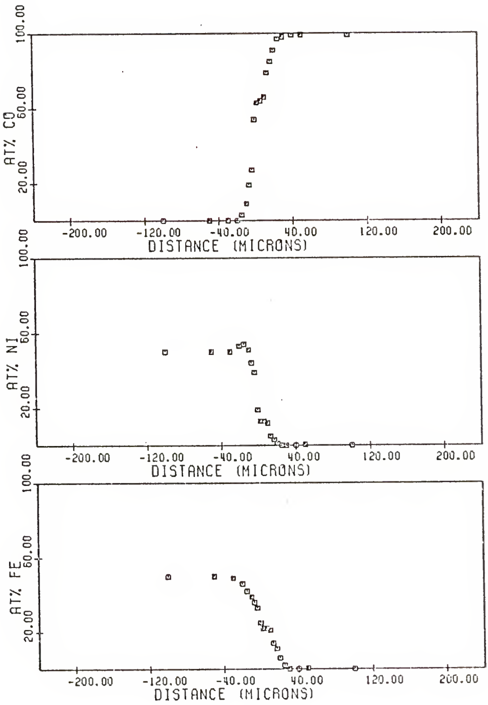

Fig. 5.5c. Concentration profile for couple FeNi/Co.

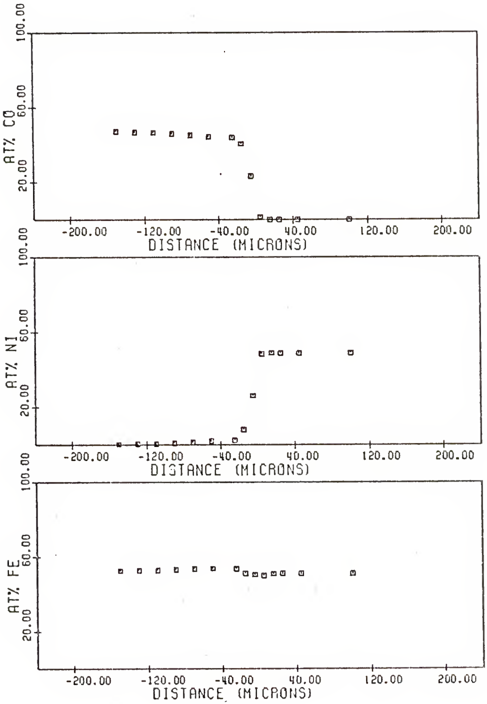

Fig. 5.5d. Concentration profile for couple FeCo/FeNi.

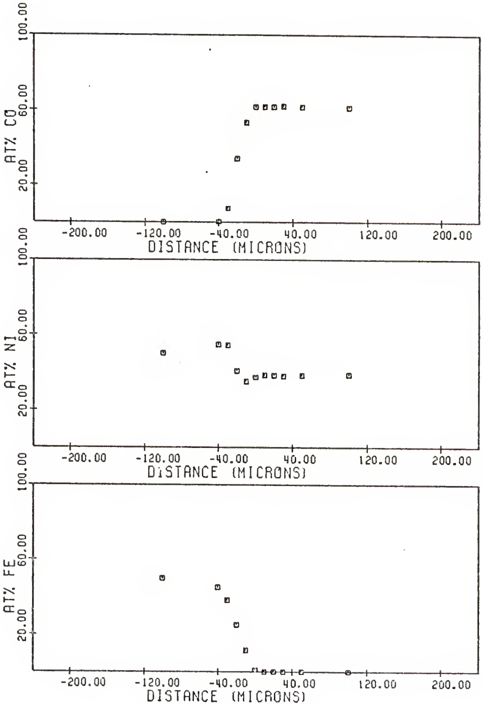

Fig. 5.5e. Concentration profile for couple FeNi/NiCo.

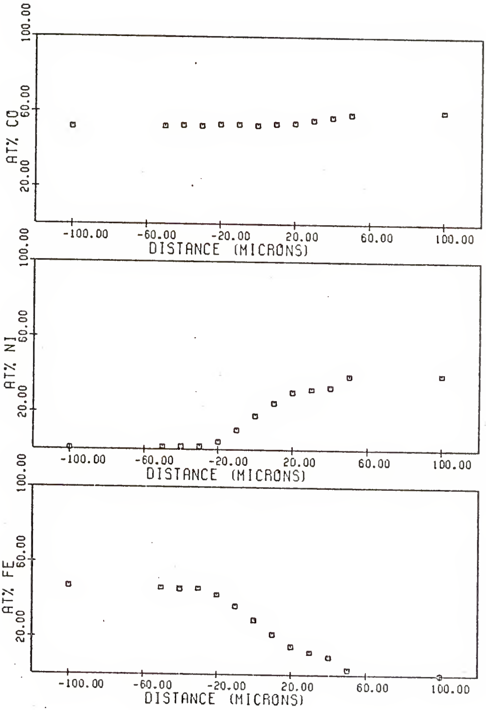

Fig. 5.5f. Concentration profile for couple FeCo/NiCo.

distortion of the concentration profile. In the composition path, this region of constant composition is projected as a single point.

For couples of the type AB/AB (Figs. 5.5d to f) the profiles are well behaved, and the conditions for diffusion with no initial concentration gradient are displayed. Consider first the FeCo/FeNi couple where the Fe concentration is initially the same on both sides of the couple (Fig. 5.5d). Due to the imbalance of fluxes between Co and Ni, the fractional concentration of Fe increases slightly on the Co-rich side and decreases on the other side. For couple FeCo/NiCo, the same reasoning suggests an undulation in the distribution of Co. However, the concentration of Co was not uniform at the beginning of the anneal (the NiCo alloy was 60 at% Co), making the detection of that effect impractical. On the other hand, the couple FeNi/NiCo displays beautifully the imbalance between the flows of Fe and Co (see Fig. 5.5c) in the form of an increase in its fractional concentration on the side that lost Fe, and a decrease on the side in which Fe penetrated. In the composition path, such undulation is revealed by the characteristic S-shaped path (Fig. 5.6).

Analysis of the diffusion paths in Fig. 5.6 permits the assignment of a ranking to the three elements. Consider first the couple FeNi/NiCo. The ends of the path point toward Fe. Consider now couple FeCo/NiCo. Again the ends point toward Fe. This suggests that Fe is the fastest moving species. From couple FeNi/FeCo, one concludes that Co out penetrates Ni. Analysis of the other paths in the system

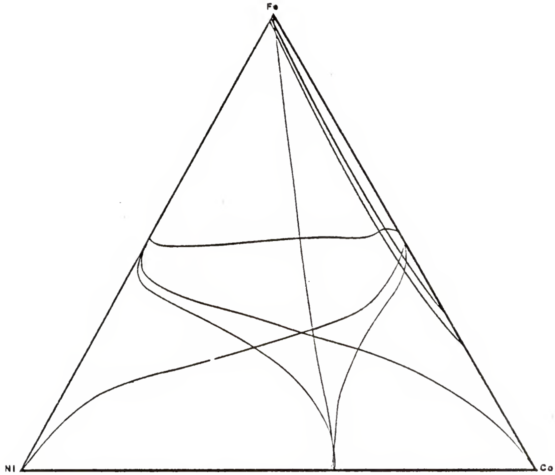

Fig. 5.6. Composition paths in the system Fe-Ni-Co.

supports the contention that the three elements have penetration tendencies in the decreasing order Fe, Ni and Co.

2. Ternary System Fe-Ni-Au

The concentration profiles for this system are illustrated in Figs. 5.7a to f. The asymmetry of the concentration profiles is evident in all couples of the system in which Au is present only in one side. This enhanced penetration depth in the Au-rich side of the couples is described by the concentration dependent case of the penetration tendency model.

Consider the couples of the type A/BC, illustrated in Figs. 5.7a to c. The theory predicts that due to the concentration dependency of the penetration tendencies, the crossover points of the composition paths will be shifted from the center of the path. The direction of the crossover shift indicates the region of the couple where the penetrations are larger. Examine the composition paths for the couples Fe/AuNi, Au/FeNi and Ni/AuFe in Fig. 5.8; the crossover shift is directed to the Au-rich side in all three couples, as predicted.

The same reasoning can be applied to the couples of type AB/AC. The direction of the crossover shift for couples AuFe/FeNi and FeNi/AuNi is toward the Au-rich side of the couple. For the couple AuFe/AuNi, the shift is directed toward AuFe. From the corresponding concentration profile (Fig. 5.7e), one cannot infer what side has larger penetration depths. Observe that the concentration gradients for Fe and Ni in Fig. 5.7e are almost linear, with a slight indication of higher

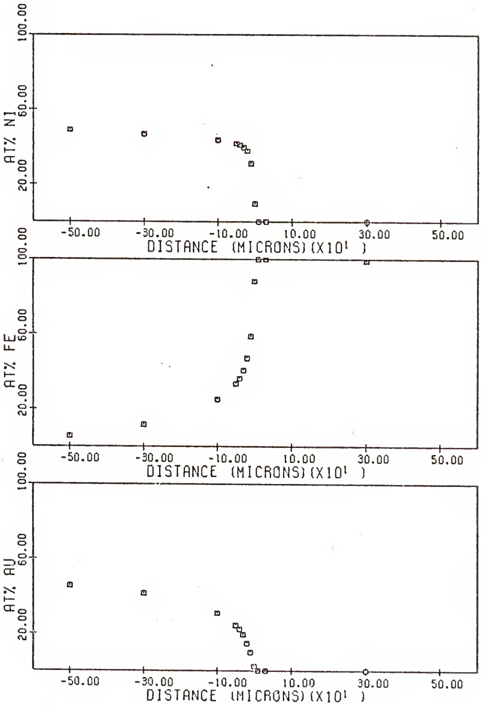

Fig. 5.7a. Concentration profile for couple AuNi/Fe.

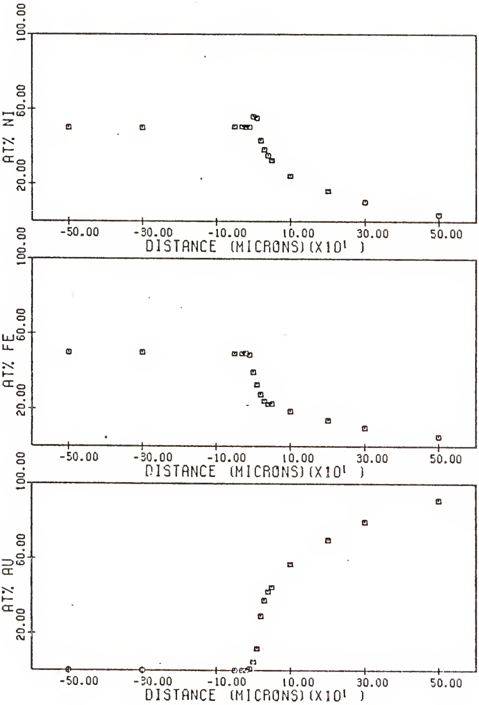

Fig. 5.7b. Concentration profile for couple FeNi/Au.

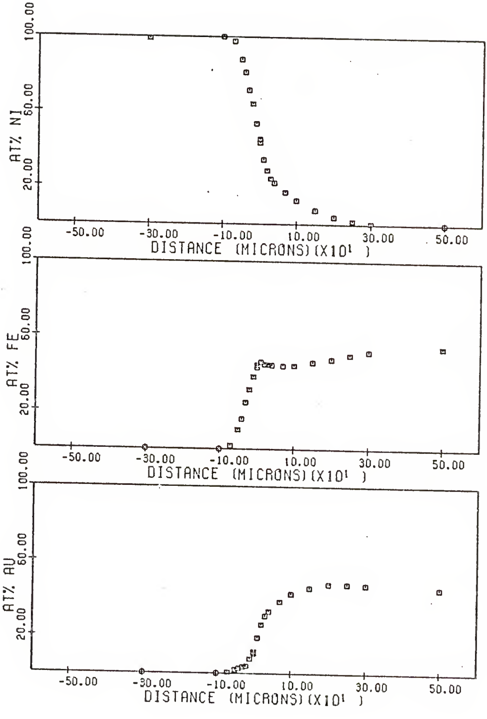

Fig. 5.7c. Concentration profile for couple Ni/AuFe.

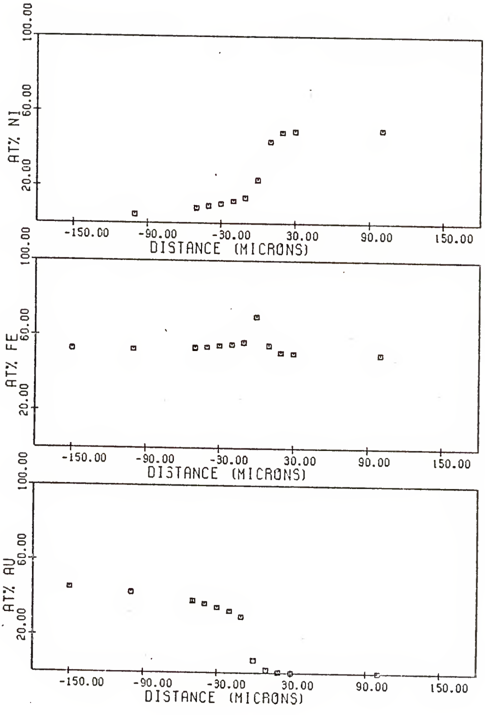

Fig. 5.7d. Concentration profile for couple AuFe/FeNi.

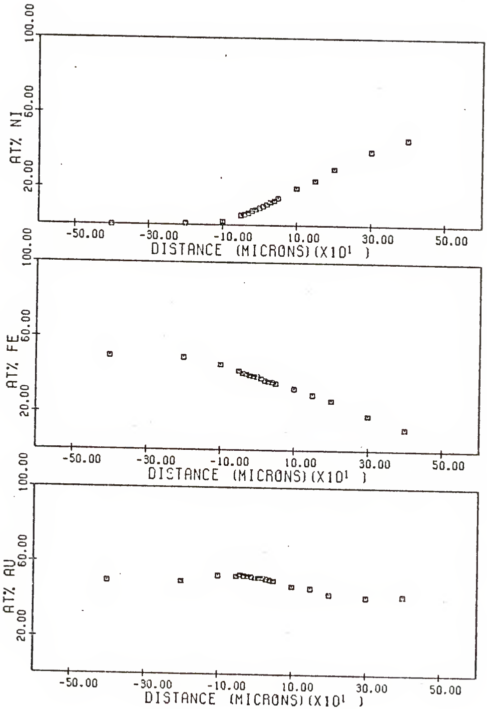

Fig. 5.7e. Concentration profile for couple AuFe/AuNi.

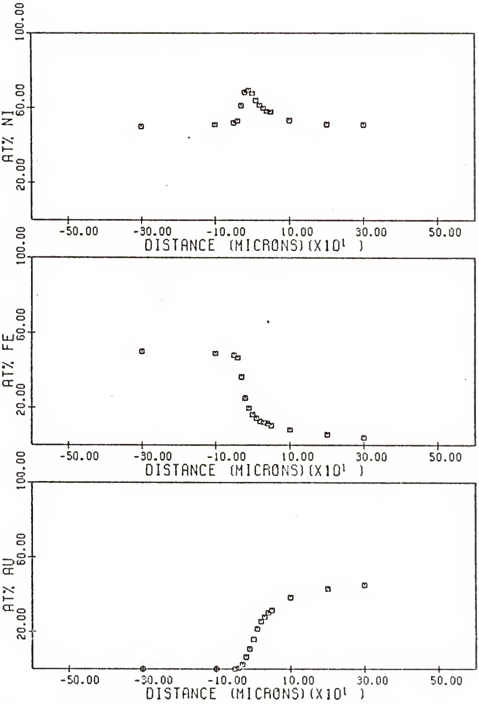

Fig. 5.7f. Concentration profile for couple FeNi/AuNi.

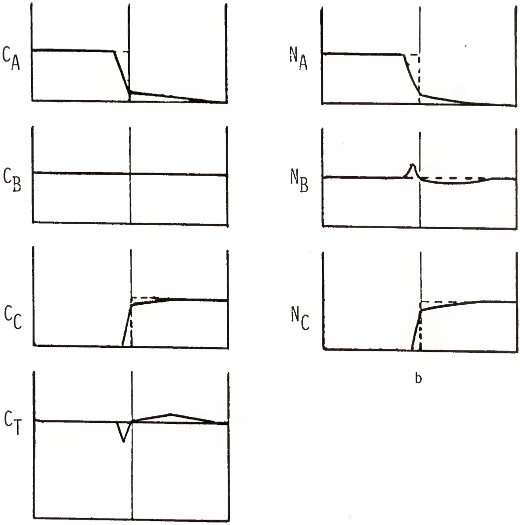

b

a

Fig. 5.7g. Penetration tendency model for couple FeNi/AuNi.

penetration favoring the AuFe side in agreement with the crossover shift. The analysis of this curve should be made having in mind the fact that the penetration depths can be inferred from the slope of the concentration profiles and from distances on those profiles measured from the Matano interface. The origin of the distance axis in Fig. 5.7e is clearly located to the left (about 200 μ) of the Matano interface, and should not be used, in this case, to compare penetration depths. Looking at the Fe profile at a grazing angle, one can detect that the upper part of the profile (FeAu side) is slightly less steep than that on the AuNi side.

The imbalance in the fluxes of Fe and Ni in Co is also illustrated in the concentration profile for Au in Fig. 5.7e. From Fig. 5.7d, the crossing of the two-phase field produced a peculiar profile for Fe in the couple AuFe/FeNi but no explanation is suggested at this point. For the couple FeNi/AuNi (Fig. 5.7f), the unusual Ni profile can be rationalized using the penetration tendency viewpoint.

Consider the penetration tendency model indicated in Fig. 5.7g, in which it is assumed that the penetration tendencies are in the order A>B>C, and concentration dependent, If, after diffusion, the concentration profiles are those indicated at the left of that figure, the resulting atomic fractions are as indicated on the right of Fig. 5.7g. Compare those profiles with Fig. 5.7f.

Analysis of the paths for the system Fe-Ni-Au (Fig. 5.8) suggests: 1) Fe is the fastest penetrator, derived from couples FeNi/AuNi (giving

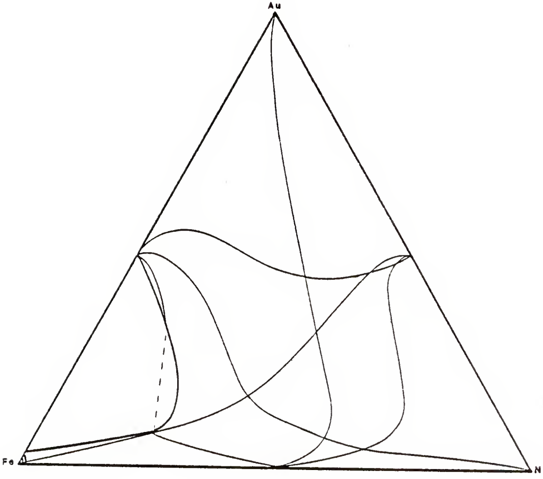

Fig. 5.8. Composition paths in the system Fe-Ni-Au.

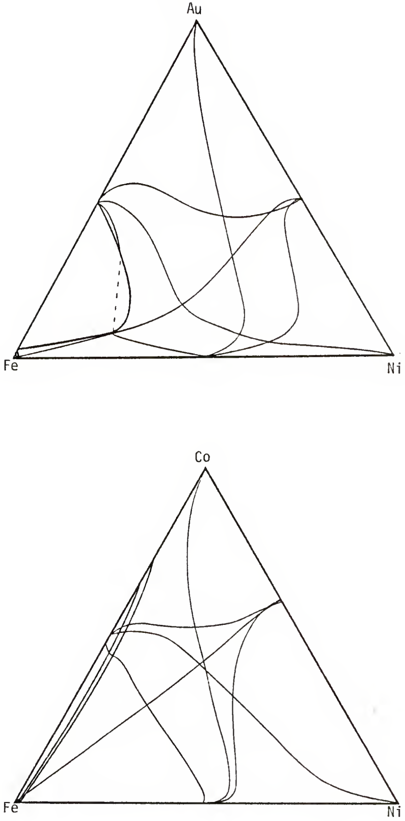

Fig. 5.9. Comparison of paths in the systems Fe-Ni-Co and Fe-Ni-Au.

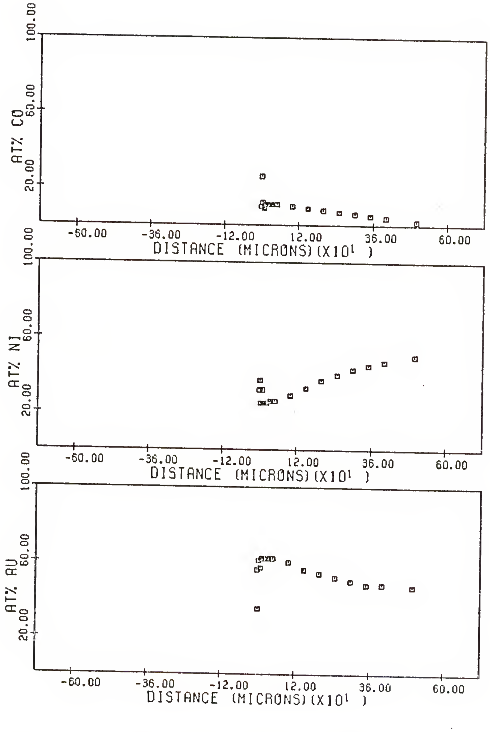

Fig. 5.10a. Concentration profile for couple AuCo/AuNi.

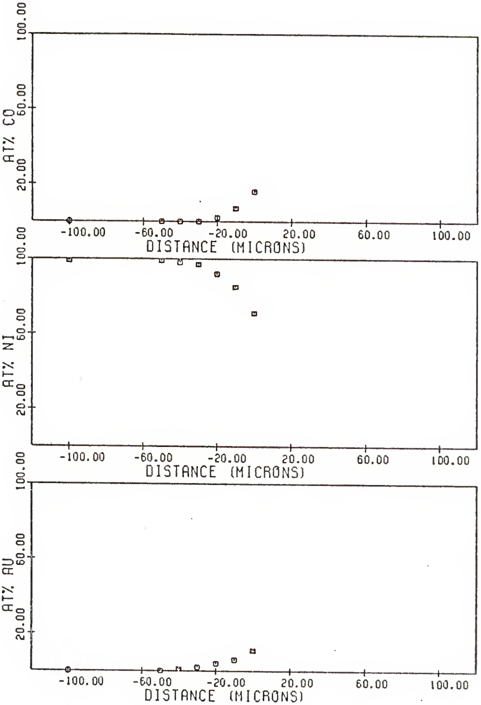

Fig. 5.10b. Concentration profile for couple Ni/AuCo.

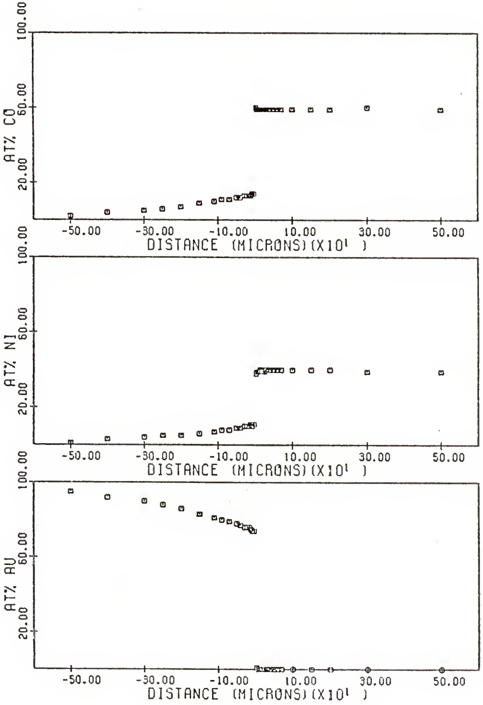

Fig. 5.10c. Concentration profile for couple Au/NiCo.

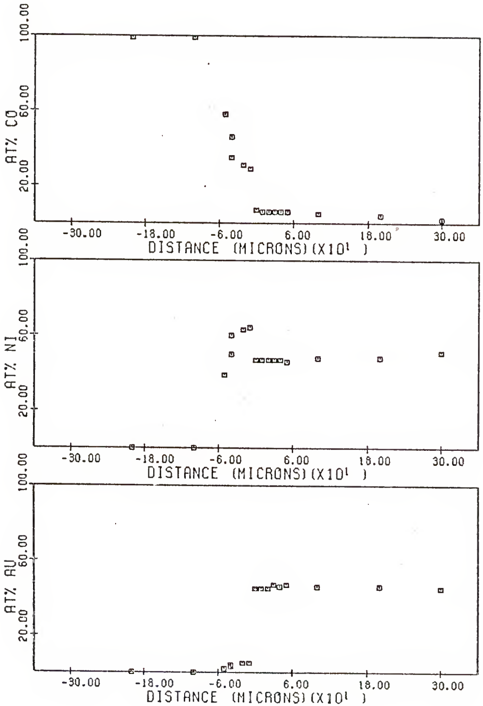

Fig. 5.10d. Concentration profile for couple Co/AuNi.

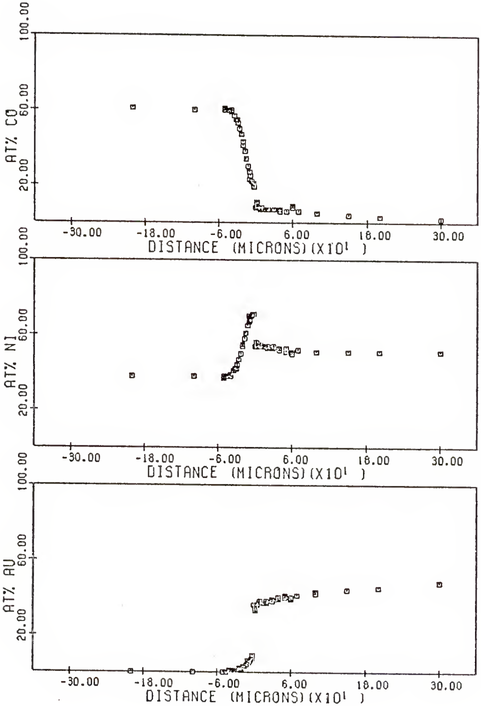

Fig. 5.10e. Concentration profile for couple NiCo/AuNi.

Fe>Au), FeAu/AuNi (Fe>Ni); 2) no conclusion can be derived about the relative penetration tendencies of Au and Ni due to the crossing of the two-phase field by the path of the deciding couple AuFe/FeNi. Analysis of the other isomorphous paths for this system and comparison with the corresponding paths in the system Fe-Ni-Co suggest that the shape of the paths is consistent with the assignment of the higher ranking for Fe and lower ranking to Ni. This is another feature of the penetration tendency viewpoint. From the shape of the paths for a given order or relative penetration tendencies, a pattern of predicted paths can be derived and used to investigate penetration tendencies, as was done above. The comparison of the diffusion paths for the two systems, Fe-Ni-Co and Fe-Ni-Au, is shown in Fig. 5.9. In spite of differences due to the concentration dependence of the penetration tendencies (as indicated by the crossover shifts) and the intervening two-phase field, it is evident that the basic features of all isomorphous paths are unchanged.

3. Ternary System Au-Ni-Co

The concentration profiles for couples in this system are presented in Figs. 5.10a to e. For couples having the AuCo two-phase alloy as one of the ends, only the isomorphous region is indicated. Once again, the difference in penetration depths between Au containing alloys (e.g. AuCo/AuNi in Fig. 5.10a) and those containing other metals (e.g. Ni/AuCo in Fig. 5.10b) is evident. The same trend is observed for the other couples of the system. The side containing Au is characterized by

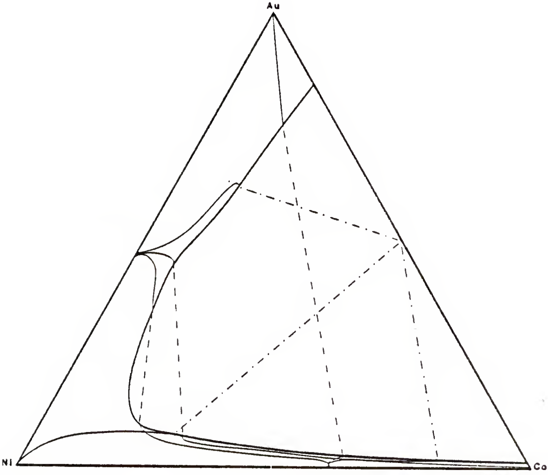

Fig. 5.11. Composition paths in the system Au-Ni-Co.

huge penetration depths, in sharp contrast with the shallow penetrations on the other side of the couple.

An interesting behavior is observed in the couple AuCo/AuNi. As illustrated by the concentration profile (Fig. 5.10a) or the composition path (Fig. 5.11), the concentration of Au in the AuNi phase increases as the interface is approached. The rationale for this effect is straightforward. At the interface of the couple, AuNi is in equilibrium with a two-phase system, so that, locally, one can consider the existence of two types of couples: one formed between AuNi and the Co-rich phase of the two-phase field; the other by AuNi and the Au-rich phase (this subject is treated more extensively in the Appendix). The flux of Ni in each of these two couples will be directed toward the two-phase AuCo alloy (specially through phase boundary diffusion). However, for Au, the direction of the flux will depend upon which couple you consider. For the "AuNI/Co-rich couple," Au will also diffuse toward the two-phase alloy. On the other hand, at the "AuNi/Au-rich couple," diffusion of Au will be directed to the AuNi side of the couple. The observed increase in concentration of Au in the AuNi side of the couple does not derive, therefore, from imbalance in the flows of Ni and Co. It results from actual diffusion of Au. Lateral diffusion of Au in front of the interface tends to homogenize the distribution of this metal along a planar section parallel to the interface. Depending on the scale of the two-phase field, this homogenization may not be completed during the diffusion anneal. The several concentration profiles obtained for each couple involving AuCo always presented small differences in the shape of the profile due to this effect. For this reason, no conclusions were definitively derived from couples having as end points two-phase alloys. The nature of the diffusion problem in those couples requires a much more complex treatment than that devised for this investigation.

One cannot derive rankings from the composition paths in Fig. 5.11 because the model for the two-phase case is still incomplete. Observe, however, that the end points of most paths point toward Au. For the penetration tendency viewpoint, this feature characterizes the fastest penetrator even if the details of the concentration profile at the interface are not understood. It will therefore be assumed, from this piece of information, that in the system Au-Ni-Co, Au is the fastest moving species.

4. Ternary System Au-Fe-Co

Concentration profiles for couples in the system Au-Fe-Co are presented in Figs. 5.12a to f. Once again, the larger penetration tendencies of all components in the side containing Au is observed. For the three couples containing the AuCo alloy (Figs. 5.12a to c), only the isomorphous part of the couple is represented.

Consider Fig. 5.12b, which represents the couple AuCo/AuFe. As in the corresponding couple of the FeNi/Au system, an increase in the concentration of Au in the AuFe side is observed. The shape of the profile, however, suggests that part of the increase in the fractional

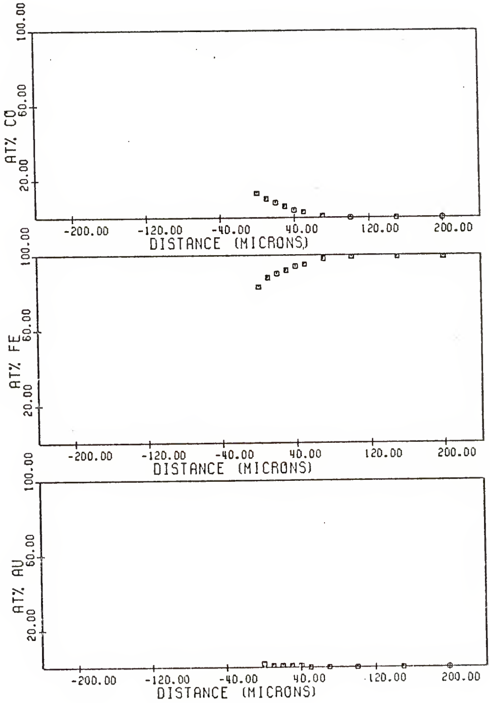

Fig. 5.12a. Concentration profile for couple AuCo/Fe.

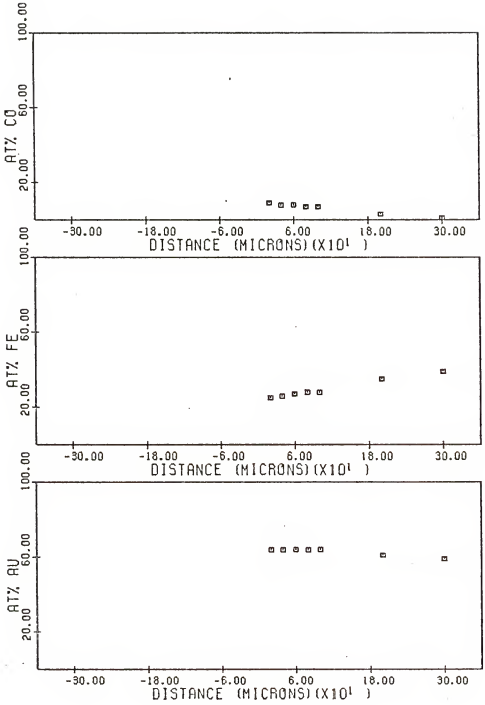

Fig. 5.12b. Concentration profile for couple AuCo/AuFe.

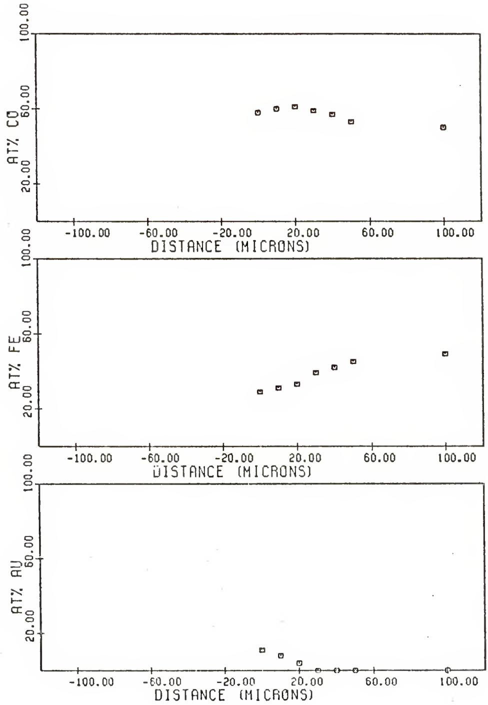

Fig. 5.12c. Concentration profile for couple AuCo/FeCo.

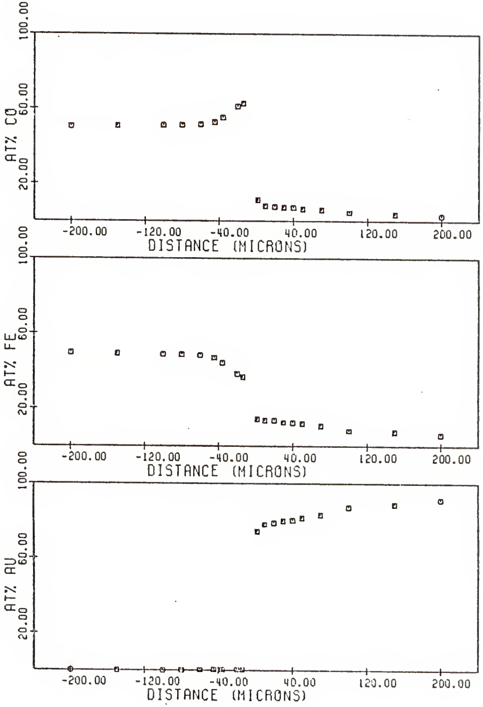

Fig. 5.12d. Concentration profile for couple FeCo/Au.

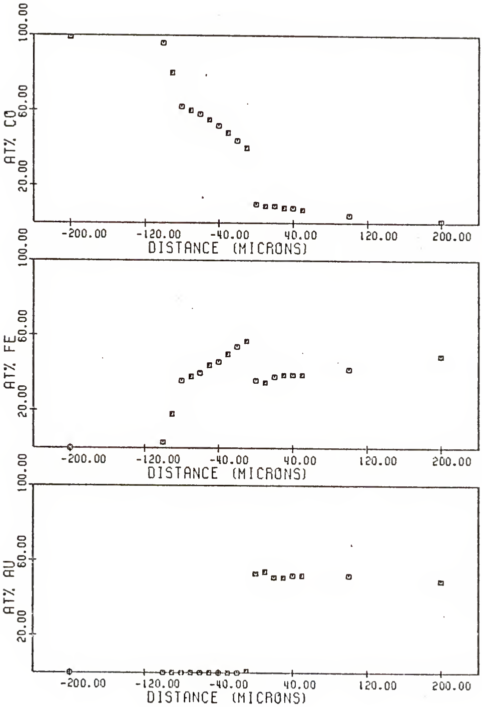

Fig. 5.12e. Concentration profile for couple Co/AuFe.

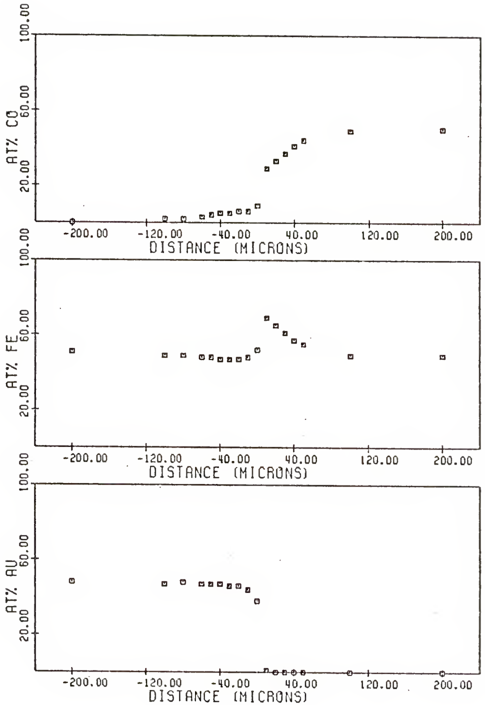

Fig. 5.12f. Concentration profile for couple AuFe/FeCo.

concentration of Au comes from the decrease in the concentration of Fe. Figure 5.12c for the couple AuCo/FeCo shows the same kind of profile for Co. In fact, the profile even suggests that Co did not redistribute. As seen in the discussion of Chapter 3 about diffusion with no initial concentration gradient, the presence of a maximum in the concentration profile may be due simply to the imbalance of atomic flows of the other two components.

As one can see, the penetration tendency viewpoint is able to explain several features of the atomic fraction profiles using physically based arguments. The possibility of associating the observed increase in fractional concentration with two different and meaningful processes is a unique feature of the model.

Analysis of the other profiles does not reveal any peculiarity in the corresponding curves (Figs. 5.12d to f). The only unusual feature observed is the crossing of the FeCo field (Fig. 5.12e) by couple Co/AuFe, producing the intermediate discontinuous section of the profile.

Inspection of the composition paths in Fig. 5.13 indicates once more that all paths are directed to Fe at their ends. For the sake of clarity, the path of couple FeCo/AuCo is not plotted in this figure; only the virtual part of the path is illustrated, indicating the point where the actual path enters the AuCo two-phase field. The end of the path on the FeCo side also points to Fe.

The only conclusion that may be unambiguously deduced from these paths is that Fe is the fastest moving species in the Au-Fe-Co system.

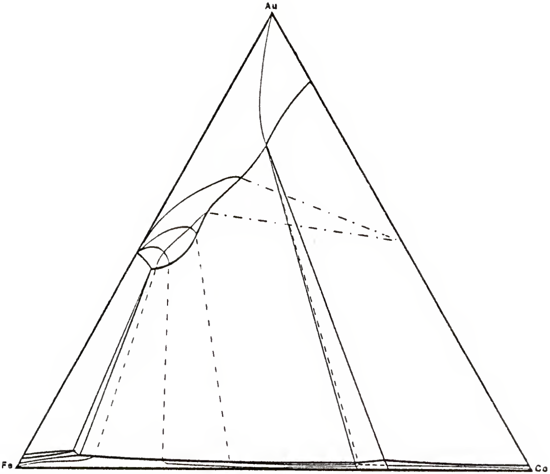

Fig. 5.13. Composition paths in the system Au-Fe-Co.

5. Quaternary Systems

The profiles for the quaternary couples are indicated in Figs. 5.14a to c. The irregular profile for the AuCo/FeNi couple (Fig. 5.14a) is due to the two-phase nature of the couple. In the region from zero to about forty microns, the structure of the diffusion zone is a very fine two-phase mixture. The profile in that region, therefore, is not a continuous and smooth curve, but rather the analysis of a sequence of points in a two-phase structure, so that the excessive scatter is expected.

For the couple AuFe/NiCo (Fig. 5.14b), the profile reveals the larger penetration on the AuFe side as opposed to the shallow penetration on the side of NiCo.

Analysis of the profile for AuNi/FeCo again indicates the larger penetration depths on the AuNi side. Observe the maximum in the profile of Co at about 80 μ. It is evident that diffusion of Fe toward the AuNi side was the factor responsible for this increase in the fractional concentration of Co. The presence of Co on the other side of the interface clearly shows that Co is in fact diffusing to the AuNi side of the couple. It seems doubtful that the Fickian approach could be used to explain this observation.

Analysis of the composition paths in Figs. 5.15a and b is necessarily superficial. The geometry of the curve in the projection may mislead the investigator about the actual direction of the path. It is possible, however, to identify the tendency of the ends of the path to point toward Fe.

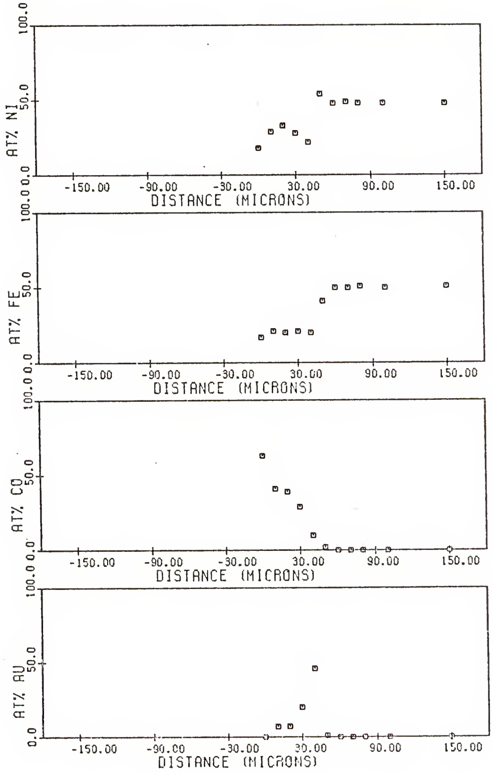

Fig. 5.14a. Concentration profile for couple AuCo/FeNi.

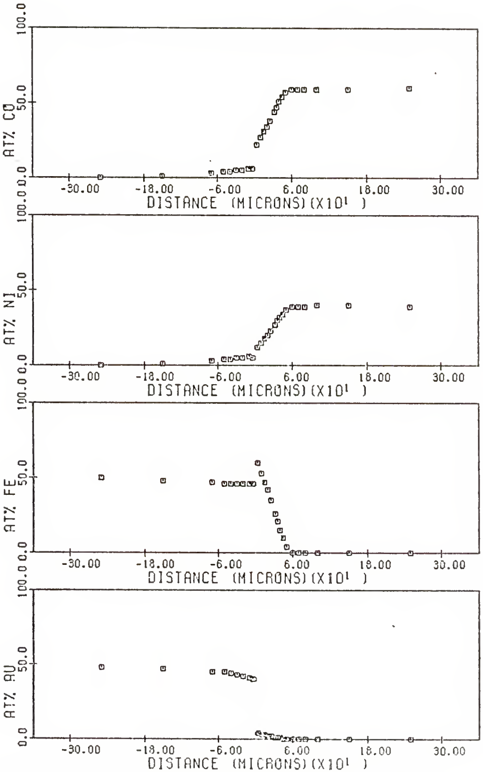

Fig. 5.14b. Concentration profile for couple AuFe/NiCo.

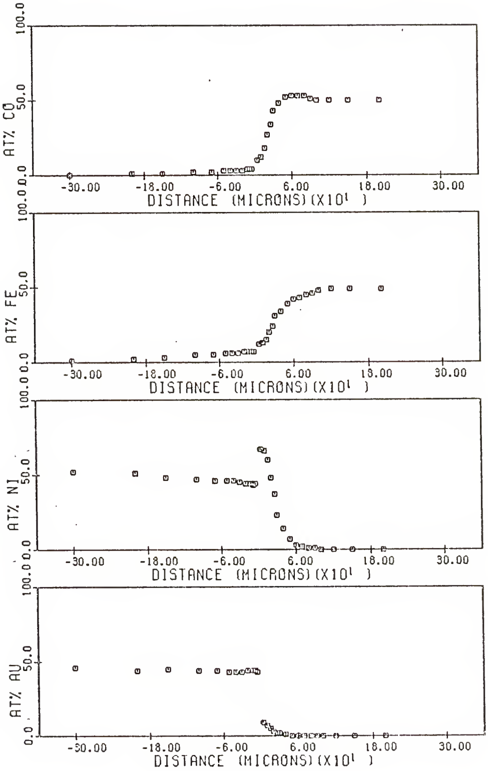

Fig. 5.14c. Concentration profile for couple AuNi/FeCo.

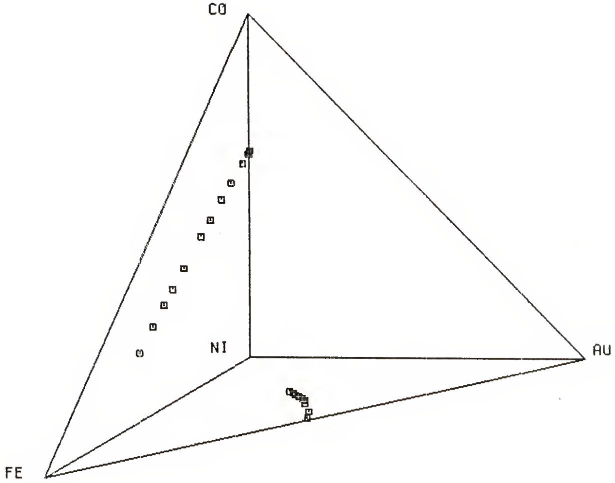

Fig. 5.15a. Composition path for couple AuFe/NiCo.

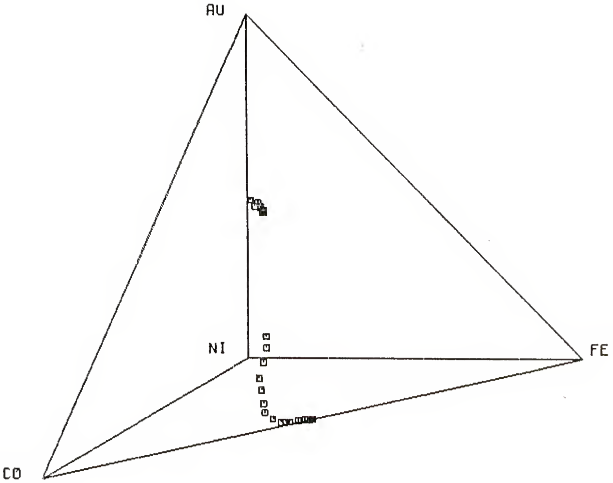

Fig. 5.15b. Composition path for couple CoFe/AuNi.

A ranking of penetration tendencies was derived from the pattern of Kirkendall shifts. According to this ranking, the metals in the Fe-Ni-Co-Au system penetrate in the decreasing order Fe, Au, Co, Ni. It was found that for compositions close to the AuNi 50-50 atomic percent, the penetration tendency for all components is enhanced. Also, the results indicate that Au out penetrates Fe in that region of compositions.

From the measured composition paths, an identical ranking of penetration tendencies was obtained. The shape of the paths for the isomorphous couples could be explained using the predictions of the model.

CHAPTER 6
CONCLUSIONS

A systematic diffusion study of the system Fe-Ni-Co-Au using the penetration tendency viewpoint has been presented.

A review of the existing models for treating multicomponent diffusion revealed the severe limitations of those models based on extensions of the Fickian approach.

An algorithm for describing diffusion phenomenon in semi-infinite two-phase diffusion couples displaying a planar interface has been introduced. Although incomplete, the proposed algorithm yielded conclusions about the role of the location and width of the two-phase field on the motion of the two-phase interface.

From the analysis of the pattern of Kirkendall shifts of binary, ternary, and quaternary couples of the system Fe-Ni-Co-Au, a qualitative model for the relative penetration tendencies of the four components was derived. The ranking of penetration tendencies thus derived is in the order Fe>Au>Co>Ni.

For couples having the AuNi alloy in one of the ends, a reversal in the ranking position of Fe and Au was required to explain the observations. This reversal seems related to the proximity of the diffusion anneal temperature to the melting point of the AuNi alloy. The simplified approach used in this investigation could not be used to explain this effect. A more sophisticated model of the relative penetration tendencies in this system must be devised to encompass this kind of result.

In all other couples, the direction of the measured Kirkendall shifts was consistent with the predictions of the model. The fact that the same qualitative model of penetration tendencies could explain the results for binary, ternary, and quaternary couples is encouraging.

Composition paths for the ternary and quaternary couples were experimentally determined and used to form the basis for an independent ranking of the penetration tendencies of the elements. Analysis of the paths in the systems Fe-Ni-Co and Fe-Ni-Au resulted in the same ranking of penetration tendencies obtained from the pattern of Kirkendall shifts. Due to the intervening two-phase fields in the ternary systems Au-Ni-Co and Au-Fe-Co, conclusions based on the shape of the path could only be derived with respect to which component was the fastest penetrator (Au in Au-Ni-Co and Fe in Au-Fe-Co). Similarly, for the two quaternary couples in which composition paths could be obtained, the presence of a two-phase field prevented a detailed analysis of the path; in both cases Fe emerged as the fastest moving species.

Analysis of the crossover point of the composition paths in the system Fe-Ni-Au using the penetration tendency model consistently indicated the larger penetration depth for all components on the Au containing side of couples. Observation of the concentration profiles for couples in which Au was present in only one side confirmed the predictions of the model.

Aspects of the diffusion behavior in multicomponent systems, such as diffusion in couples with no initial concentration gradient of one of the elements, were rationalized in a physically meaningful way using the penetration tendency viewpoint. The possibility of associating changes in the fractional concentration of one component with the imbalance in the flows of the other components permits a more realistic visualization of the processes taking place in the diffusion couple. Only a model based on intrinsic fluxes, such as the penetration tendency viewpoint, has the capability to describe this kind of phenomenon. It is expected that the occurrence of this "diffusion with no concentration gradient" will become more frequent as the number of components in the system increases.

The ability of the penetration tendency viewpoint to qualitatively explain the diffusion results over most of the quaternary system Fe-Ni-Co-Au using an extremely simple model attests to the validity of the approach.

APPENDIX
DETERMINATION OF PHASE BOUNDARIES IN TERNARY SYSTEMS USING TWO-PHASE BINARY DIFFUSION COUPLES

Introduction

It is the purpose of this work to report a new technique for determination of phase boundaries in ternary isotherms utilizing diffusion couples formed with two-phase binary alloys. Besides revealing the boundaries of the two-phase regions, the new method provides information about the diffusion paths in the system under study, from which the relative ratio of penetration of the three constituent elements can be estimated.

Review of Available Methods

Consider a ternary system displaying a miscibility gap at some temperature T, as indicated in Fig. A1. In order to determine the boundaries of the miscibility gap several techniques could be used. The most straightforward methods call for the preparation of several alloys with compositions uniformly distributed across the diagram as indicated in Fig. A1. After equilibrating samples of those alloys at the temperature T, they are quenched to room temperature and examined metallographically and by x-ray methods to determine which ones display two-phase structure. Quantitative analysis of those two-phase samples using a microprobe may yield the composition of the phase boundaries in the form of tie lines (see Fig. A1). When a microprobe is not available, measurement of lattice spacings can be used to reveal the boundaries of the two-phase region. In this case alloys with compositions lying along one line, e.g. AD (Fig. A1), are annealed at T°C, quenched, and the lattice spacing plotted as a function of composition as indicated in Fig. A2. For an alloy of composition P, the lattice spacings of α_1 and α_2 in equilibrium will correspond to the compositions defined by the tie line on which P lies. Thus, all two-phase alloys lying along AD will have the lattice spacings of α_1 and α_2 in equilibrium determined. If the boundaries of the two-phase region are known, the end compositions of the tie lines can be obtained when contours of equal lattice spacings are drawn in the ternary diagram. The phase boundaries are marked by sharp changes in the slope of the lattice spacing curves and may be defined over the whole field by working with alloys whose compositions lie along other lines in the ternary diagram. The main disadvantage of the method is its dependence on the lattice spacing variation. Thus if the contours of equal lattice spacing are parallel to the phase boundary, the solubility curve may be well defined but the tie lines cannot be determined. It is also appropriate to emphasize the large number of samples necessary to delineate the phase boundaries, even if tie lines are not to be determined.

Diffusion couple methods have been reported in the literature as early as 1957 (35), when Rhines and Clark studied the Al-Mg-Zn system.

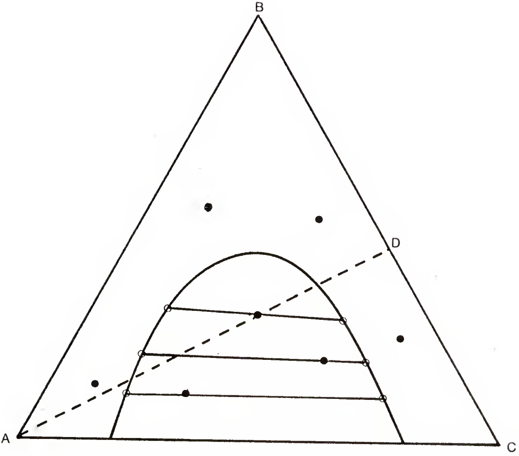

Fig. A1. Ternary system displaying a miscibility gap.

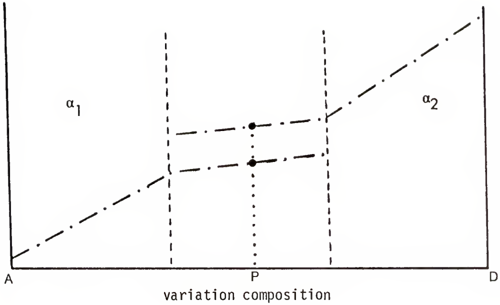

Fig. A2. Lattice parameter variation with composition.

Although their method was criticized (36) for being essentially metallographic, they were able to observe new phases as well as derive some rules for the composition path in ternary systems. The technique is based on the diffusion anneal of several couples whose end composition crosses over the ternary diagram in such a way as to delineate the location of the phase boundaries. If a planar interface is formed in a two-phase couple, the composition of each phase at the interface corresponds to the end points of a tie line, as indicated schematically in Fig. A3. One of the restrictions usually made to diffusion couple methods is the possibility of some equilibrium intermediate phase not being formed in the diffusion zone. Also it has been argued whether or not equilibrium is attained at the interface so that tie line compositions can be obtained. However, excellent agreement between diffusion couple methods and equilibrated alloys has been reported in the Mo-Ni system (106) and the diffusion couple technique has been used with success in the Ti-Ni-Cu system (107).

Although the possibility of missing one or more intermediate phases may represent a stumbling block for those interested in the true equilibrium diagram, there are many cases in which it is more important to know what phases are actually formed under the conditions usually encountered in real life, such as a dissimilar joint at high temperature.

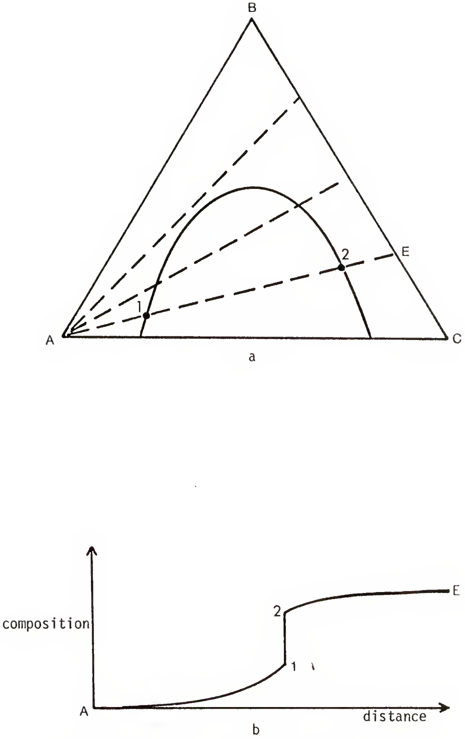

Fig. A3. Concentration profile in a diffusion couple.

Description of the Technique

The technique to be discussed in this work is a variation of the diffusion couple method having as its distinguishing feature the use of two-phase binary alloys. The main advantage of the present technique is the possibility of delineating the two-phase boundaries with as few as one diffusion couple, as will be shown later. Due to the heterogeneity of the sample with respect to a planar front of diffusion, the theoretical arguments on which the technique is based will be presented.

Consider a diffusion couple formed by joining pure B to some two-phase AC alloy, as indicated in Fig. A4. Upon diffusion B will penetrate into the AC side, while A and C will diffuse into B. The resulting composition path will in general be curved, with its ends pointing toward the fastest moving species (in the present discussion it was arbitrarily assumed that the penetration tendencies were in the order A>B>C). At some point E along the two-phase boundary the path will enter the two-phase region and traverse in the direction of the composition 50-50 AC. If the lateral dimensions of the two-phase aggregate are small compared to the size of the diffusion zone, it is reasonable to assume that lateral diffusion will eliminate concentration gradients inside each of the phases α_1 and α_2 as indicated schematically in Figs. A5d and e. In other words, if one considers the idealized case represented in that figure, it can be seen that along two different lines 1 and 2, the concentration of a given component, say B,

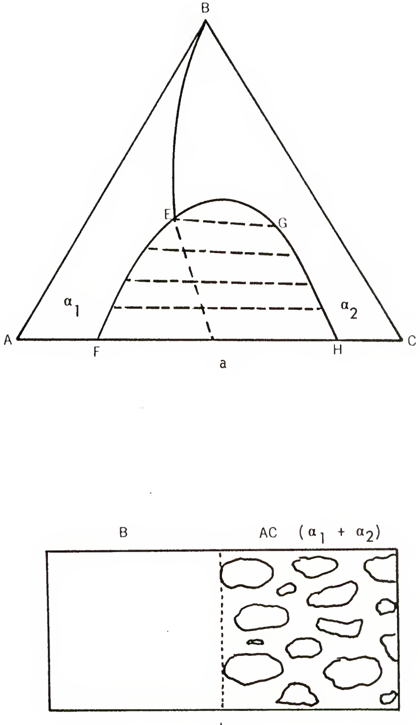

Fig. A4. Diffusion couple using a binary two-phase alloy.

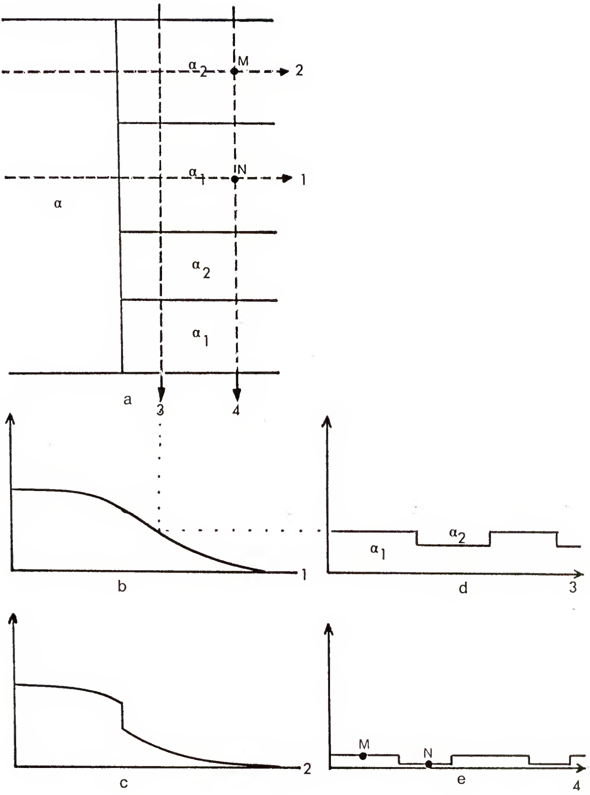

Fig. A5. Composition profiles in a two-phase structure.

varies with distance according to the curves presented in Figs. A5b and c, respectively. If equilibrium at the interface α_1/α_2 is maintained, the composition of these interfaces will represent tie lines on the two-phase region. Further, since the phases α_1 and α_2 are laterally uniform, to obtain the compositions at the interface α_1/α_2 one can analyze each of the phases α_1 and α_2 at some region removed from the interface, as indicated by the points M and N in Figs. A5a and e. It can be questioned why should the composition path in the isomorphous region BE (see Fig. A4) be the same along lines 1 and 2. Looking at Fig. A5a, it is possible to consider lines 1 and 2 as two different couples, one formed by joining alloys with compositions B and F and the other by joining alloys with compositions B and H. Assuming that along each direction the concentration profiles initially formed are different, one can see that lateral diffusion in the isomorphous region α will tend to eliminate concentration gradients in the direction parallel to the interface, producing the single path BE. At the same time, assuming that in the two-phase region of the couple the compositions initially formed in α_1 and α_2 are outside the boundaries of the miscibility gap, the fact that α_1 and α_2 are in direct contact with each other assures that equilibrium at the interface α_1/α_2 may be attained; thus the two-phase field is partially delineated (see Fig. A6). The fraction of the two-phase field illuminated will depend on several factors such as end couple composition, relative penetration tendency of the three elements and shape of the two-phase field, since these will

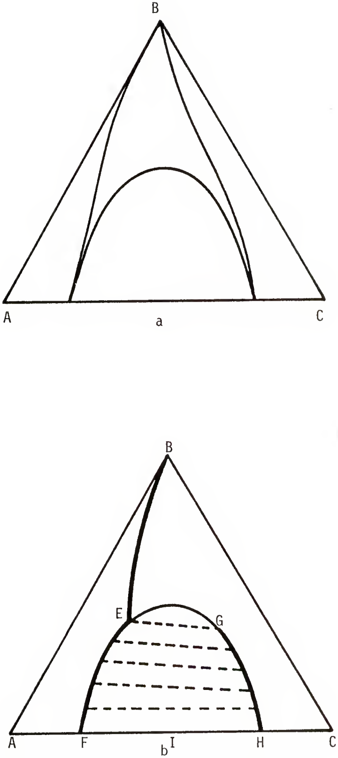

Fig. A6. Initial and later stages of a local diffusion couple.

dictate the composition path and its intersection with the boundaries of the miscibility gap.

Now that the basic features of the method have been illustrated in an ideal situation, more realistic cases will be treated. In general the condition illustrated in Figs. A5d and e where the chemical potential of each element is constant at each front perpendicular to the diffusion direction is not observed. The scale of the two-phase structure may be too coarse to permit lateral homogenization, and, in addition, diffusion along the α_1/α_2 boundary may play a significant role. When this occurs, the determination of the tie lines becomes very difficult since the composition corresponds to equilibrium only at the interface α_1/α_2, as indicated in Fig. A7, and the analytical determination of composition at interfaces is rather imprecise. As will be seen, these circumstances do not affect the capability of the method for the determination of phase boundaries.

Considering the case in which the two-phase region is present as in an interconnected network, phase boundary diffusion is expected to increase the size of the diffusion zone by providing a short circuit path for the penetration of the diffusing species. As a result the composition at some point located at the boundary but well removed from the original interface may be affected by such high diffusivity condition. Fig. A7a illustrates a situation in which volume diffusion would produce a diffusion zone extending up to the plane defined by RS, and yet as a result of boundary diffusion, the composition at point

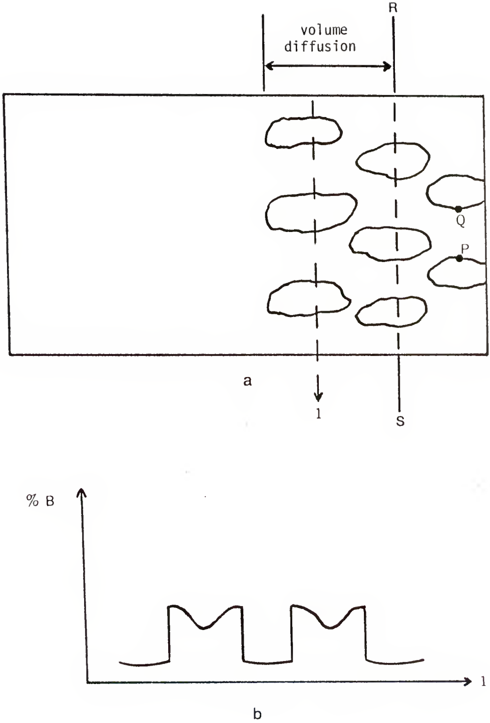

Fig. A7. Composition profile across a particle in a two-phase structure.

Q is altered due to the connectedness of the two-phase aggregate. The information obtained in a two-dimensional section, such as that shown in Fig. A7a, is incomplete since it does not reveal the connectivity of the structure. Thus, two points, such as P and Q in Fig. A7a, that are located at the same distance from the original interface may be at different distances from the original interface with respect to delivery of solute through boundary diffusion. Such a possibility does not affect whatsoever the technique.

Consider first point Q, Fig. A8. Component B, having attained the tie line concentrations $C_{\alpha_1}^{B}$ and $C_{\alpha_2}^{B}$ at the boundary, diffuses laterally into the phases α_1 and α_2 which initially have compositions C_1 and C_2, respectively. Analysis of compositions along the line QT would yield a composition profile starting in $C\alpha_1$ and finishing in C_1. Analysis of these paths will depend again on the ratio of diffusivities among the constituent elements, but they do not have to be S-shaped as required in semi-infinite couples by mass balance considerations (37). The continuous feeding of B atoms at Q through the boundary and removal of part of these atoms by lateral diffusion into α_1 and α_2 gives rise to a complex problem of conservation of species, whose solution is beyond the scope of the present study. However, if one considers the region QT as representing a finite couple one can easily surmise that conservation of species does not hold, at least for component B. In fact the situation is more complicated because the compositions $C\alpha_1$ and $C\alpha_2$ at the point Q are not constant during the

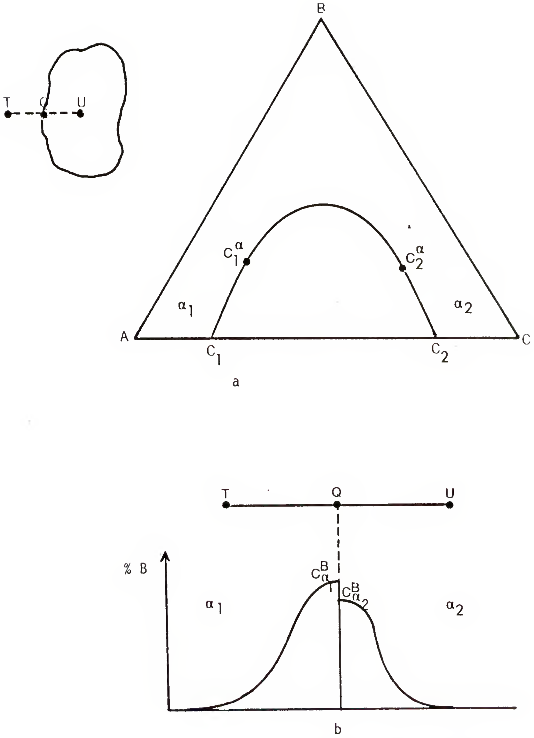

Fig. A8. Effect of phase boundary on a two-phase diffusion couple.

process, but increase steadily from the initial values C_1 and C_2 to some final value C_{α_1} and C_{α_2} at the end of the diffusion anneal. At some intermediate time during the annealing period the compositions at Q will be somewhere inbetween those two pairs of value, always representing the end points of a tie line. One can see that a model for the study of diffusion along the line QT would be similar to one of vapor-solid state diffusion with the composition of the gas, and consequently the equilibrium concentration of solute at the interface, being varied during the process. Studies of vapor-solid diffusion couples in the systems Cu-Zn-Mn (63) and Zn-Cd-Ag (64) under conditions of constant concentration at the vapor-solid interface indicate that a slightly C-shaped composition path may be obtained. Referring again to Fig. A8, one can see that a C-shaped path starting in C_{α_1} and ending in C_1 could roughly delineate part of the phase boundary $\alpha_1/\alpha_1+\alpha_2$. However there is no guarantee that this will always happen, since the boundary of the two-phase region may be very curved, the C-shaped path may be curved in the opposite direction and the two curves may have in common just the points C_1 and C_{α_1}.

The same reasoning developed above would apply to point P or any other boundary point, except for the interfacial compositions C_{α_1} and C_{α_2} which will vary from point to point. Fortunately, one does not depend on these paths to obtain the phase boundaries, as will be shown.

Up to this point in the discussion, it was assumed that the compositions at the center of the phases α_1 and α_2 were equal to the initial concentrations C_1 and C_2, respectively, due to the inability of lateral diffusion to homogenize each phase. Such a statement implies that all regions of α_1 and α_2 that are being analyzed in the polished section are large with respect to lateral dimensions. It is not necessary to thus restrict the analysis. In a two-phase section, one can always find some regions of a given phase having small lateral dimensions, e.g., particle 1 in Fig. A9. Analysis of this particle along the direction a could result in a concentration profile for component B as indicated in Fig. A9a. Observe that such a profile may result from (1) lateral diffusion along direction a, if the section cut a thin particle of that phase or (2) downward or upward diffusion (normal to the plane of the section) if the section just touched the top or bottom of a big particle. In either case, if the concentration of B along direction a approaches a constant value, as depicted in Fig. A9a, one can say that it is approaching some equilibrium interface composition. The same reasoning can be applied to the profile obtained along line b, illustrated in Fig. A9b. Due to their proximity with the interface α_1/α_2 most of the points along line b will have attained a composition very close to some equilibrium composition. Although it is possible to determine the adjacent equilibrium composition in the other phase, such a procedure is not recommended due to the imprecision associated with interface analyses, unless the concentration gradients in the other phase are also negligible. In both systems analyzed in this investigation, such conditions were observed. When this happens,

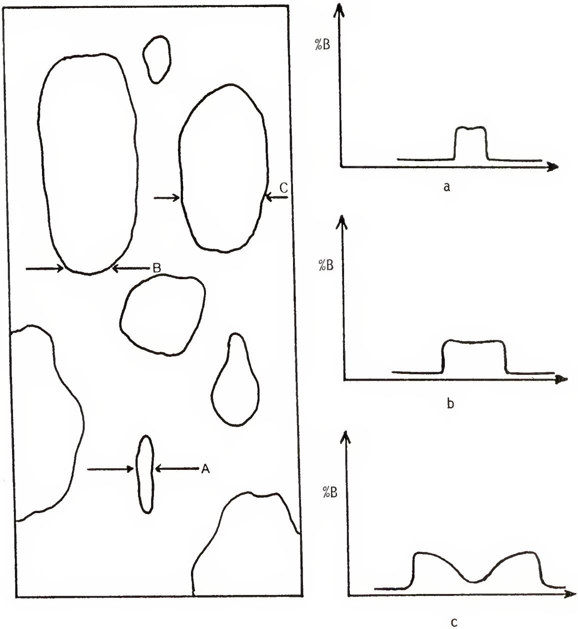

Fig. A9. Different concentration profiles resulting from phase boundary diffusion.

tie line compositions may be obtained by analyzing adjacent regions of each phase. However, due to drift problems in the microprobe used in this study, the evaluation of tie lines from analysis of neighboring regions could not be attempted. In Fig. A9a, the hypothetical profile for component B along a thick part of particle 2 is illustrated for comparison. The equilibrium compositions at the interface α_1/α_2 along lines a, b and c are not the same, although they can be very close due to the high diffusivity of the grain boundaries.

One can see now that in a single section of a diffusion couple such as that indicated in Fig. A4 there is a complete sequence of interface compositions capable of delineating the boundaries of the two-phase field, from the point where the diffusion path enters it up to the two-phase binary, as indicated by lines EF and GH in Fig. A6. In order to obtain these lines, one has simply to analyze several regions of the sample, each located at different distance from the original interface but always following the conditions discussed in detail above. It may happen that the path BI enters the two-phase field too close to the binary side to provide very much information (see Fig. A10). When this happens, one can select a different couple, such as KI in Fig. A10, which illuminates a considerable part of the two-phase field. The relative penetration tendency viewpoint (26,31,78) with its ability to model patterns of composition paths from tracer diffusivity data and Kirkendall shifts may prove to be invaluable in helping to select couples for such experiments. In case more than one couple is used,

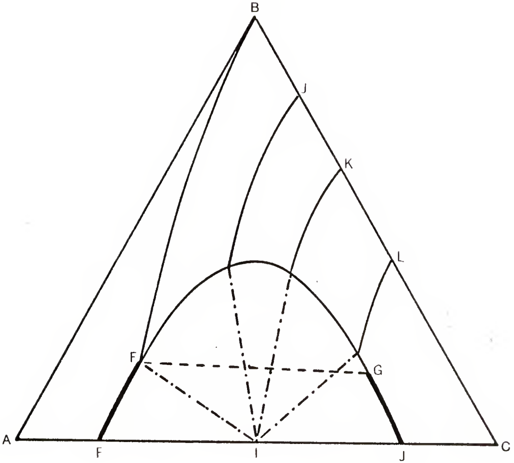

Fig. A10. Selection of couple to illuminate two-phase field.

the limits of the two-phase region obtained with one couple may be used to check those parts of the phase boundaries which are common to other couples. As a result, what could represent an undesirable increase in the number of specimens must also be regarded as an internal check to the validity of the method.

One final point to be mentioned refers to the applicability of the method. During this discussion, a system displaying a miscibility gap was analyzed. The technique is not limited to such systems. Some examples will be given here, very briefly, of situations where the method can be applied.

1. Crossing Two-Phase Field

This is a very common type of system, as illustrated in Fig. A11a. Observe that in this case, the selection of the couple KI is trivial. At the original interface (joint), several local "couples" may be formed such as: $K\alpha/I\alpha$ (pt 1), $K\alpha/I\beta$ (pt 2), $K\beta/I\alpha$ (pt 3) and $K\beta/I\beta$ (pt 4). How the paths on these regions will be shaped during the diffusion anneal is not clear. However, on both sides of the couple, direct contact between α and β will provide for equilibrium condition at any interface α/β. The α and β interfacial compositions at some point P on the K side far removed from the joint will be $K\alpha$ and $K\beta$ (see Fig. A11a). Similarly at some distant point N on the I side the composition at an α/β interface will be $I\alpha$ and $I\beta$. If one now considers regions successively closer to the original interface, the α/β interfacial compositions will correspond to tie lines of the two-phase

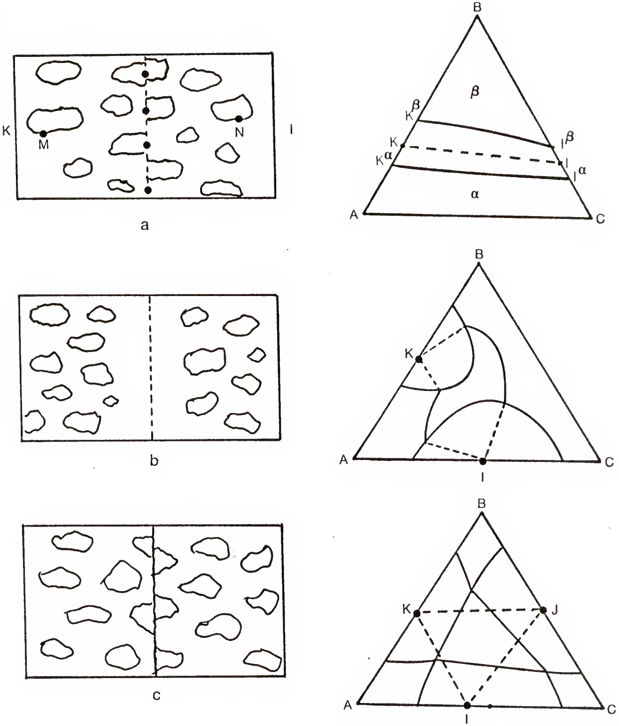

Fig. A11. Different two-phase cases in which the technique can be used.

field. In other words, as one approaches the original interface from both sides, the binary tie lines Kα/Kβ and Iα/Iβ start moving toward each other, delineating the two-phase field, until they meet inside the ternary, indicating the tie line compositions corresponding to the original interface. Analysis of a single section, therefore, can provide the location of the phase boundaries. Furthermore, if adjacent regions of α and β can be found in the couple such that the concentration gradients in both phases are negligible, a mapping of the set of tie lines may also be obtained.

2. More Than One Two-Phase Field

Figs. A11b and c illustrate two examples where more than one two-phase field is present. The selection of couples is not as obvious in the first case, since a couple may produce a path that illuminates satisfactorily one two-phase region but not the other, as shown in Fig. A11b. It may be necessary to prepare more than one couple.

With respect to the three-phase reaction indicated in Fig. A11c, it seems reasonable to assume that two of the three two-phase fields can always be investigated with a properly selected single couple, such as couple JI in that figure. To get information on the other two-phase region, an additional couple would have to be examined (see couples KI or KJ).

A schematic view of the metallographic structures probably encountered in these two cases is shown at the side of each system.

3. Quaternary Systems

Perhaps the most striking feature of the new technique is its potential ability to determine the location of phase boundaries in quaternary systems with a reasonable number of samples. Consider a quaternary system with a miscibility gap, as indicated in Fig. A12a. The determination of the surface bounding the miscibility gap using available techniques would require an inordinate amount of alloy preparation (quaternary alloys of different compositions!) in addition to long anneals to equilibrate the samples at the temperature of interest. One can apply the present technique by preparing several couples, all of them having in one side a two-phase binary alloy CD, such as I in Fig. A12a., and in the other side binary alloys AB of varied compositions. For each couple, the composition path will move from the binary side AB into the isomorphous region of the tetrahedron and proceed in a curved path until it enters the two-phase field at some point E along the bounding surface. Subsequently, the virtual path somehow gets to point I. In Fig. A12b, the bounding surface is shown, together with the lines EF and GH that represent end points of tie lines inside the two-phase volume. The surface EFGH is not necessarily plane.

The same reasoning developed for ternary systems can be applied here with respect to the role of boundary diffusion in extending the diffusion zone and providing a means to determine tie line compositions. Therefore, from each annealed couple one can obtain curves such as EF

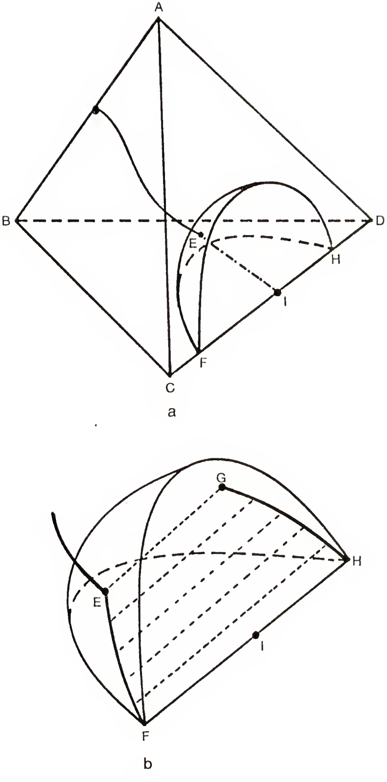

Fig. A12. Composition path in a quaternary system displaying miscibility gap.

and GH (even if tie lines cannot be obtained connecting the two) by analyzing separately selected areas of each phase. Figure A13 shows an hypothetical case where six couples were used to investigate a system. One can see that if the paths do not enter the two-phase field very close to the CD binary, the segments of curves delineated on the surface bounding the two-phase field permit a rough sketch of the miscibility gap to be drawn. In the example given, two of the couples used were ternary alloys, having as purpose the illumination of the ternary boundaries of the miscibility gap. If the ternary isotherms are known, other quaternary couples can be used to better define the two-phase field.

Determination of Two-Phase Fields in the Systems Au-Ni-Co and Au-Fe-Co

Experimental support for the proposed technique is provided by investigations in the systems Au-Ni-Co and Au-Fe-Co, at 900°C. An alloy within the two-phase field on the Au-Co binary was used as one side of the couples in both systems.

The microprobe results for the system Au-Ni-Co are presented in Figs. A14a, b and c. The operating conditions of the probe were as indicated in Table A1. Due to the appreciable difference in hardness between the Au-rich and Co-rich phases of the two-phase Au-Co alloy, surface relief was produced during polishing, mainly at interfaces. Added to that, the small take-off angle (18°) of the microprobe used

Table A.1
Operational Conditions for the Acton Microprobe (MS 64)

Accelerating Voltage	20 KV
Specimen Current	100 nA
Beam Size	≈1 μ
Take-Off Angle	18°
Counting Time (background)	100 s
Counting Time (peak)	10 s

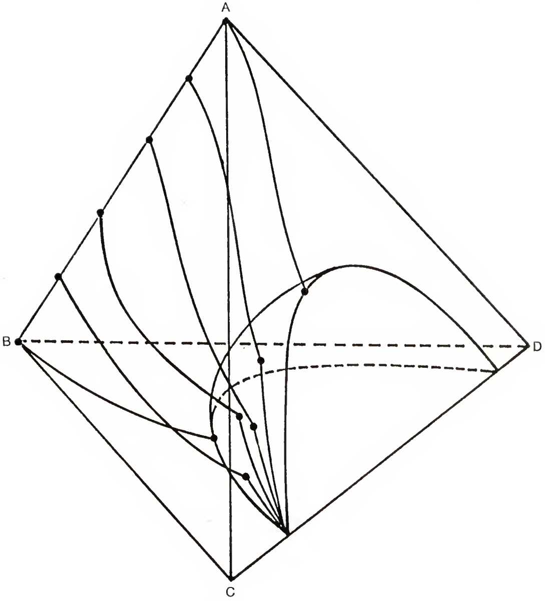

Fig. A13. Application of the technique to the determination of a quaternary two-phase field.

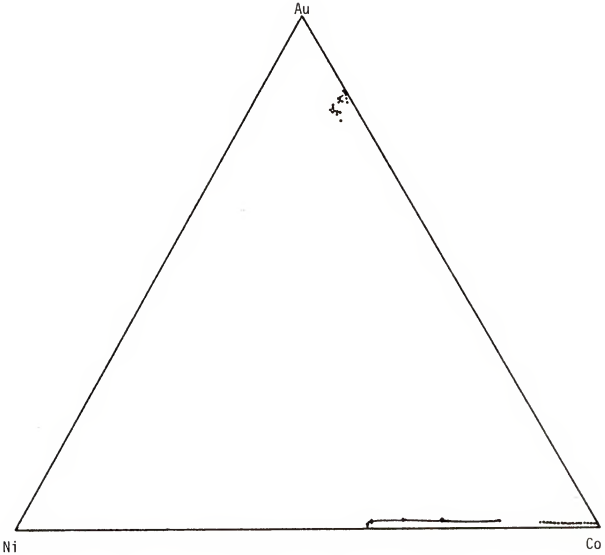

Fig. A14a. Microprobe results for the NiCo/AuCo couple.

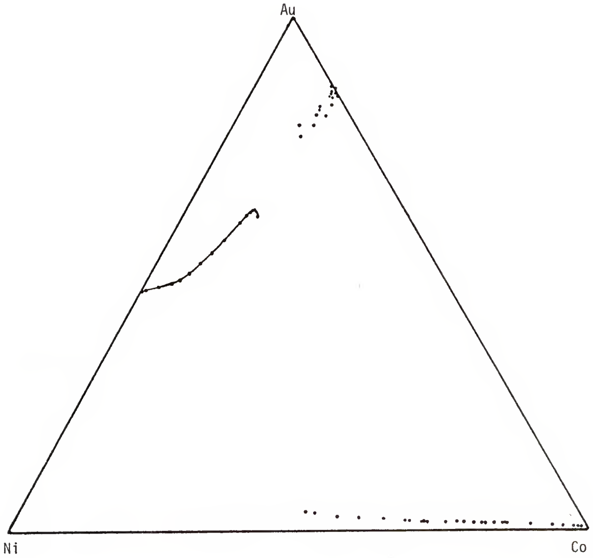

Fig. A14b. Microprobe results for the AuNi/AuCo couple.

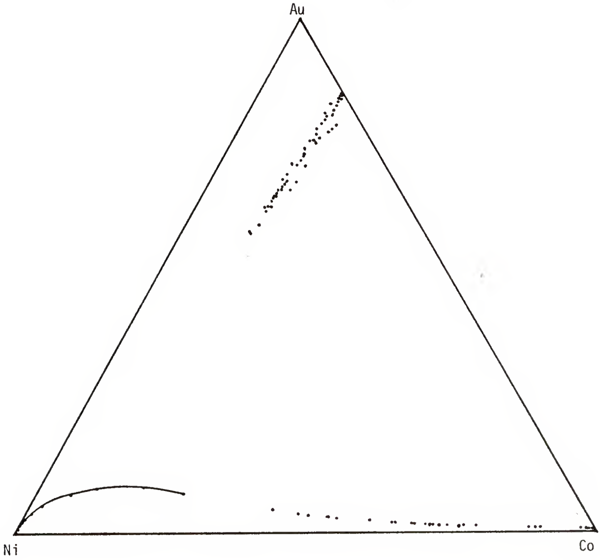

Fig. A14c. Microprobe results for the Ni/AuCo couple.

in the investigation required careful selection of the regions to be analyzed to avoid biasing the results with surface effects. If the applicability of the technique were dependent on analysis of compositions at interfaces, it could not be used in this study.

The microprobe utilized in this investigation was presenting a drift of the electron beam associated with the composition of the region under analysis in such a way that the beam would always drift when going from one phase to another. For this reason, tie line compositions could not be established with confidence. Looking at the points obtained for the phase boundaries in Fig. A14a, b and c, one can feel that they roughly define the shape of the miscibility gap. The larger scattering on the Au-rich side seems to be due to the presence of very small Co-rich particles in the Au-rich matrix, making the selection of Au-rich regions for analysis difficult, if one recalls that the samples for microprobe study are unetched. Even when the probe is hitting a pure matrix region, adjacent Co-rich particles located in the direction of one detector may be traversed by x-rays coming from below the surface of the analyzed region, giving rise to absorption, enhancement and other effects not taken into account during the processing of data. The fact that even with so many potential problems threatening the outcome of the analysis in this particular system the results come out satisfactorily deserves mention. Figure A15 shows the data for the three couples; the consistency of results in the Co-rich phase boundary is remarkable. On the Au-rich side more scatter is evident, but a rough sketch of the phase boundary can be drawn without problem.

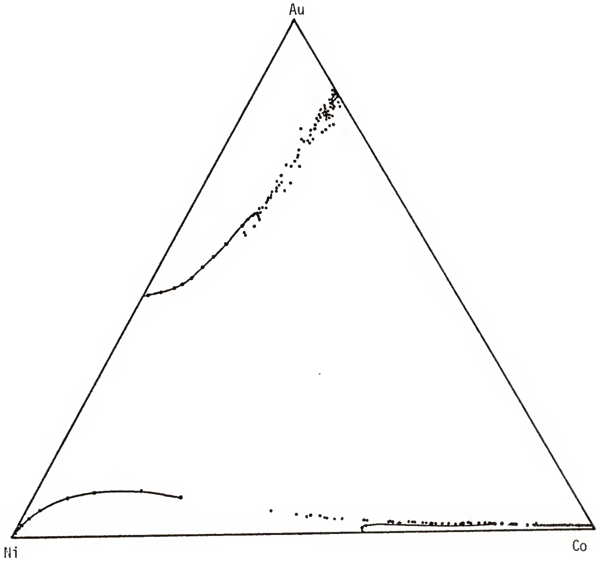

Fig. A15. Collection of results for the Au-Ni-Co system.

The results for the System Au-Fe-Co are shown in Figs. A16a, b and c. Again, the same problems were faced with respect to surface relief and the fine disperson of the Co-rich phase. In addition, the presence of three other two-phase fields and two three-phase reactions increased the complexity of the analysis. Only the two-phase field extending to the Au-Co binary was studied in this investigation. Plotting the results for the three couples in one graph, Fig. A17, shows once more an excellent agreement in the Co-rich side and a satisfactory minimal scatter on the Au-rich side. The three-phase reactions as well as the other two-phase fields were drawn in a speculative way, since no attempt was made to determine them quantitatively in this study. Their determination would require couples with binary alloys within each two-phase field, but that was not in line with the diffusion project that motivated the development of this technique in the first place.

Conclusions

A new technique for determining two-phase boundaries in ternary systems using two-phase binary alloys has been fully described, in order to completely justify the application of the method under a variety of situations commonly encountered in practice. A unique feature of the proposed technique is its ability to determine the phase boundaries of ternary systems with as few as one single diffusion couple. The fact that binary alloys are used as end couple compositions

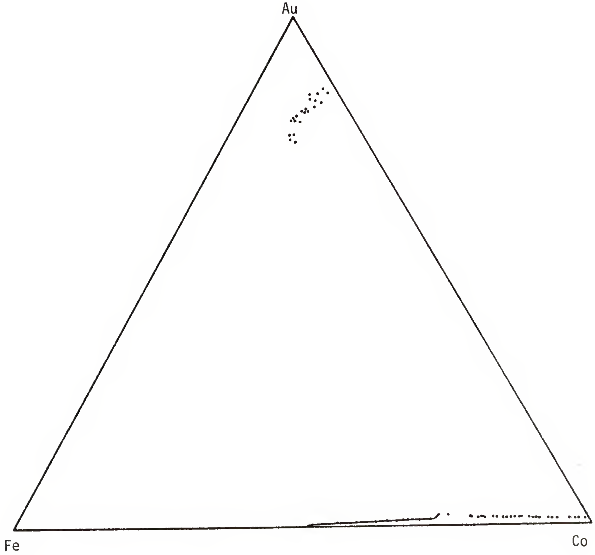

Fig. A16a. Microprobe results for the couple FeCo/AuCo.

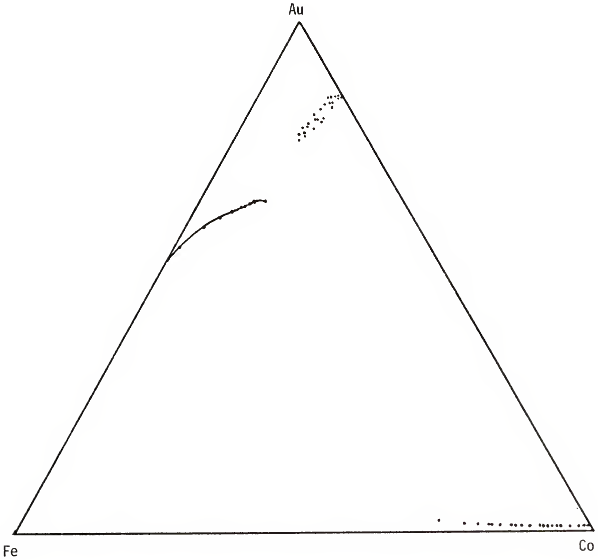

Fig. A16b. Microprobe results for the couple AuFe/AuCo.

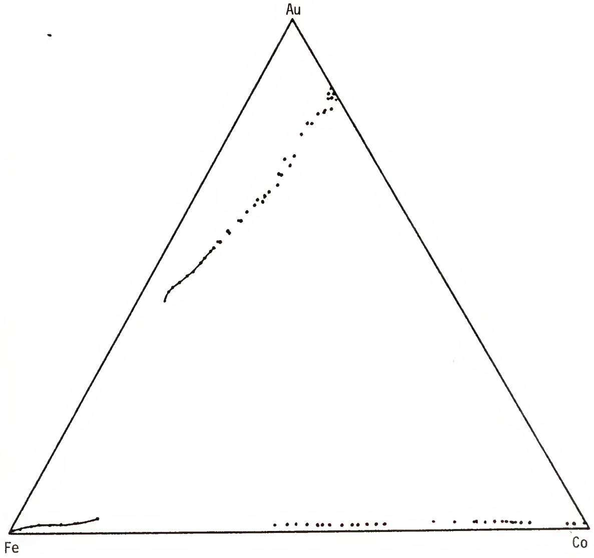

Fig. A16c. Microprobe results for the couple Fe/AuCo.

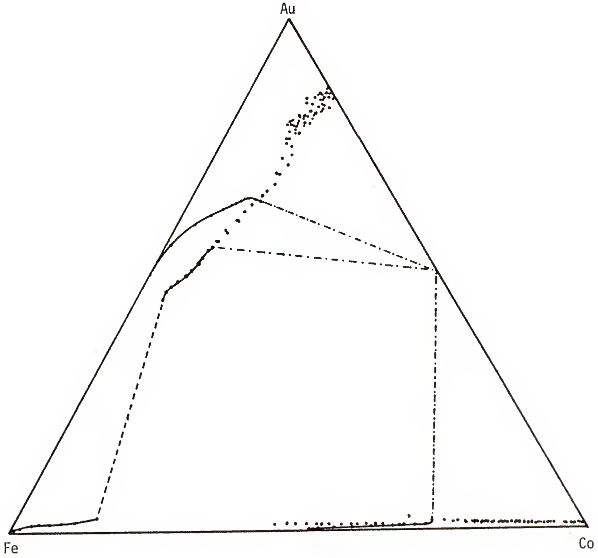

Fig. A17. Collection of results for the Au-Fe-Co system.

makes the method extremely appealing. Experimental support for the technique was obtained by determining the phase boundaries of the Au-Co two-phase field in the systems Au-Ni-Co and Au-Fe-Co. Although those systems present some experimental difficulties due to the difference in hardness between the two phases, the results were reproducible in describing one side of the two-phase region, and satisfactory on the other. It is expected that in other systems where such peculiarities are nonexistent, the proposed technique can be applied with success to both phase boundaries.

Finally, the possibility of using the method in quaternary systems has been pointed out. In case this prediction is confirmed experimentally, it could provide a practical means for the determination of phase diagrams for that type of multicomponent system.

REFERENCES

1. J. Fourier, The Analytical Theory of Heat, 1955, Dover Publications, Inc., New York.
2. A. Fick, Pogg. Ann., 94, 59 (1855).
3. H. S. Carslaw and J. C. Jaeger, Conduction of Heat in Solids, 1959, Oxford University Press, London.
4. J. Crank, Mathematics of Diffusion, 1956, Oxford University Press, London.
5. J. Jost, Diffusion in Solids, Liquids, Gases, 1952, Academic Press, Inc., New York.
6. L. Boltzmann, Ann. Phys. Leipzig, 53, 959 (1894).
7. C. Matano, Japan J. Phys., 8, 109 (1933).
8. P. Shewmon, Diffusion in Solids, 1963, McGraw-Hill Book Company, New York.
9. E. O. Kirkendall, L. Thomassen, C. Upthegrove, Trans. AIME, 133, 186 (1939).
10. E. O. Kirkendall, Trans. AIME, 147, 104 (1942).
11. A. C. Smigelskas and E. O. Kirkendall, Trans. AIME, 171, 130 (1947).
12. L. C. Correa da Silva and R. F. Mehl, Trans. AIME, 191, 155 (1951).
13. L. S. Darken, Trans. AIME, 175, 184 (1948).
14. F. Seitz, Phys. Rev., 74, 1513 (1948).
15. F. Seitz, Acta Cryst., 3, 355 (1950).
16. A. D. Le Claire, Phil. Mag., 3, 921 (1958).
17. J. S. Kirkaldy and G. R. Purdy, Can. J. Phys., 40, 208 (1962).

18. R. T. DeHoff, Trans. AIME, 242, 608 (1968).

19. L. Onsager, Phys. Rev., 37, 405 (1931) and 38, 2265 (1931).

20. L. Onsager, Ann. N.Y. Acad. Sci., 46, 241 (1945).

21. P. J. Dunlop and L. J. Gosting, J. Phys. Chem., 63, 86 (1959).

22. H. Fujita and L. J. Gosting, J. Phys. Chem., 64, 1256 (1960).

23. D. G. Miller, J. Phys. Chem., 62, 767 (1958).

24. D. G. Miller, J. Phys. Chem., 63, 570 (1959).

25. A. Vignes and J. P. Fabatier, Trans. AIME, 245, 1795 (1969).

26. C. C. Wan, Doctoral Dissertation, University of Florida, Gainesville, 1973.

27. T. O. Ziebold, Doctoral Dissertation, Massachusetts Institute of Technology, Cambridge, 1965.

28. G. R. Mason, Master's Thesis, McMaster University, Hamilton, Ontario, 1959.

29. L. S. Darken, Atom Movements, 1951, American Society for Metals, Metals Park.

30. R. F. Mehl, AIME Technical Publication No. 726 (1936).

31. K. J. Anusavice, Doctoral Dissertation, University of Florida, Gainesville, 1970.

32. L. J. Darken, Trans. AIME, 180, 430 (1949).

33. F. N. Rhines, R. A. Meussner, R. T. DeHoff, Trans. AIME, 212, 860 (1958).

34. F. N. Rhines and R. F. Mehl, Trans. AIME, 128, 205 (1938).

35. J. B. Clark and F. N. Rhines, Trans, ASM, 51, 119 (1959).

36. J. S. Kirkaldy and D. G. Fedak, Trans. AIME, 224, 490 (1962).

37. J. S. Kirkaldy and L. C. Brown, Can. Met. Quart., 2, 89 (1963).

38. J. B. Clark, Trans. AIME, 227, 1250 (1963).

39. C. W. Taylor, M. A. Dayananda, R. E. Grace, Met. Trans., 1, 127 (1970).

40. L. E. Wirtz and M. A. Dayananda, Met. Trans., 8A, 567 (1977).

41. J. S. Kirkaldy, Can. J. Phys., 35, 435 (1957).

42. J. S. Kirkaldy, Can. J. Phys., 36, 899 (1958).

43. J. S. Kirkaldy, Can. J. Phys., 36, 907 (1958).

44. J. S. Kirkaldy, Can. J. Phys., 36, 917 (1958).

45. J. S. Kirkaldy, Can. J. Phys., 37, 30 (1959).

46. C. Zener, J. A. Physics, 20, 950 (1949).

47. D. E. Coates, Doctoral Dissertation, McMaster University, Hamilton, Ontario, 1970.

48. L. Chandrasekar, Hydrodynamic and Hydromagnetic Stability, 1959, Oxford University Press, London.

49. D. E. Coates, Met. Trans., 3, 1203 (1972).

50. R. T. DeHoff, private communication.

51. T. O. Ziebold and R. E. Ogilvie, Trans. AIME, 239, 942 (1967).

52. A. G. Guy, V. Leroy, T. B. Lindemer, ASM Trans. Quart., 59, 517 (1966).

53. T. B. Lindemer and A. G. Guy, Trans. AIME, 239, 1924 (1967).

54. G. F. Johnson, Master's Thesis, Brooklyn Polytechnic Institute, Brooklyn, 1969.

55. J. E. Lane and J. S. Kirkaldy, Can. J. Phys., 42, 1643 (1964).

56. J. Philibert and A. G. Guy, Compt. Rend., 257, 2281 (1963).

57. R. D. Sisson, Jr., and M. A. Dayananda, Met. Trans., 8A, 1849 (1977).

58. M. A. Dayananda and R. E. Grace, Trans. AIME, 233, 1287 (1965).

59. T. D. Moyer and M. A. Dayananda, Met. Trans., 7A, 1035 (1976).

60. T. Heumann, Z. Phys. Chem., 201, 168 (1952).

61. T. Heumann and P. Lohmann, Z. Electrochem., 59, 849 (1955).

62. A. G. Guy and V. Leroy, The Electron Microprobe, 1966, John Wiley & Sons, New York, p. 543.

63. M. A. Dayananda, P. F. Kirsch, R. E. Grace, Trans. TMS-AIME, 242, 855 (1968).

64. P. T. Carlson, M. A. Dayananda, R. E. Grace, Met. Trans., 3, 819 (1972).

65. J. S. Kirkaldy, Advances in Material Research, volume 4, 1970, Interscience, New York.

66. J. S. Kirkaldy and J. E. Lane, Can. J. Phys., 44, 2059 (1966).

67. A. R. Cooper, Phys. Chem. of Glasses, 2, 55 (1965).

68. Y. Oishi, Journal Chem. Phys., 43, 1611 (1965).

69. Y. Oishi, "Analysis of Ternary Diffusion: Diffusion Equations in Terms of Intrinsic Diffusion Coefficients," incomplete reference.

70. P. K. Gupta and A. R. Cooper, Physica, 54, 39 (1971).

71. R. T. DeHoff, K. J. Anusavice, C. C. Wan, Met. Trans., 5, 1113 (1974).

72. J. S. Kirkaldy, D. H. Weichert, Zia-Ul Haq, Can. J. Phys., 41, 2166 (1963).

73. H. T. Cullinam, I and EC Fund, 4, 133 (1965).

74. F. B. Hildebrand, Methods of Applied Mathematics, 1952, Prentice-Hall, Inc., New York.

75. S. R. de Groot and P. Mazur, Nonequilibrium Thermodynamics, 1969, North Holland, New York.

76. H. Engelke, Thesis, Universität Erlangen-Nürnberg, 1972.

77. A. K. Varshneya, Doctoral Dissertation, Case Western Reserve University, Cincinnati, 1970.

78. C. C. Wan and R. T. DeHoff, Acta Met., 25, 287 (1977).

79. K. J. Anusavice and R. T. DeHoff, Met. Trans., 3, 1279 (1972).

80. C. V. Iswaran, to be published.

81. C. V. Iswaran, F. C. Rizzo Assunção, R. T. DeHoff, TMS-AIME Fall Meeting, Chicago (1977).

82. Metals Handbook, 8th Edition, volume 8.

83. M. Hansen, Constitution of Binary Alloys, 1958, McGraw-Hill Book Company, New York.

84. R. P. Elliott, Constitution of Binary Alloys, 1st supplement, 1965, McGraw-Hill Book Company, New York.

85. F. A. Shunk, Constitution of Binary Alloys, 2nd supplement, 1969, McGraw-Hill Book Company, New York.

86. W. Guertler, WACD Technical Report 58-615, part 1, March 1959.

87. F. N. Rhines, Phase Diagrams in Metallurgy, 1956, McGraw-Hill Book Company, New York.

88. F. N. Rhines, Advanced Phase Diagrams, lecture notes, University of Florida, Gainesville.

89. R. Cribb, Doctoral Dissertation, University of Florida, Gainesville, 1975.

90. T. B. Lindemer and A. G. Guy, Welding Research Journal, 47, 2225 (1968).

91. C. C. Wan, Master's Thesis, University of Florida, Gainesville, 1969.

92. J. W. Colby, Bell Telephone Lab, Inc., Allentown, Pennsylvania (1969).

93. H. Yakowitz, Practical Scanning Electron Microscopy, Chapter IX, 1975, Plenum Press, New York.

94. S. J. B. Reed and J. V. P. Long, X-Ray Optics and X-Ray Microanalysis, 1963, Academic Press, New York, p. 317.

95. E. J. Rapperport, Advances in Electronics and Electron Physics, supplement 6, 1969, Academic Press, New York, p. 117.

96. P. K. Gupta, J. Phys. D. Appl. Phys., 3, 1919 (1970).

97. A. S. Norkiewicz, Master's Thesis, Lehigh University, Bethlehem, 1972.

98. J. W. Colby, Proceedings of the 6th International Conference on X-Ray Optics and Microanalysis, 1972, University of Tokyo Press, Tokyo, p. 247.

99. J. I. Goldstein and J. W. Colby, Practical Scanning Electron Microscopy, 1975, Plenum Press, New York, Chapter XII.

100. H. Yakowitz and J. E. Goldstein, Practical Scanning Electron Electron Microscopy, 1975, Plenum Press, New York, Chapter XI.

101. H. Yakowitz and K. F. J. Heinrich, Mikrochim. Acta, 5, 182 (1968).

102. H. Yakowitz, ASTM-STP 430, 383 (1968).

103. M. L. Picklesimer and G. Hallerman, Report ORNL-TM-1591 (1966).

104. Y. Adda and J. Philibert, La Diffusion dans les Solides, 1966, Presses Universitaires de France, Paris.

105. R. W. Ballufi, Acta Met., 2, 194 (1955).

106. C. P. Heijwegen and G. D. Rieck, Zeit. Met., 64, 450 (1973).

107. J. Hegger, Intern Report 1972, University of Technology, Eindhoven, Netherlands.

BIOGRAPHICAL SKETCH

Fernando Cosme Rizzo Assunção was born on July 9, 1947, in Rio de Janeiro, Brasil. In December, 1965, he finished high school in Liceu Franco Brasileiro. In June, 1970, he received the degree of Bachelor of Science in Metallurgical Engineering from Pontificia Universidade Catolica (PUC), Rio de Janeiro. In December, 1973, he received his Master of Science in Materials Science from Instituto Militar de Engenharia, Rio de Janeiro.

From August, 1970, to March, 1975, he worked in a faculty position in the Department of Materials Science and Metallurgy at PUC.

In March, 1975, he came to the United States and enrolled at the University of Florida to pursue a degree of Doctor of Philosophy in the Department of Materials Science and Engineering.

He is a fellow member of Alpha Sigma Mu, Tau Beta Pi and is a joint student member of the American Society for Metals and the Metallurgical Society of AIME.

Fernando Cosme Rizzo Assunção is married to the former Maria Louiza Portes and they have one son, Mauricio.

I certify that I have read this study and that in my opinion it conforms to acceptable standards of scholarly presentation and is fully adequate, in scope and quality, as a dissertation for the degree of Doctor of Philosophy.

R.T. DeHoff

R. T. DeHoff, Chairman
Professor of Materials Science
and Engineering

I certify that I have read this study and that in my opinion it conforms to acceptable standards of scholarly presentation and is fully adequate, in scope and quality, as a dissertation for the degree of Doctor of Philosophy.

A. G. Guy
Professor of Materials Science
and Engineering

I certify that I have read this study and that in my opinion it conforms to acceptable standards of scholarly presentation and is fully adequate, in scope and quality, as a dissertation for the degree of Doctor of Philosophy.

R.E. Reed-Hill

R. E. Reed-Hill
Professor of Materials Science
and Engineering

I certify that I have read this study and that in my opinion it conforms to acceptable standards of scholarly presentation and is fully adequate, in scope and quality, as a dissertation for the degree of Doctor of Philosophy.

A. I. Khuri

A. I. Khuri
Assistant Professor of Statistics

This dissertation was submitted to the Graduate Faculty of the College of Engineering and to the Graduate Council, and was accepted as partial fulfillment of the requirements for the degree of Doctor of Philosophy.

December 1978

Wayne H. Chen

Dean, College of Engineering

Dean, Graduate School